2017

Assessing Responses of *Betula papyrifera* (Paper Birch) to Climate Variability in a Remnant Population Along the Niobrara River in Nebraska Through Dendroecological and Remote Sensing Techniques

Evan Bumann
University of Nebraska - Lincoln, ebumann@huskers.unl.edu

ASSESSING RESPONSES OF *BETULA PAPYRIFERA* (PAPER BIRCH) TO CLIMATE VARIABILITY IN A REMNANT POPULATION ALONG THE NIOBRARA RIVER IN NEBRASKA THROUGH DENDROECOLOGICAL AND REMOTE SENSING TECHNIQUES

By

Evan P. Bumann

A THESIS

Presented to the Faculty of

The Graduate College at the University of Nebraska

In Partial Fulfillment of Requirements

For the Degree of Master of Science

Major: Natural Resources Sciences

Under the Supervision of Professor Tala Awada

Lincoln, Nebraska

December, 2017

ASSESSING RESPONSES OF *BETULA PAPYRIFERA* (PAPER BIRCH) TO CLIMATE VARIABILITY IN A REMNANT POPULATION ALONG THE NIOBRARA RIVER VALLEY IN NEBRASKA THROUGH DENDROECOLOGICAL AND REMOTE SENSING TECHNIQUES

Evan P. Bumann, M.S.

University of Nebraska, 2017

Advisor: Tala Awada

Remnant populations of the boreal species *Betula papyrifera,* found along north-facing canyons and river banks of the Niobrara River Valley in north-central Nebraska, represent one of the southernmost distributions of the species in North America. Although, the species has persisted in the Great Plains after the Wisconsin Glaciation due to the local topography and microclimatic conditions, canopy dieback has been reported in recent years, which is believed to be attributed to temperature change. Therefore, the goals of this research are to: 1) use dendroecological techniques, or the study of tree rings to assess the responses *B. papyrifera* to intra- and inter-annual micro-environmental variability between 1950 and 2014, and identify the abiotic factor(s) which best describe the observed growth trends in this species; and 2) determine whether the use of satellite imagery from Landsat 5 TM (1985-2011) and MODIS (2000-2014) can serve as a proxy for assessing tree health by relating indices like the Normalized Difference Vegetation Index (NDVI) to tree rings characteristics.

Results showed that growing-season streamflow and precipitation were positively and significantly correlated with raw tree ring widths, basal area increment increase, and standardized ring widths ($p < 0.05$), while high late fall and spring precipitation and streamflow seemed to have a negative effects. The strongest predictor for standardized tree ring growth was the Palmer's Drought Severity Index (PDSI), suggesting that *B. papyrifera* is highly responsive to a combination of temperature and water availability. GLMMs and Pearson R^2 correlations indicated that increasing winter and spring temperatures were unfavorable for tree growth while increasing summer temperatures were favorable in the absence of drought.

Maximum and accumumlated NDVI derived from satellite imagery showed potential of these techniques to be used as a proxy for ex-situ monitoring *B. papyrifera* performance through high Pearson's R^2 values (≥ 0.76) at the pixel level. Landsat 5 TM derived max-value NDVI correlations identified adjacent rangeland of moderate bison grazing on rough landscape - similar to those occupied by *B. papyrifera* – as a likely reliable proxy for predicting seasonal growth and performance the species.

Results from this study have significant management implications and are critical to the development of biogeographical and ecophysiological predictive models aimed at forecasting the dynamics and performance of this species in the face of future climate variability, extremes, and change in both remnant populations and across its current habitat range in more northern latitudes.

ACKNOWLEDGEMENT

A special thanks goes to my advising committee that helped me every step of the way to design and implement the research for my thesis. Drs. Brian Wardlow and Michael Hayes were invaluable in teaching me how to analyze and interpret remotely sensed and climate-based data. Mr. Chris Helzer facilitated the usage of the Niobrara Valley Preserve for research purposes and shared invaluable information on land use and ecology of the area. Dr. Paolo Cherubini helped me understand new implications associated with the use of dendrochronological data, and his laboratory in Switzerland (WSL) assisted with processing tree ring samples.

Dr. Tala Awada took a chance and gave me an opportunity I never thought I would see. Through the past few years she spent countless hours helping me to understand perspectives of environmental and plant physiological sciences. As this project draws to a close, I can confidently say I would not want to repeat this work under any other advising professor. Tala pushed me to really make something of this opportunity; it has been an invaluable experience in both life and learning and I am grateful to have had Tala showing me the way.

This project required consultation and assistance from many of my colleagues, most notably Tasos Mazis and Jeremy Hiller. These two gentlemen dedicated many hours helping me collect tree cores on a rough terrain and process samples. A special thanks also goes to Dr. Drew Tyre for his input and advice on the statistical models.

I want to give special acknowledgement to my teammates, coaches, and trainers at the Lincoln Boxing Club. Cruz and Aaron Quintana, Art Shiers, and Ethan Hopp (and so, so

many more) were a second family to me over the past few years, through the good times and the bad, and not only provided wonderful community outside of my studies, but also experiences which will last through my final days.

I wish to thank my family for encouraging me all along the way. I could not have made it anywhere near this far without their love and support.

Finally, this study was supported by the McIntire Stennis Forest Research Fund, United States Department of Agriculture, and I am thankful for financially supporting my research endeavors.

Table of Contents

1. INTRODUCTION

Paper birch (*Betula papyrifera*) is a widely distributed deciduous tree species across the continental North America. It grows in the boreal forest from Newfoundland in eastern Canada all the way to northwestern Alaska in the U.S., crossing the Canadian prairies in Manitoba, Saskatchewan and Alberta. *B. papyrifera* also extends south from Washington in the western U.S. to Montana, and through the Lake States to New England in the eastern U.S. Scattered populations can be found in the Great Plains of Montana and North Dakota, the Black Hills of South Dakota, the Appalachian Mountains, and the Front Range of Colorado (Burns and Honkala 1990) (Fig. 1). As a boreal species, *B. papyrifera* is adapted to the cold northern climate and can rarely be found in regions where July monthly average temperature exceeds 21°C (Stroh and Miller 2009; USDA 1965). In fact, *B. papyrifera* has been found to have mixed responses to temperature especially early in the growing season. Warming temperatures in the spring can result in an earlier bud burst which can have positive impact on growth rates when water is available (Karlsson et al. 2004; Li et al. 2016), but this comes with a risk of early season re-freeze, which can damage and kill newly emerging buds and rootlets (Pomerleau 1991), and may result in crown dieback. Water availability has also been shown to positively affect the performance of the species (Li et al. 2016), on the other hand water stress - including both excess water and drought - can cause defoliation (Wang et al. 2016), leading to suppressed tree ring growth and performance for up to four years following defoliation (Karlsson et al. 2004). Drought conditions have also been shown to suppress seed

production and encourage vegetative propagation of the species (Burns and Honkala 1990). Water availability can be strongly influenced by the presence of invasive species adding pressure to evapotranspirational demands on an ecological system, thereby creating a potential deficiency for less competitive/native species, such as the case with *Phragmites Australis* of the Republican River Basin, USA (Mykleby et al. 2016) and *Juniperus virginiana* in the Great Plains (Awada et al. 2013).

After the Wisconsin Glaciation, remnant stands of *B. papyrifera* are the last of what was once reflective of boreal vegetation in nature (Wright 1970; Stroh and Miller 2009) and have persisted in the Great Plains with notable current, yet declining presence. One of these ecotypes can be found along the Niobrara River Valley in north-central Nebraska, where the species can be found in north-facing canyons and along river banks.

The Valley plays an important ecological role as an ecotone where grassland and forest species converge, supporting a diverse array of vegetation that can be rarely found in close proximity elsewhere (Stroh and Miller 2009). Short grass species from the semi-arid grasslands of the surrounding Sandhills, as well as grasses representing the mixed and tall grass prairies can be found alongside forest species representing the western coniferous, eastern deciduous and boreal communities. Localized microclimate has been associated with species distribution and health of this unique ecosystem.

Dieback in canopy-sized *B. papyrifera* has been reported in recent years and is thought to have started around the 1980's. In a study that focused on temperature fluctuation and its impacts on *B. papyrifera* health and performance, Stroh and Miller (2009) concluded that the healthy trees seemed to be associated with annual minimum temperature regimes and

distance from the river bank. Healthy trees experienced mean summer temperatures of approximately 22°C, about 1°C cooler than the surrounding local weather stations, and decreased freeze/thaw conditions in the spring which likely prevent rootlet injuries and dieback, and promote the persistence of the species in healthy stands (Stroh and Miller 2009). On a continental scale, one of the main threats to *B. papyrifera* is increased climate variability, extremes, and change (Canada Parks and Wilderness Society). The species rarely occurs in areas where average July temperature exceeds 21˚C, in comparison, the Niobrara River Valley July average temperature is approximately 23.8˚C. It is unknown how this species in its remnant southern locations will respond to increasing climate change, weather variability, and extremes. In more northern latitudes *B. papyrifera* was reported to respond positively to warming summer and winter air temperatures in Greenland (Hollesen 2015), and Siberian populations declined under drought conditions (Kharuk et al. 2014).

As this population is a remnant of the more northern Boreal forest, we can observe how it has behaved in the face of changing climate and apply that knowledge to climate predictions for the northern boreal forest to better understand and mitigate the effects of climate change. Growth habits of *B. papyrifera* and other boreal species have also shown warming temperatures and drying climate to be highly unfavorable for growth, which are expected to persist in the near future (Girardin et al. 2016; Chen et al. 2017; Hogg et al 2017).

At present, few studies have been conducted on the environmental factors that impact health and performance of the remnant *B. papyrifera* population of the Niobrara River Valley, which represents one of the southernmost distributions in North America.

Therefore, the goals of this research are to: 1) use dendrochronological techniques, or the study of tree rings to assess the past responses of *B. papyrifera* to intra- and inter-annual micro-environmental variability, and identify the abiotic factor(s) which best describe the observed growth trends in this species; and 2) determine if the use of satellite imagery can serve as a proxy for assessing tree health by relating indices like the Normalized Difference Vegetation Index (NDVI) to tree rings characteristics.

Dendrochronological techniques, or the study of tree rings, can be applied to investigate ecological processes and tree responses to the localized environment, which are then related to tree performance and forest health (Campelo and Cherubini 2009; Cherubini and Amoroso 2015; Cherubini and Simcha 2014). Factors such as site characteristics, abiotic and biotic environment, management practices, species growth habit, and genetics influence the formation and growth of tree rings (Cherubini and Simcha 2014). This study examined a time period spanning between 1950–2014.

NDVI is a vegetation index commonly used in remote sensing applications and can be related to plant health, vitality, and population characteristics such as leaf area index (Lee et al. 2017). The index examines the ratio of spectral reflectance between the red and near-infrared regions of the electromagnetic spectrum. This study used max-value growing season NDVI obtained from Landsat 5 TM (Thematic Mapper) imagery between 1985-2011, and accumulated NDVI over various periods of the growing season from MODIS (Moderate Resolution Imaging Spectroradiometer) between 2000-2014. NDVI derived from Landsat 5 TM and MODIS were then related to tree ring growth to identify pixel-based locations with strong correlation to *B. papyrifera* growth. We examined characteristics of these locations, and used that information to identify geographical areas

which could be used as a proxy to estimate and infer *B. papyrifera* growth and performance for scattered individuals in near real-time from satellite imagery.

Results from this study have significant management implications and are critical to the development of biogeographical and ecophysiological predictive models aimed at forecasting the dynamics and performance of this species in the face of future climate variability and change in both remnant populations and across its current habitat range in more northern latitudes.

2. MATERIALS AND METHODS

2.1. Sites selection

The study area was located at the Nature Conservancy Niobrara Valley Preserve, north-central Nebraska, centered at 42.7834° N, 100.0280° and encompasses nearly 227 km^2 (Fig. 2). Four north-facing study sites of *Betula papyrifera* were selected along a 27 km section of the river owned by The Nature Conservancy. All observed distribution of *B. papyrifera* were close to the river's edge and accompanied by other deciduous, riparian vegetation. There was a distinct change from deciduous vegetation at the water's edge to coniferous vegetation further upslope. The Valley is 60 to 90 m deep, and ranges between 0.8 to 3.2 km in width. Most of the river banks are steep, more so on the south side. The water flow in the adjacent Niobrara River and its tributaries is in part determined by groundwater contribution (Szilagyi et al. 2002), as the water itself flows over bedrock, therefore creating a high water table. Soil type is mostly alluvial fine-grained sand with a small amount of coarser material (Cady and Sherer 1946). Water moves in an easterly

direction at a rate of roughly 0.3 md^{-1} through aquifers at a downward slope of anywhere from 2.5 – 13 m per every kilometer of easterly travel (Bradley 1956).

2.2. Microclimate

Precipitation data were acquired from the Ainsworth Weather Station via the High Plains Regional Climate Center, University of Nebraska-Lincoln (HPRCC, http://climod.unl.edu/). This station is located approximately 35 km from the study sites, and is the closet station with long term records. Long-term (1901-2015) annual precipitation ranged between 241 and 938 mm, and average monthly precipitation ranged between 15.9 to 63.8 mm. During the study period between 1950 and 2014, average annual precipitation was 572 mm, with 80-90% falling during the growing season (Fig. 3).

Monthly streamflow rate was acquired from the USGS National Water Information System (www.waterdata.usgs.gov), Sparks NE (Station code: 06461500; 42°54'14"N, 100°26'13"W). The stream gauge is located approximately 30 km from the study sites. Average monthly streamflow ranged between 16.9 and 26.4 m^3s^{-1}. Streamflow during the growing season, March through October (Uchytil 1991), ranged between 15.6 and 27.7 m^3s^{-1}. Mean annual streamflow during the study period (1950–2014) ranged between 6.9 and 10.9 m^3s^{-1} (Fig. 3).

Temperature data were acquired from the Springview Weather Station, via the HPRCC. This station is located approximately 30km from the study sites. January average minimum and maximum temperatures were -12.3 and 0.4 °C, respectively, and July average minimum and maximum temperatures were 16.5 °C and 31.2 °C, respectively

(Fig. 4). The Springview station is closer to the study sites but had a less complete precipitation record than the Aisnworth station, and therefore Ainsworth precipitation data were used.

Monthly and annual Palmer's Drought Severity Index (PDSI) data were acquired from NOAA (www.ncdc.noaa.gov), calculated for the region of north-central Nebraska. Monthly PDSI during the study period ranged between -5.9 and 8.1, with a mean monthly PDSI of 0.9 (Appendices A and B). Annual PDSI ranged between -4.9 and 6.7 with a mean of 0.9. (Fig. 3)

2.3. Tree core collection

Sites were located visually and accessed via the river, by a canoe. Sites were identified, marked and GPS location acquired for all trees (Fig. 2). Trees were found only on north-facing slopes and growing from pre-existing root crowns; there were not any trees on examined sites which emerged from seeds. We selected one trunk from each sampled root crown based on healthiest appearance and largest diameter measured at breast height (DBH). A total 180 cores from 45 trees were sampled, at 1.3 m from the root crown, at 90° intervals around the trunk; representing the north, south, east, and west faces of the trunk (Maeglin 1979). Diameter at breast height (DBH, cm) was recorded. The oldest ring record dated back to 1894, with the majority of consistent records across trees rings dating back to the 1950's, thus the time frame selection for this study.

2.4. Tree rings parameters

Cores were placed on core trays and were dried in open air for several weeks post-collection. Once dried, cores were glued to wooden dowels and sanded flat and smoothed with 150, 220, 440, and 600 grit sandpaper. Cores from southern and western facing slopes were sent to the Dendrochronology laboratory, Swiss Federal Institute for Forests, Snow and Landscapes, WSL, Switzerland for ring width measurements, while the northern and southern facing cores remained at the Forest Ecophysiology Lab at UNL for assessment using complementary methods. South and West facing cores were originally intended for isotopic analysis of carbon and hydrogen by the WSL lab but many of the rings were simply too small to gather a reliable measurement. The cores at UNL were scanned at 3200 dpi and individual ring widths were measured to the nearest 0.01 mm and cross-dated with the Windendro software platform. At WSL, Switzerland, the rings were measured under a microscope to the nearest 0.01 mm using a linear table, "LINTAB" (Rinn 2003). All measurements were visually and mathematically crossdated in TSAPWin (Time Series Analysis and Presentation; Rinn 2003; Stokes and Smiley 1968). Missing rings were inserted manually with a value of 0 to complete the chronology. The visually crossdated data was imported to CONFECHA for statistical analysis to check crossdating accuracy (Grissino-Mayer 2001).

Outer bark measurements were extrapolated as many peeled and were lost during transport; B. papyrifera bark is papery and loose in general and does not typically remain attached to the core upon removal from the tree. During transport, many of the bark samples came loose and could not reliably be replaced to their appropriate core. Extrapolation was done by stand. Bark measurements were gathered in Windendro; for measurements of inner and outer bark for the cores which still had it. First the inner bark

length was averaged by stand and direction, then filled in to the 2016 values that lacked inner bark measurement followed by repeating the process for outer bark measurements. In this fashion, Inner and outer bark average length was extrapolated to missing measurements by direction, and by stand. Some cores lacked structural integrity were removed from the analysis records, ultimately resulting in 153 included of 180 sampled from a total of 43 trees.

From the cores that did contain pith or rings very close to pith, 5-10 rings were removed to discount early/sapling growth. Ring width from up to four cores per tree were correlated to each other, and were averaged using Tukey's robust average to create a single measurement for each year for each tree. From this we calculated basal area increment (BAI) increase. Standardized measurements were calculated from each core using the "detrendeR" package in "R" (Campelo 2012); single detrending, spline length 20, bandwidth 0.65, $p < 0.05$. Standardization removes biological factors of the individual samples due to age, disturbance, crowding, and size, leaving a value influenced primarily by climate.

Tree ring chronologies ranged between 21 – 122 years of age and averaged 68 years. DBH was significantly correlated with age ($p>0.001$).

2.5. Tree rings statistical analysis

Statistical analysis was carried out in R (R core team 2015) using linear mixed modeling through the package "Lme4" (Bates et al. 2015). In all models considered, predictor variables were represented by monthly cumulative precipitation, mean streamflow, mean temperature, and annual Palmer's Drought Severity Index (PDSI) with year, stand, and

sample (tree ID) as random effects. Monthly inclusion began in the growing season of the previous year through October of the current year. All models considered 1950-2014 for the time period and individual trees considered as separate response variables. Through early model creation, all parameters of spatial distinction were eliminated as they did not show any statistical significance (slope, aspect, distance/elevation to ridgeline and river edge). They were thus not considered for final models creation. The general linear mixed model in matrix notation:

$$Y = \beta_0 + \beta_1 X_1 + \cdots + \beta_{r-1} X_{r-1} + \varepsilon$$

Stepwise backward selection is a process wherein a model is selected by removing one variable each step of the process based on t-statistics of their estimated coefficients (UCLA 2006). It is useful for selecting models from a moderate-sized pool of all potential inclusions. Concerns arise from this method as variables that are significant to the project at hand may be removed in early selection. When this method is employed, one must give consideration to the legitimacy of the selected product from a real-life perspective (Burnham and Anderson 2002)

All variables for consideration were included in a "global model" from which variables were systematically removed: At every step, all variables were individually tested for removal using a Chi-square test. Whichever variable's removal after testing produced the highest P-value was removed, and a new model was created using the remaining variables. This process was repeated until the highest calculated P-value of variable removal was $p<0.05$. At this point, model selection was finished and the final model

considered determined. In the generalized linear mixed models: stand, sample (tree ID), and year were used as random effects.

2.6. Landsat and MODIS imagery analysis

Landsat 5 TM offers the highest spatial resolution at the most frequent time intervals available for the study period. The imagery was acquired from Google Earth Engine, described as "…a platform for petabyte-scale scientific analysis and visualization of geospatial datasets, both for public benefit and for business and government users…", using the "LANDSAT/LT5_L1T_32DAY_NDVI" dataset with the Landsat cloud score algorithm applied to every available scene through the growing season, March through October, from 1985-2011. Pixels identified as "cloud" (or primarily water) were removed. All imagery considered was of identical spatial reference and 30-m pixel dimension. Normalized Difference Vegetation Index (NDVI) was calculated from retained pixels. NDVI is the ratio of reflectance between the red (630-690 nm) and near-infrared (760-900 nm) regions of the electromagnetic spectrum. NDVI = (NIR-red)/(NIR + red) which results in a number ranging -1 – 1. A high positive number indicates healthy vegetation, while a low positive number indicates unhealthy or dead vegetation. As NDVI illustrates characteristics such as chlorophyll content, leaf structure, and leaf area (NASA 2000); phenologically speaking, the maximum NDVI value should be seen around the peak of the growing season.

The NDVI images which were available for each year were "stacked" and the maximum values at each pixel location gathered to create a single raster representing the maximum value of cloud-free pixels of available image scenes by year.

This does allow for some pixel locations' max-value NDVI to come from a point outside of the growing season (not summer) which results in some amount of noise in the pixel-based correlation which will lead to a slightly decreased R^2 value. Some years contained too many "cloud" pixels during the summer scenes to create a representative raster of peak season pixels and were removed from analysis. Annual representative images which primarily were comprised of data from summer months (June, July, August) during 1988, 1990-2001, and 2003-2007 to create a raster of pixel-based correlation (Pearson's R^2) values against both average standardized and average tree ring widths.

While Landsat imagery provides a high spatial resolution, the drawbacks to using it come by way of cloud obstruction; therefore we applied similar methods for comparison to MODIS imagery which offers consistent, high temporal resolution multispectral dataset useful for examining surface changes throughout the year with imagery recorded every 1-2 days since December 1999 to present at 250-1000 m pixel resolution. NDVI (red 620-670 nm, near infrared: 841-876nm) image data were acquired through Google Earth Engine from the MODIS Terra Daily NDVI (Image collection: 'MODIS/MOD09GA_NDVI') data set for all available dates between March and October from 2000-2014.

Produced biomass is a direct cause of photosynthetic performance, and accumulated NDVI over time from MODIS imagery (Reed et al. 1996; Li et al. 2015; Kumar and Mutanga 2017) has been shown to provide a stronger estimate of aboveground biomass, and therefore seasonal productivity, than single-date NDVI. Therefore, accumulated NDVI through distinct portions of the growing season were also examined and correlated with raw and standardized tree ring growth. NDVI images were "stacked" for the time

periods of March – October (full season), March – May (early season), June – August (mid-season), August – October (late season), May, June, July, and August. The NDVI images were added together to determine "accumulated-NDVI", or "area under the curve" to examine how aggregate NDVI, over various time periods correlates (Pearson's R^2) at the pixel level with tree ring width and standardized ring width.

2.7. Relationship between tree rings and NDVI

Tree ring chronologies have been shown to reflect a strong, significant correlation with NDVI (Jicheng and Xuemei 2005; Forbes et al. 2010). Focus on the relationship of *B. papyrifera* and pixel-based NDVI signal during the peak growing season is facilitated by comparison with a plot-based vegetation sampling performed in 2016 by The Nature Conservancy (TNC) on the Niobrara Valley Preserve property. This was accomplished by calculating a Pearson's R^2 value between averaged annual ring growth (raw, BAI, standardized) and the annual representative NDVI values at each pixel location over the observed area. The R^2 values were organized in a single raster representing the pixel-level correlation to growth.

2.8. Vegetation validation

The forest population of *B. papyrifera* was not dense enough to reliably establish any pixel from Landsat or MODIS imagery as homogenous to *B. papyrifera,* and the population is so close to the river's edge, the vegetation signal was most often masked by water and therefore removed from NDVI analysis. Nearby grasslands were used as a proxy. Vegetation was sampled from 8 plots, established by TNC, across a series of management areas along the Niobrara Valley Preserve on June 27, 2016. These plots

were placed so TNC could track inter-annual changes in vegetation structure across the various treatments of: rotational grazing (plots 1, 2, 3); patch-burn cattle grazing (plot 4); patch-burn cattle grazing, burned in 2015 (plot 5); unburned cattle grazing, control (plot 6); bison grazing, burned in 2015 (plot 7); and bison grazing, unburned (plot 8). In the patch-burn grazed areas, there were no burns in 2016, so the two grids in each site were in unburned (for at least several years) areas vs areas burned in 2015. The patch-burn cattle control site is unburned, but grazed season-long at the same stocking rate as the patch-burn cattle pasture, which is supposed to have a portion of it burned each year. In the rotational grazing treatments, each pasture is grazed at a different time each year. Each plot consisted of an 8 m x 6 m grid (8 east – west, 6 north – south) of GPS points encompassed in a 640 x 480 m^2. At each GPS point, a 1 m^2 quadrat was dropped and vegetation sampled. Canopy height was measured using a meter stick and a piece of Styrofoam board; the meter stick was placed vertically at the soil level and the Styrofoam dropped on to the canopy to measure canopy height. Percent of each vegetation functional group (grass, shrubs and forbs), as well as litter, standing dead and bare soil, were recorded. Topography and vegetation composition were considered in reference to pixel-based NDVI and tree ring growth correlation of *B. papyrifera* to identify potential areas of proxy monitoring based on their vegetation and/or topographical characteristics.

3. RESULTS

3.1. Site microclimate

Annual cumulative precipitation for the area during the study period of 1950 – 2014 ranged from 241.3 to 938.0 mm with a mean annual precipitation of 572.6±17.6 mm.

During the 65-year study period, annual precipitation did not show any obvious increasing or decreasing trend over time, instead precipitation varied annually around the mean (Fig. 3). The majority (80-90%) of the annual precipitation fell during the growing season between April and September (Fig. 5). Average annual streamflow ranged between 16.9 and 26.4 m^3S^{-1} with a mean annual streamflow of 21.7±0.3 m^3S^{-1} (Fig. 3). During the study period, average annual streamflow showed a decreasing trend, which was significant at $p < 0.1$ ($p = 0.09$). Streamflow increased in the spring with snow melt and declined in July through September with decrease in precipitation and increase in temperature and evapotranspirational demands, before increasing again in October with decline in temperatures (Fig. 5). Annual Palmer's Drought Severity Index (PDSI) ranged from -4.9 to 6.7, with a long-term average of 0.9±0.3. During the study period, annual regional PDSI exhibited a significant ($p < 0.1$ ($p = 0.054$)) upward (wetting) trend (Fig. 3). Despite this wetting trend, years of moderate to severe droughts were common and constituted around 32% of the 65-year period of study (1950 to 2014).

Annual air temperature averaged 8.9±0.1 °C (Fig. 4), with January mean temperature ranging between -15.1 to 3.0 ºC, and showing a slight and statistically significant warming over time ($p<0.01$). January minimum temperature ranged between -20.4 and -3.5 ºC, January maximum temperatures ranged between -9.8 and 9.6 ºC, and neither showed a significant positive or negative trend. July minimum temperature ranged between 13.1 and 19.3 ºC, July maximum temperature ranged between 24.4 and 37.4 ºC, and neither showed an increasing or decreasing trend. July mean temperature met or exceeded 21 ºC nearly every year except for 1992 (Fig. 4). March minimum temperatures ranged between -12.2 and 0.4 ºC and did not show an increasing or decreasing trend,

while March maximum temperatures ranged between 1.8 and 17.6 ºC and displayed a significant decreasing trend ($p = 0.048$). April minimum temperatures ranged between -3.8 and 5.1 ºC, April maximum temperatures ranged between 9.7 and 21.5 ºC and neither showed a significant increasing or decreasing trend.

3.2. Tree rings characteristics

Sampled chronologies were dated back to 1894 with a majority of the records dating back to around 1950's (Appendix R). Therefore, we chose the time period between 1950 - 2014 for analysis. Raw tree ring widths ranged between 0.087 and 4.355 mm, with an average annual growth of 1.21±0.02 mm (Fig. 6). Basal area increment (BAI) increase ranged between 11.3 and 1327 mm^2 with a mean BAI of 325.3±4.27 mm^2 (Fig. 6). Both tree ring width and BAI showed a significant decline in growth over time ($p< 0.001$), and significant variability in response to the environment. Data standardization, which removed age-related trends, reduced variance, and eliminated the impacts of abnormalities associated with disturbances, resulted in the removal of any significant trend ($p = 0.74$), and showed variability around the mean (0.99±0.006 mm) which reflected inter- and intra-annual fluctuations of the environment (Fig. 6). A decline in tree ring growth rate was observed in five periods, early 1960s, mid 1970s, late 1980s, early 1990s, and early 2000s. This reduction in growth was also observed during years with near zero or negative (drought) PDSI, or in years with lower than average air temperatures. Above average tree ring width, standardized ring width, and BAI were observed during wet years or positive annual PDSI (e.g. 1983, 1995, and 2009).

3.3. Climate correlations

Previous and current year streamflow from July through November were positively and significantly correlated with raw tree ring width, BAI, and standardized ring width ($p < 0.05$). Increasing streamflow during fall through spring had negative, albeit statistically non-significant, impacts on tree performance (Fig. 7). Current and previous year precipitation of July and October were generally positively correlated with tree growth, but only October precipitation was significant for standardized ring width. High precipitation and streamflow rates during April of current and previous year seemed to have a negative effect on tree ring growth. Increased air temperatures of both current and previous year were generally negatively correlated with all measured tree parameters, with few exceptions (Fig. 8). The strongest predictor for standardized tree ring width was PDSI, where values were significantly and positively correlated at $p < 0.05$ for both previous and current year. While PDSI was generally positively correlated to tree ring width and BAI, the relationship was not significant (Fig. 8, Appendix C).

3.4. Stepwise linear regression

Generalized linear mixed modeling considered monthly variables of precipitation, streamflow, mean temperature, and annual Palmer's Drought Severity Index (PDSI) with year, stand, and sample (tree ID) as random effects. Final Models were created from a pool of all available variables which were removed one-by-one using a Chi-square test to determine which removed variable would improve the model the most until variable removal no longer improved the model at the $P = 0.05$ level (Appendix D). One model was created each for raw tree ring width (Raw), standardized ring width (Std), and basal

area increment increase (BAI) from the same pool of variables. The selected models highlighted the effects of mid-season water availability for both previous and current year, early season temperature of the current year, and late-season temperature of both the previous year and current year (Table 1).

3.5. Comparison of climate correlation and GLMM

Precipitation was included in the raw tree ring width model (Raw model) for current March only and reflected a positive influence on growth during that time, while the Pearson's R^2 showed significant negative correlation with previous year April and significant positive correlation with previous year July. The BAI model showed that precipitation had a positive influence on growth for previous year July and current June while the R^2 only showed significance with previous April. The standardized ring width model is the most relevant since data standardization removes the effects of biological factors of due to age, disturbance, crowding, and size. This model indicated only a negative influence of previous November precipitation on growth while the R^2 showed significant positive correlation with previous October and December precipitation. R^2 correlations were also significantly negative in previous January and positive in current June, current October, and current November. The Raw and BAI models, and Pearson R^2 all highlight previous early season precipitation as negatively impacting growth while previous and current mid and early season precipitation is favorable. Standardized tree ring width showed a disagreement where the model shows late previous season precipitation as negatively impacting growth while the Pearson R^2 showed significant positive correlation to late season precipitation of both previous and current year.

The GLMM and climate correlations all considered virtually the same pool of variables yet produced slightly different results, while the overall messages were similar. When using backwards selection, one must consider that variables can be dropped early in the model creation process which could later show significance. Variables may be dropped in the selection process which could later show significance. Therefore one must consider the overall model as a whole and interpret its meaning within the ecological context of the data itself.

Streamflow was included as having a negative influence for previous July and current May in the Raw model and previous July in the BAI model. Otherwise the positive influence was agreed upon by the both the Raw and BAI models, and Pearson R^2 of previous and current August. Significant Pearson R^2 correlations were observed additionally to raw tree ring width and BAI during previous and current September, current July and August. The influence of streamflow during previous July on the raw tree ring width and BAI models is the only major contrast between the GLMMS and Pearson R^2 correlations which generally show streamflow as a positive influence across raw ring width, BAI and standardized growth.

Temperature was agreed upon by the Raw GLMM and Pearson R^2 as a negative impactor of growth for current January. Increasing temperature during previous and current January and March in the Raw and BAI models, and previous April and previous June in the standardized model, both showed significant negative correlation to growth. While only current January of the Raw model was included as significant in the GLMM and Pearson R^2, the overall message portrayed from the GLMMs and Pearson R^2 correlations was that increasing winter and spring temperatures are unfavorable for growth while

increasing summer temperatures are favorable for growth in the absence of drought (Table 1, Fig. 7 and 8, Appendix E).

3.6. NDVI as a proxy for vegetation and *B. papyrifera* health

Average raw tree ring width and average standardized ring width were correlated (Pearson's R^2) with Landsat 5 annual max-value NDVI and MODIS sum-value NDVI over various time periods during the growing season (March – October, March – May, June – August, July, August – October, August, June, and May), at the pixel level for the Niobrara Valley Preserve area owned by TNC between 1985-2011 (Landsat) and 2000-2014 (MODIS), (Fig. 9). For Landsat imagery, every pixel "stack" of maximum available annual NDVI values between March and October of each included year (1988, 1990-2001, 2003-2007) was considered individually via the maximum available value. For annual MODIS imagery, all concurrent values for every scene of the prescribed time period at the pixel level were added together across the growing season.

Correlation (R^2) of raw tree ring width to Landsat 5 TM max-value NDVI between 1985 and 2011 within the confines of the Preserve boundary ranged between -0.85 – 0.93. Correlation (R^2) of standardized tree ring width to Landsat 5 TM max-value NDVI between 1985 and 2011 within the confines of the Preserve boundary ranged between -0.69 – 0.91.

Correlation (R^2) of raw tree ring width to MODIS sum-NDVI between 2000 and 2014, within the confines of the Preserve boundary at various monthly intervals were as follows: May ranged between -0.68 – 0, June ranged between -0.44 - 0.01, July ranged between -0.15 – 0.53, August ranged between -0.37 - 0.08, August-October ranged

between -0.42 – 0.08, June-August ranged between -0.37 – 0.13, March-May ranged between -0.31 – 0.15, and March-October ranged between -0.49 – 0.10.

Correlation (R^2) of standardized tree ring width to MODIS sum-NDVI between 2000 and 2014 within the confines of the Preserve boundary at various monthly intervals were as follows: May ranged between -0.58 – 0.14, June ranged between -0.15 – 0.32, July ranged between -0.07 – 0.70, August ranged between -0.09 – 0.45, August-October ranged between -0.23 – 0.34, June-August ranged between 0.01 – 0.56, March-May ranged between -0.28 - 0.14, March-October ranged between -0.14 - 0.42 (Appendix F).

The pixel-level correlation values in raster form were assigned a "heat map" style colorway in ArcGIS to indicate direction and magnitude of the correlation at each pixel. The raster was made semi-transparent and overlain on a triangulated irregular network to examine a possible relationship between ring growth of nearby *B. papyrifera* samples, and topography and/or vegetation (Fig. 10 and 11).

Vegetation composition adjacent to the *B. paryrifera* stands were sampled for groundtruthing purposes. We sampled 8, 640 x 480 m plots on June 27, 2016 on the Niobrara Valley Preserve. Results indicated that grasses percent cover ranged between 31.9 and 49% and averaged 37.6±0.9% (Fig. 12). Forb percent cover ranged between 5.4 and 20.7, and averaged 11.5±0.5%. Forb composition was significantly higher in plot 4 (20.7%) and plot 5 (16.3%) compared to the other plots. Shrub percent cover ranged between 6.2 - 27.4% and averaged 17.8±1.1%. Litter percent cover ranged between 36.7% - 67.2% and averaged 52.4±1.5%. Litter composition was significantly lower in plot 4 (38.4%) and plot 7 (36.1%) relative to the others. Standing dead vegetation percent

cover ranged between 2.3% - 6.2% and averaged 6.2±0.5%. Bare ground percent cover ranged between 28.8% - 54.5% and averaged 41.8±1.5%. Bare ground composition was significantly high in plots 4 (54%), 5 (54%), and 7 (53%) relative to others. Canopy height ranged between 26.9 – 41.6 cm and averaged 34.0±1.4 cm (Fig. 12, Appendix G)

Max-value Landsat 5 NDVI from all 8 vegetation sampling plots followed the standardized growth trend of *B. papyrifera* (Fig. 13). Average R^2 correlation value among each plot ranged between 0.35 and 0.63 for the raw tree ring width, and between 0.36 and 0.76 for the standardized ring width measurement. Average plot-level correlation was highest in plot 6 for raw ring width at 0.63 and plot 2 for standardized ring width at 0.76. Average plot-level correlation was lowest in plot 8 for both raw ring width and standardized ring width at 0.35 and 0.36, respectively (Fig. 14, Appendix H).

A notable significant drop in Landsat max-value NDVI was observed in 2002. Climate records indicate this year as one of low precipitation, low streamflow, warm temperature, and drought, along with decreased ring growth from the collected *B. papyrifera* dendrochronological record. MODIS sum-NDVI for the periods of July, August, and August – October reflect the same notable drop in 2002 NDVI for all 8 plot locations as seen in the Landsat 5 max-value NDVI (Appendix I).

MODIS Sum-NDVI from all 8 vegetation sampling plots were positively correlated with the raw tree ring growth of *B. papyrifera* during the month of July, and standardized tree ring width behavior closest for July and June-August (Appendix I). A statistical summary of both raw and standardized growth correlation to various time periods is seen in Appendix (J). Average plot level correlation for tree ring width and July sum-NDVI was

highest in plot 8 at 0.42 and lowest in plots 4 and 5 at -0.01. Average plot-level correlation for standardized tree ring width and July sum-NDVI was highest in plot 6 at 0.6 and lowest in plot 5 at 0.27. Average plot-level correlation for standardized ring width and August – October sum-NDVI was highest in plot 3 at 0.31 and lowest in plots 6 and 8 at $p < 0.05$.

Pixel-level correlation of raw tree ring width and standardized tree ring width between Landsat max-value NDVI and MODIS sum-value NDVI during the summer months showed very similar results when compared to topography and plot-level vegetation composition (Fig 9, 10, 11, 12).

4. DISCUSSION

4.1 Dendrochronology

Throughout the study period of 1950-2014, precipitation did not show an increasing or decreasing trend with strong variation above and below the mean. Standardized tree ring growth followed this precipitation trend fairly closely both intra- and inter-annually. Annual temperature and summer (July) temperature have remained reasonably stable with no upward or downward trends. However, the area did see a warming trend in January (Fig. 4) which indicates winter temperatures around the Niobrara Preserve area are becoming a bit warmer. Warming winter and spring trends have been linked to facilitation of birch stand densification, increased ring growth, and treeline advancement into neighboring tundra areas (Kharuk et al. 2014), as well as wider seasonal rings created as a result of increased cambial growth due to extending the growing season,

facilitated by earlier bud burst (Karlsson et al. 2004; Yang et al. 2017). Increased ring growth of birch species has been observed to be encouraged by earlier snowmelt which allows soils to drain and warm quicker (Hollesen et al. 2015). In this study however, the ring width model (Table 1) shows warming January air temperature as having a negative effect on growth. This may be due to re-freezing of the roots in the early season and ultimately leading to tree damage, crown dieback (Greenidge 1953; Redmond 1955), or death of the tree (Pomerleau 1991). Water availability can have a similar effect in that availability has been shown to encourage establishment and growth of birch species (Li et al. 2016), while water logging of soil has been shown to decrease leaf area of birch species (Wang et al. 2016). Such may be the case in the Niobrara as the standardized model highlights a negative growth effect from increased precipitation during previous November and current May, or late-previous and early-current season. The defoliation response to water may very well translate to problematic bud formation in the late-previous season and bud-burst in the spring.

The shallow fibrous root system of *B. papyrifera* combined with its defoliation stress response to both too little and too much water may partially explain why it was only found in small areas which may facilitate a more reliable underground flow of water, as streamflow is primarily dictated by groundwater movement in the area (Szilagyi et al. 2002) which flows lateral in an easterly direction (Bradley 1956; www.NPS.gov). USGS well level data from the surrounding area showed a significant positive correlation only to groundwater levels located to the east of the observed B. papyrifera sites (Appendix Q).

Palmer's Drought Severity Index (PDSI) displayed an upward (wetting) trend, (P= 0.054). Standardized ring width followed the PDSI behavior very closely, which suggests that inter and intra-annual growth of paper birch of the Niobrara River valley is strongly dependent on a combination of temperature and water availability, in that warm and wet conditions during the growing season facilitate more growth. These results were supported by Li et al. (2016).

Both raw tree ring width and BAI showed a sharp decline overall between 1950 – 2014 (Fig. 6). This decrease can be attributed to the normal growth behavior of paper birch in general, as growth is rapid for the first 30 years or so and then sharply declines through maturity (Burns and Honkala 1990). It should also be considered that as a tree ages, cambial tissue must be distributed over a greater surface area which results in smaller and smaller rings produced as a tree ages. Standardized tree ring width removes these age and competition related trends leaving only a scaled growth measurement in response to climate and environmental factors. Standardized ring width of *B. papyrifera* in this study overall showed neither an increase nor a decrease, suggesting the population might remain reasonably stable given current conditions even though no seed-based propagation was observed in the areas of this study. Current conditions are expected to change, however, as drought conditions are expected to increase in frequency and duration for the future of the Great Plains (Woodhouse and Overpeck 1998) which may very well cause a temperature-influenced decrease in growth.

Growth did however show a strong response to drought conditions as indicated by the selected standardized model wherein current year PDSI has the strongest estimate of the four included variables and significant Pearson's R^2 values for every month of both

current and previous year PDSI suggesting that *B. papyrifera* of the Niobrara River Valley is highly responsive to a combination of temperature and water availability. This can be seen notably by the rapid reductions in standardized ring width during years of low (dry) PDSI in the late 1980s to early 1990s and the early 2000's versus an increase in standardized growth during years of high (wet) PDSI in the early 1980s, mid 1990s, and late 2000's which agrees with other publications (Li et al. 2016, Karlsson et al. 2004). (Table 1, Fig. 3, 6, and 8, Appendix B).

Climate correlations showed streamflow from April through November of both previous and current year to be in significant positive relation with growth (Fig. 7), agreeing with inclusion of August streamflow of both current and previous year, but disagreeing with the negative influence of July streamflow to raw growth and BAI as displayed by the selected models (Table 1). This influence of streamflow on growth might be explained by some of the unique geology of the Niobrara River Valley in that the river water, which flows directly over bedrock, is fed by lateral (easterly) movement of groundwater (Szilagyi et al. 2002). We observed *B. papyrifera* only growing in close proximity to the water's edge in small pockets (Appendix K). Combining the shallow fibrous root system of paper birch, and the influence of drought-related conditions on growth, one can observe that close proximity to the water table is necessary for this species' access to water be it by precipitation or streamflow. The future of Niobrara River Valley *B. papyrifera* will be dependent on climate and water availability at key points of the growing season. Invasive woody species such as *J. virginiana,* are invading the upland sites. These species have been shown to impact soil water availability and groundwater recharge, therefore increasing competition for the limited available water, which might

exacerbate the impact of climate on *B. papyrifera* and should therefore be monitored by forest managers.

4.2 Satellite Imagery

In this study, NDVI derived from satellite imagery via both Landsat 5 TM and MODIS satellites showed potential toward being used as a proxy for ex-situ growth monitoring *B. papyrifera* growth through high Pearson's R^2 values between ring growth and NDVI at the pixel level. The correlation rasters were made semi-transparent and overlain on a TIN representation of topography which allowed us to observe any relationship between topography and/or vegetation composition as characteristics for identifying other sites of comparative use. Based on R^2 values and vegetation communities within the 8 sampled plots on NVP property, there was no obvious link between vegetation type and NDVI correlation to ring growth, as plots which contained significant differences of population composition typically showed a lower mean R^2 value (Fig. 9, Appendix G). Percentage of bare ground did not appear to have a significant relationship to the plot-level correlations either (Appendix H). Rather what we do see is the noticeable difference in topography; plots 2, 6, 5, and 3 are all located on rougher areas of land with a greater variation in topographical relief and comprise the top half of mean R^2 of standardized ring width to pixel-level max-value Landsat NDVI while plots 4, 7, 1, and 8 are located on flatter ground and comprise the bottom half of R^2 of standardized ring width to pixel-level max-value Landsat NDVI. (Fig. 14, Appendices L and M). This observed topographical influence appeared to be unrelated to aspect or direction, rather better characterized by the land contour of the general area in question.

MODIS sum-value NDVI showed the strongest relationships during July to both raw and standardized growth, and June-August to standardized growth. Concerning these three time-period correlations, none of the stronger correlated plots contained any significant differences in their vegetation communities (Fig. 12) However, there was a consistency of the higher mean-correlated vegetation sampling plots and rough topography, which mostly agrees with the Landsat 5 TM max-value NDVI results at the plot level (Fig. 10, 11, 14; Appendices N and O) .

Other studies have linked satellite NDVI to climate variables such as temperature, precipitation, and drought conditions (Baird et al. 2012; Gensuo and Epstein 2003); and tree ring width to NDVI (Coops et al. 1999; Forbes et al. 2010; Vincente-Serrano 2016). As we have already established tree ring growth to having a strong relationship to climate conditions, it becomes apparent that observing NDVI of bison and cattle pasture land with relatively high variability in topographical relief can provide a reasonably reliable representation of *B. papyrifera* performance.

5. CONCLUSION

The dendrochronological technique of statistical modeling using tree rings as a response to climatic variables (Iverson 2008) was applied to determine the most significant climatic drivers of *B. papyrifera* growth of the Niobrara River Valley. Cumulative precipitation, average temperature, and average streamflow, by month, and annual PDSI, from both current and previous year were considered as predictors for growth. Growth response was considered from three perspectives of: raw tree ring width, basal area increment increase (BAI), and standardized tree ring width. Models were created from an

all-encompassing pool of every variable in consideration and systematically removed using backwards selection until a small representative model was determined. The results of these models highlighted the effects of mid-season water availability for both previous and current year, early season temperature of the current year, and late-season temperature of both the previous year and current year. Further, these climatic variables were considered individually through Pearson's R^2 correlation to the three perspectives of growth measurements. Both analyses produced similar results with minor disagreements which overall illustrated that *B. papyrifera* of the Niobrara River Valley does not perform well under drought conditions, which are expected to increase in frequency and duration for the future of the Great Plains (Woodhouse and Overpeck 1998). Warming conditions are as well expected in the northern Boreal forest (Soja et al 2007) which have been shown to impact a stronger demand on riparian water systems leading to decreased biomass of riparian species and greater overall species richness; boreal riparian communities are predicted to be replaced with more water-competitive terrestrial communities (Strom et al 2011).

Water levels in the Ogallala aquifer have dropped or reduced aquifer storage by about 9% since 1950 (Karl et al. 2009). *B papyrifera* is strongly dependent on groundwater that directly feed the into the stream, especially during periods of increased temperature, which is projected to continue rising with a 95% likelihood within the next two decades by approximately 0.3 to 2.2ºC (Karl et al. 2009). Management of the demand placed on groundwater supply could be a viable method to sustaining the local population. This could be accomplished in part through reducing anthropogenic demand via alternative land use practices. Additionally, controlling and managing invasive species in the area

could help to sustain groundwater levels through reduced evapotranspirational demands on the regional water system as a whole (Mykleby et al. 2016).

Pixel-based NDVI derived from Landsat 5 TM and MODIS satellites in bison pastureland owned by The Nature Conservancy adjacent to the *B. papyrifera* sample sites showed strong correlation to annual raw tree ring width and standardized ring width of *B. papyrifera* in areas of rough topography and moderate grazing intensity. Vegetation composition at sampled sites did not appear to have a strong influence on this NDVI signal's correlation to *B. papyrifera* growth. Overall, this shows that pixel-based NDVI from satellite imagery of bison and cattle pasture land with relatively high variability in topographical relief could serve as a proxy by which one may monitor a sparsely populated and/or remote species growth behavior ex-situ. The methods can be applied to any tree ring data set during which suitable NDVI imagery is available.

This research could very well continue by identifying high correlation value pixel locations outside of the 2016 vegetation plots, and both within and outside of the preserve boundary, to further refine our understanding of vegetation, topography, and land-use qualities to relationships of satellite imagery pixel-based vegetation index and tree ring growth. These locations can then be observed from remote locations to derive an estimation of how a sparse or difficult to reach vegetation population, such as *B. papyrifera*, is performing in near-real time.

These results from both dendrochronological analysis and satellite NDVI correlation could be verified by comparison to imagery and ring width records from the more northern *B. papyrifera* population. Additionally, the methods could be repeated with

another vegetation index, such as EVI, to further understanding of the relationship between pixel-based vegetation indices and tree ring growth.

REFERENCES

Amoroso M, Daniels LD, Villalba R, Cherubini P (2015) Does Drought Incite Tree Decline and Death in Austrocedrus Chilensis Forests? Journal of Vegetation Science, 26:1171-1183.

Awada T, El-Hage R, Geha M, Wedin DA, Huddle JA, Zhou X, Msanne J, Sudmeyer RA, Martin DL, Brandle JR (2013) Intra-annual variability and environmental controls over transpiration in a 58-year-old even-aged stand of invasive woody *Juniperus virginiana* L. in the Nebraska Sandhills, USA. Ecohydrology, 6:731-740.

Baird RA, Verbyla D, Hollingsworth TN (2012) Browning of the Landscape of Interior Alaska Based on 1986-2009 Landsat Sensor NDVI. Canadian Journal of Forest Research, 42:1371-1382. doi:10.1139/X2012-088.

Bates D, Maechler M, Bolker B, Walker S (2015) Fitting Linear Mixed-Effects Models Using lme4. Journal of Statistical Software, 67:1-48. doi:10.18637/jss.v067.i01.

Bradley E (1956) Geology and GroundWater Resources of the Upper Niobrara River Basin, Nebraska and Wyoming. US Geological Survey Water-Supply Paper 1368.

Burnham KP, Anderson DR (2002) Model Selection and Multimodel Inference: A Practical Information-Theoretical Approach 2nd ed. New York: Springer-Verlag.

Burns RM, Honkala BH (1990) Silvics of North America. US Department of Agriculture – Forest Service.

Cady RC, Scherer OJ (1946) Geology and ground-water resources of Box Butte County, Nebraska. U. S. Geological Survey Water-Supply Paper 969.

Campelo F, Nabais C, Garcia-Gonzalez I, Cherubini P, Gutierrez, Freitas H (2009) Dendrochronology of Quercus Ilex L. And Its Potential Use for Climate Reconstruction in the Mediterranean Region. Canadian Journal of Forest Research. 39:2486-2493. doi:10.1139/X09-163.

Campelo F (2012) DetrendeR: Start the detrendeR Graphical User Interface (GUI). R package version 1.0.4. https://CRAN.R-project.org/package=detrendeR.

Canada Parks and Wilderness Society (2017) Boreal Forest. *http://cpaws.org/campaigns/boreal-forest,* Web. Accessed 25 September 2017.

Cherubini P, Simcha LY (2014) The Olive Tree-Ring Problematic Dating. Antiquity, 88(339):290-291.

Chen L, Huang JG, Alam SA, Zhai L, Dawson A, Stadt K, Comeau PG (2017) Drought causes reduced growth of trembling aspen in western Canada. Global Change Biology, 23:2887-2902. doi: 10.1111/gcb.13595.

Coops N, Bi H, Barnett P, Ryan P (1999) Estimating Mean and Current Annual Increments of Stand Volume in a Regrowth Eucalypt Forest Using Historical Landsat Multi Spectral Scanner Imagery. Journal of Sustainable Forestry. 9(3-4):149. doi:10.1300/J091v09n03_07.

Forbes BC, Fauria MM, Zetterberg P (2010) Russian Arctic Warming and 'Greening' Are Closely Tracked by Tundra Shrub Willows. Global Change Biology, 16:1542-1554. doi:10.1111/j.1365-2486.2009.02047.x.

Gensuo JJ, Epstein HE (2003) Greening of Arctic Alaska 1981-2001. Geophysical Resource Letters, 30:20 doi:10.1029/2003GL018268.

Girardin MP, Bouriaud O, Hogg EH, Kurz W, Zimmermann NE, Metsaranta JM, Jong Rd, Frank DC, Esper J, Buntgen U, Guo XJ, Bhatti J (2016) No growth stimulation of Caada's boreal forest under half-century of combined warming and CO2 fertilization

Greenidge KNH (1953) Further studies of birch dieback in Nova Scotia. Canadian Journal of Botany, 31(5): 548– 559.

Grissino-Mayer HD (2001) Evaluating crossdating accuracy: A manual and tutorial for the computer program COFECHA. Tree-Ring Research 57(2):205-221.

Hogg EH, Michaelian M, Hook TI, Undershultz ME (2017) Recent climatic drying leads to age-independent growth reductions of white spruce stands in western Canada. Global Change Biology 23:(12) 5297-5308.

Hollesen J, Buchwal A, Rachlewicz G, Hansen BU, Hansen MO, Stecher O, Elberling B (2015) Winter Warming as an Important Co-Driver for Betula Nana Growth in Western Greenland during the past Century. Global Change Biology, 21(6):2410-2423.

Iverson LR, Prasad AM, Matthews M (2008) Modeling potential climate change impacts on the trees of the northeastern United States. Mitigation and Adaptation Strategies for Global Change, 13(5-6):487–516.

Jicheng H, Xuemei S (2005) Relationships between tree-ring width index and NDVI of grassland in Delingha. Chinese Science Bulletin. 51(9):1106-1114. doi:10.1007/s11434-006-1106-4.

Karl TM, Melillo JM, Peterson TC (2009) United States Global Change Research Program: Global climate change impacts in the United States. Cambridge University Press, New York, New York, USA.

Karlsson PS, Tenow O, Bylund H, Hoogesteger J, Weih M (2004) Determinants of Mountain Birch Growth in Situ: Effects of Temperature and Herbivory. Ecography. 27(5):659-667.

Kharuk VI, Kuzmichev VV, Sergey T Im, Ranson KJ (2014) Birch Stands Growth

Increase in Western Siberia. Scandinavian Journal of Forest Research. 29(5):421-426. doi: 10.1080/02827581.2014.912345.

Kumar L, Mutanga O (2017) Remote Sensing of Above-Ground Biomass. Remote Sensing. 9, 935; doi:10.3390/rs9090935.

Lee B, Kwon Hyojung, Miyata A, Lindner S, Tenhunen J (2017) Evaluation of a Phenology-Dependent Response Method for Estimating Leaf Area Index of Rice Across Climate Gradients. Remote Sensing. 9:1-16. ISSN: 20724292.

Li B, MMPD Heijmans, Berendse F, Blok D, Maximov T, Sass-klaassen U (2016) The Role of Summer Precipitation and Summer Temperature in Establishment and Growth of Dwarf Shrub Betula Nana in Northeast Siberian Tundra. Polar Biology. 39(7):1245-1255.

Li L, Guo Q, Tao S, Kelly M, Xu G (2015) LiDAR with multi-temporal MODIS provide a means to upscape predictions of forest biomass. ISPRS Journal of Phtogrammetry and Remote Sensing. 102: 198-208.

Maeglin RR (1979) Increment cores: How to collect, handle, and use them. General tech report, FPL 25, United States Forest Service

Mykleby PM, Lenters JD, Cutrell GJ, Herman KS, Istanbulluoglu E, Scott DT, Twine TE, Kucharik CJ, Awada T, Soylu ME, Dong B (2016) Energy and Water Balance Response of a Vegetated Wetland to Herbicide Treatment of Invasive Phragmites Australis. Journal of Hydrology, 539: 290-303. doi:10.1016/j.jhydrol.2016.05.015.

NASA (2000) Measuring Vegetation: NDVI and EVI. https://earthobservatory.nasa.gov/Features/MeasuringVegetation/measuring_vegetation_2.php. September 2017

Pomerleau, R (1991) Experiments on the causal mechanisms of dieback on deciduous forests in Québec. Québec Region Canadian Forest Service, Information Report LAU-X-96, 47

R Core Team (2015) R: A language and environment for statistical computing. R Foundation for Statistical Computing, Vienna, Austria. URL https://www.R-project.org/.

Redmond DR (1955) Studies in forest pathology: XV. Rootlets, mycorrhiza, and soil temperature in relation to birch dieback. Canadian Journal of Botany. 33(6):595–627. doi: 10.1139/b55-048

Reed BC, Loveland TR, Tieszen LL (1996) An approach for using AVHRR data to monitor U.S. Great Plains Grasslands. Geocarto International. 11(3): 13-22. doi:10.1080/10106049609354544

Rinn F (2003) TSAP-Win: Time Series Analysis and Presentation for Dendrochronology and Related Applications. Version 0.55 User reference. Heidelberg, Germany (http://www.rimatech.com).

Soja AJ, Tchebakova NM, French NH, Flannigan MD, Shugart HH, Stocks BJ, Sukhinin AI, Parfenova, EI, Stuart Chapin III F, Stackhouse Jr PW (2007) Climate-induced boreal forest change: predictions versus current observations. Glob Planet. Change. 56:274–296.

Stokes MA, Smiley TL (1968) An Introduction to Tree-ring Dating. University of Arizona Press, Tucson, AZ.

Stroh ED and Miller JP (2009) Paper birch decline in the Niobrara River Valley, Nebraska: weather, microclimate, and birch stand conditions. U.S. Geological Survey Open-file Report 2009–1221

Strom L, Jansson R, Nilsson C, Johansson ME, Xiong S (2011) Hydrologic effects on riparian vegetation in a boreal river: an experiment testig climate change predictions. Landscape Ecology Group, Department ofEcology and Environmental Science, Umed University

Szilagyi J, Harvey FE, Ayers JF (2002) Regional estimation of base recharge to ground water using water balance and a base-flow index. Ground Water 41(4):504-513.

Uchytil RJ (1991) Betula papyrifera. In: Fire Effects Information System. http://www.fs.fed.us/database/feis. U.S. Department of Agriculture, Forest Service, Rocky Mountain Research Station, Fire Sciences Laboratory. Accessed 2 April 2017

UCLA (2006) Introduction to Generalized Linear Mixed Models, UCLA: Statistical Consulting Group. http://stats.idre.ucla.edu/other/mult-pkg/introduction-to-generalized-linear-mixed-models. Accessed 15 September 2017

U.S. Department of Agriculture (1965) Silvics of forest trees of the United States: Forest Service Agricultural Handbook No. 271

Vincente-Serrano SM, Camarero JJ, Olano JM, Martin-Hernandez N, Pena-Gallardo M, Tomas-burguera M, Gazol A, Azorin-Molina C, Bhuyan U, El Kenawy A (2016) Diverse Relationships between Forest Growth and the Normalized Difference Vegetation Index at a Global Scale. Remote Sensing of Environment. 187(15):14-29. doi: 10.1016/j.rse.2016.10.001

Wang AF, Roitto M, Sutinen S, Lehto T, Heinonen J, Zhang G, Repo T (2016) Waterlogging in Late Dormancy and the Early Growth Phase Affected Root and Leaf Morphology in Betula Pendula and Betula Pubescens Seedlings. Tree Physiology, 36:86-98. doi:10.1093/treephys/tpv089

Woodhouse C, Overpeck J (1998) 2000 years of drought variability in the central United States. Bulletin of the American Meteorological Society. 79(12):2693-2714.

Wright HE (1970) Vegetational history of the central plains. In: Dort W, Jones JK (eds) Pleistocene and recent environments of the central Great Plains: Lawrence, University of Kansas Press, p. 157–172.

Yang B, He M, Shishov V, Tychkov I, Vaganov E, Rossi S, Ljungqvist FC, Brauning A, Grießinger J (2017) New Perspective on Spring Vegetation Phenology and Global Climate Change Based on Tibetan Plateau Tree-Ring Data. Proceedings of the

National Academy of Sciences of the United States of America, 114(27):6966-6971

TABLES

Table 1. Results from generalized linear mixed models (GLMM), predictor variables including monthly precipitation, streamflow, mean temperature, and annual Palmer's Drought Severity Index (PDSI) with year, stand, and sample (tree ID) were considered as random effects. Monthly inclusion began in July of the previous year through October of the current year. Final GLM models were selected via backwards selection, their variables and their influence (positive or negative), estimate, standard error, and T value for tree ring width, BAI, and standardized ring width.

			Raw				BAI				Std	
Variable	**+/-**	estimate	std.error	T value	**+/-**	estimate	std.error	T value	**+/-**	estimate	std.error	T value
Previous year												
July precipitation					+	0.0077	0.00336	2.292				
July streamflow	-	-0.01634	0.005468	-2.988	-	-0.14818	0.068989	-2.148				
August streamflow	+	0.026224	0.006558	3.999	+	0.255626	0.088493	2.889				
November precipitation									-	-6.83E-04	2.47E-04	-2.769
November mean temperature	-	-0.01111	0.00475	-2.34								
PDSI	+	0.01668	0.006549	2.547								
Current year												
January mean temperature	-	-0.01519	0.003284	-4.625								
March precipitation	+	0.001339	0.000514	2.602								
May precipitation									-	-2.52E-04	9.18E-05	-2.747
May streamflow	-	-0.0093	0.00275	-3.381								
June precipitation					-	-0.00776	0.003397	-2.285				
June mean temperature	+	0.013132	0.006497	2.021								
August streamflow	+	0.024494	0.005016	4.884	+	0.162025	0.063533	2.55				
August mean temperature	+	0.034575	0.008929	3.872					+	6.03E-03	2.74E-03	2.201
September mean temperature	-	-0.01989	0.006412	-3.101								
PDSI	-	-0.01917	0.006843	-2.801					+	8.52E-03	1.64E-03	5.2

FIGURES

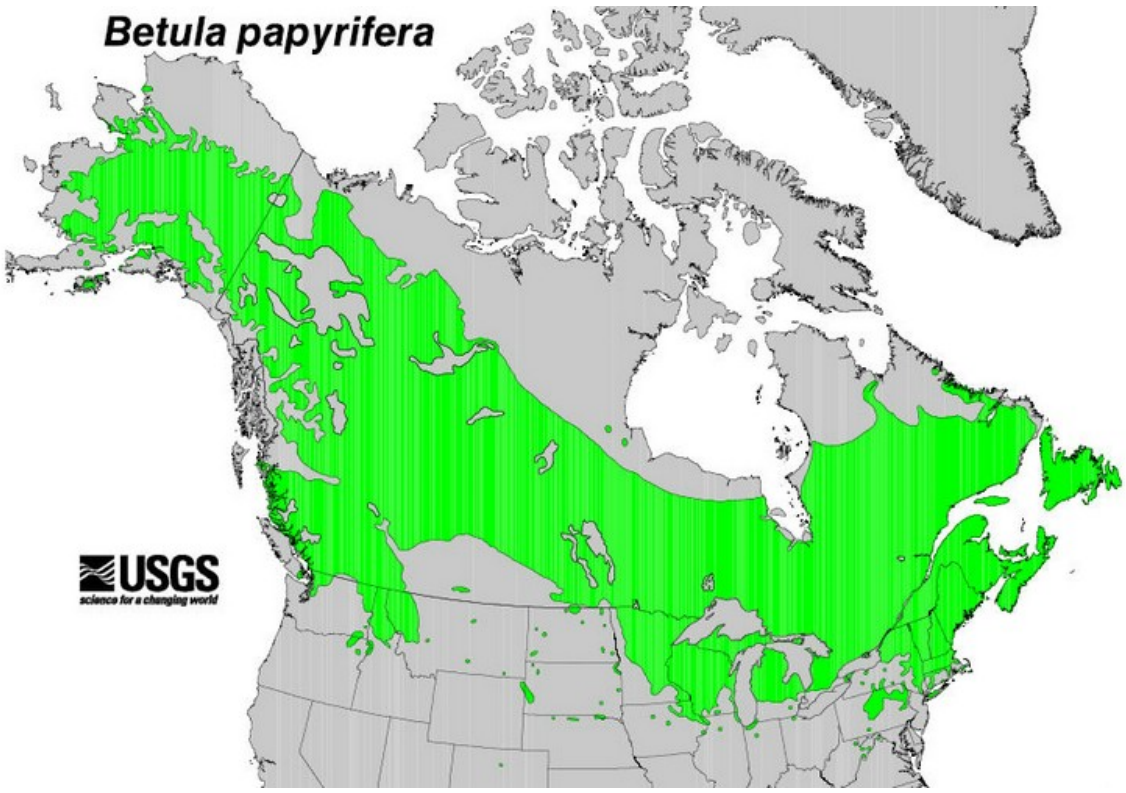

Figure 1. North America distribution of Paper birch (green). Source: USGS (http://nativeplantspnw.com/wp-content/uploads/2014/06/Distribution-of-Betula-papyrifera.png)

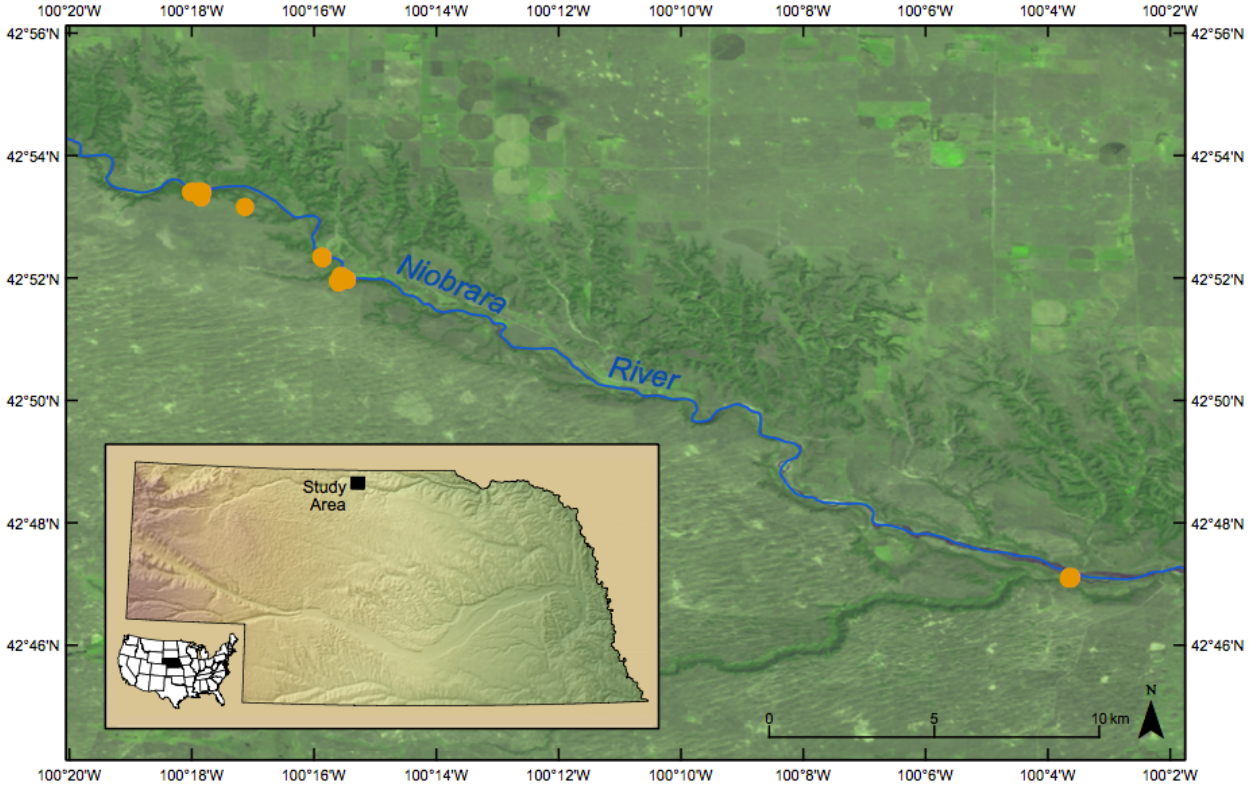

Figure 2. Location of the study area in north-central Nebraska, USA. Locations of the examined *B. papyrifera* sites are marked with orange.

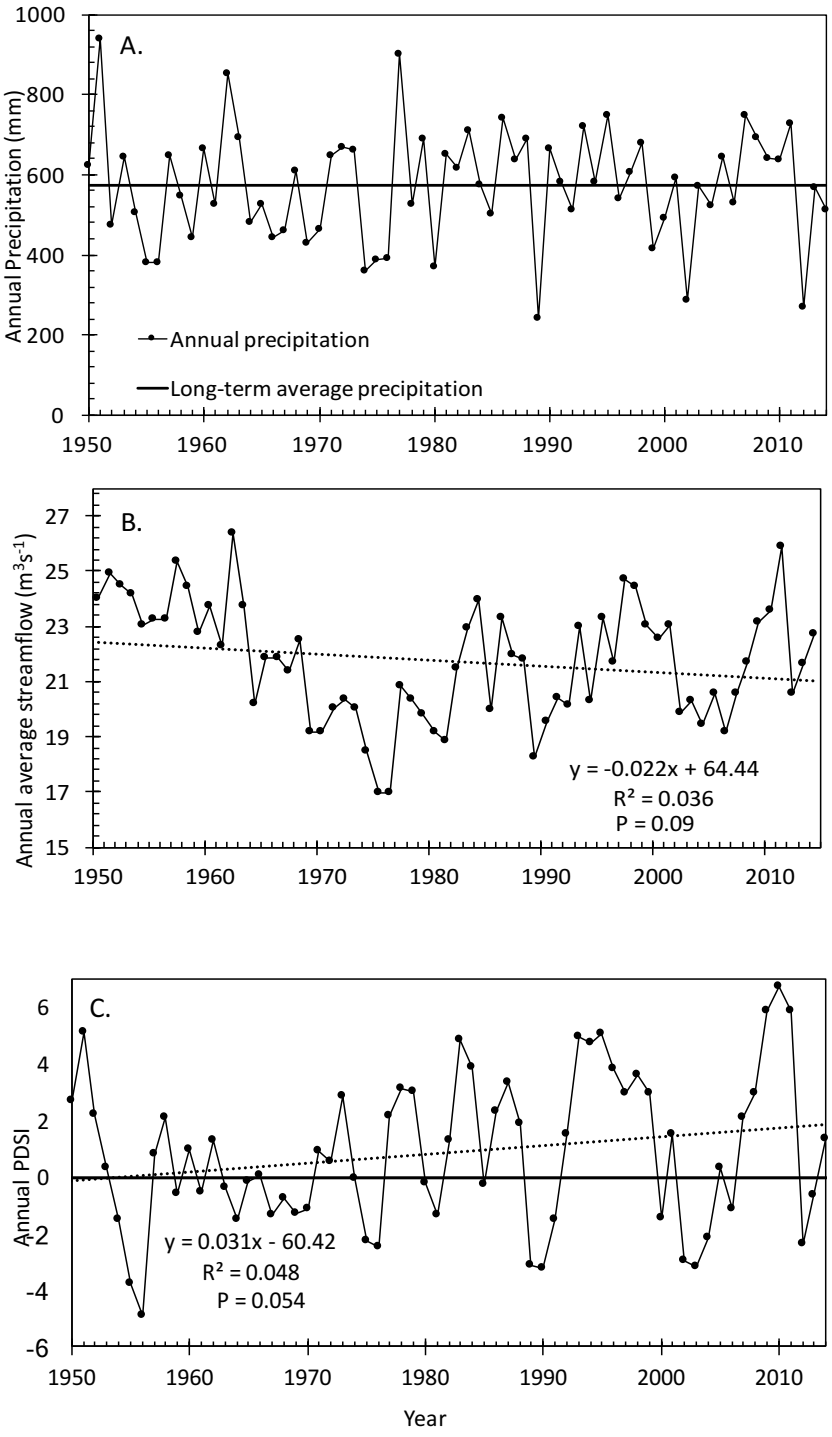

Figure 3. (A) Annual precipitation (mm) recorded by the Ainsworth, NE weather station between 1950 and 2014. (B) Annual average streamflow of the Niobrara River (m^3s^{-1}) recorded by the USGS near Sparks, NE between 1950 and 2014. (C) Annual Palmer's Drought Severity Index for the region of North-Central Nebraska, obtained from NOAA for the period of 1950 to 2014.

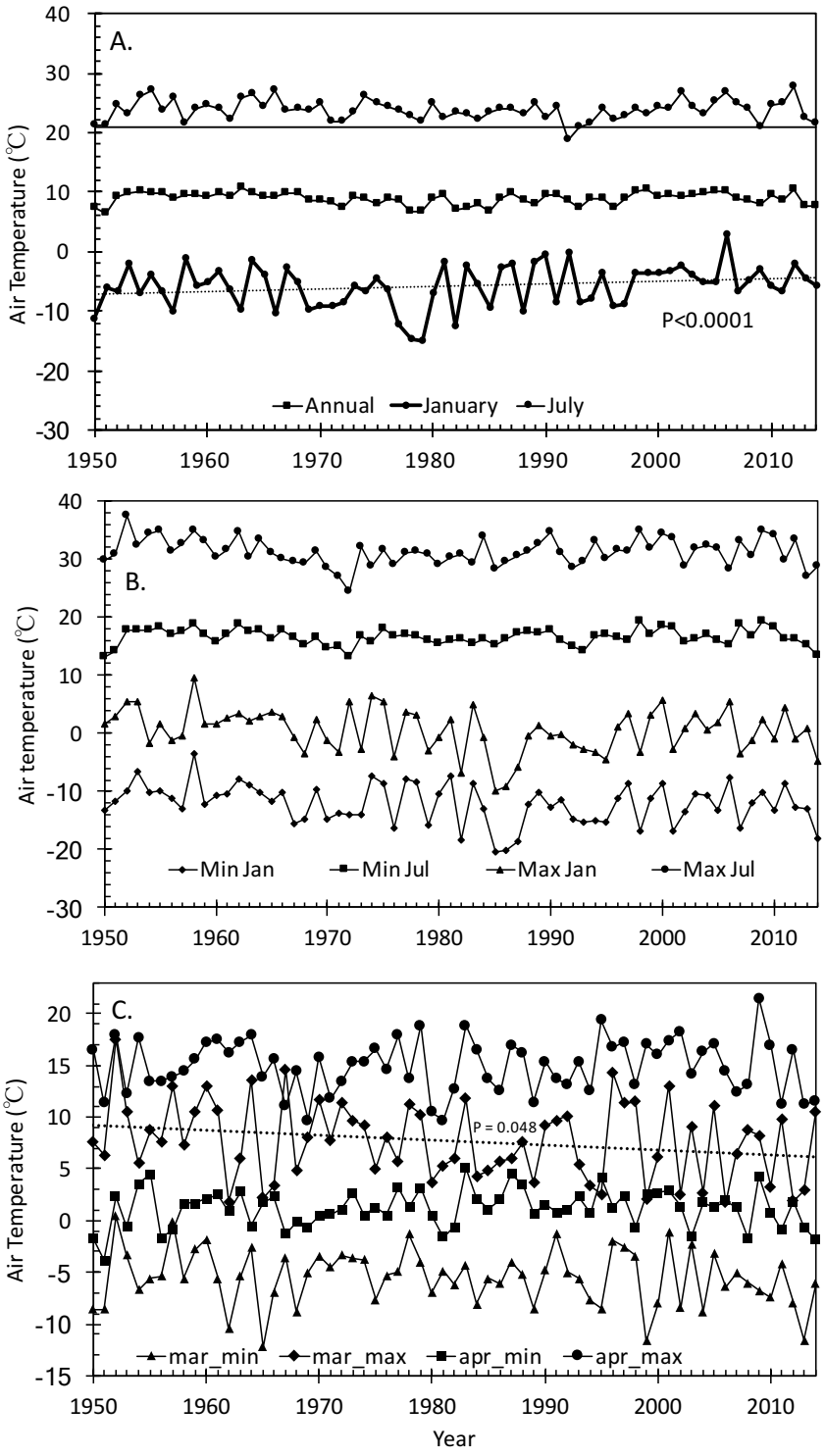

Figure 4. (A) Annual average, January average, and July average air temperature °C recorded by the Springview, NE weather station between 1950 and 2014. January temperature was observed to be increasing significantly increasing (P<0.0001). (B) Annual January minimum and maximum, July minimum and maximum air temperature °C recorded by the Springfield, NE weather station between 1950 and 2014.

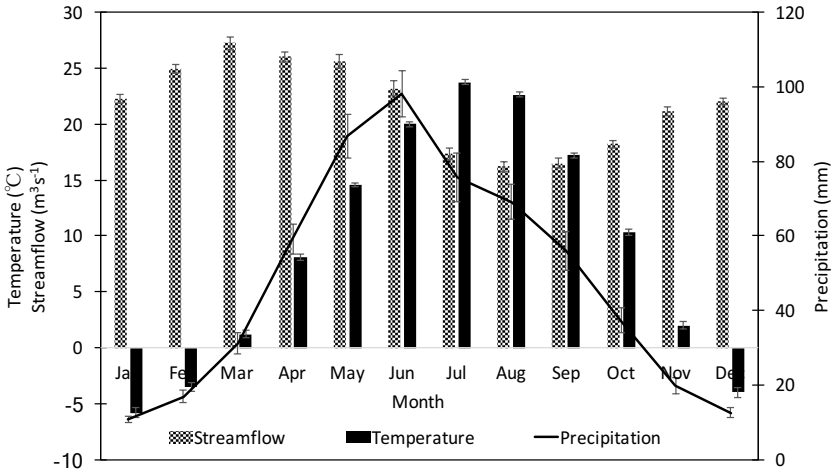

Figure 5. Average monthly streamflow of the Niobrara River (m^3s^{-1}) recorded by the USGS near Sparks, NE between 1950 and 2014, average monthly air temperature °C recorded by the Springview, NE weather station between 1950 and 2014, and average monthly precipitation (mm) recorded by the Ainsworth, NE weather station between 1950 and 2014

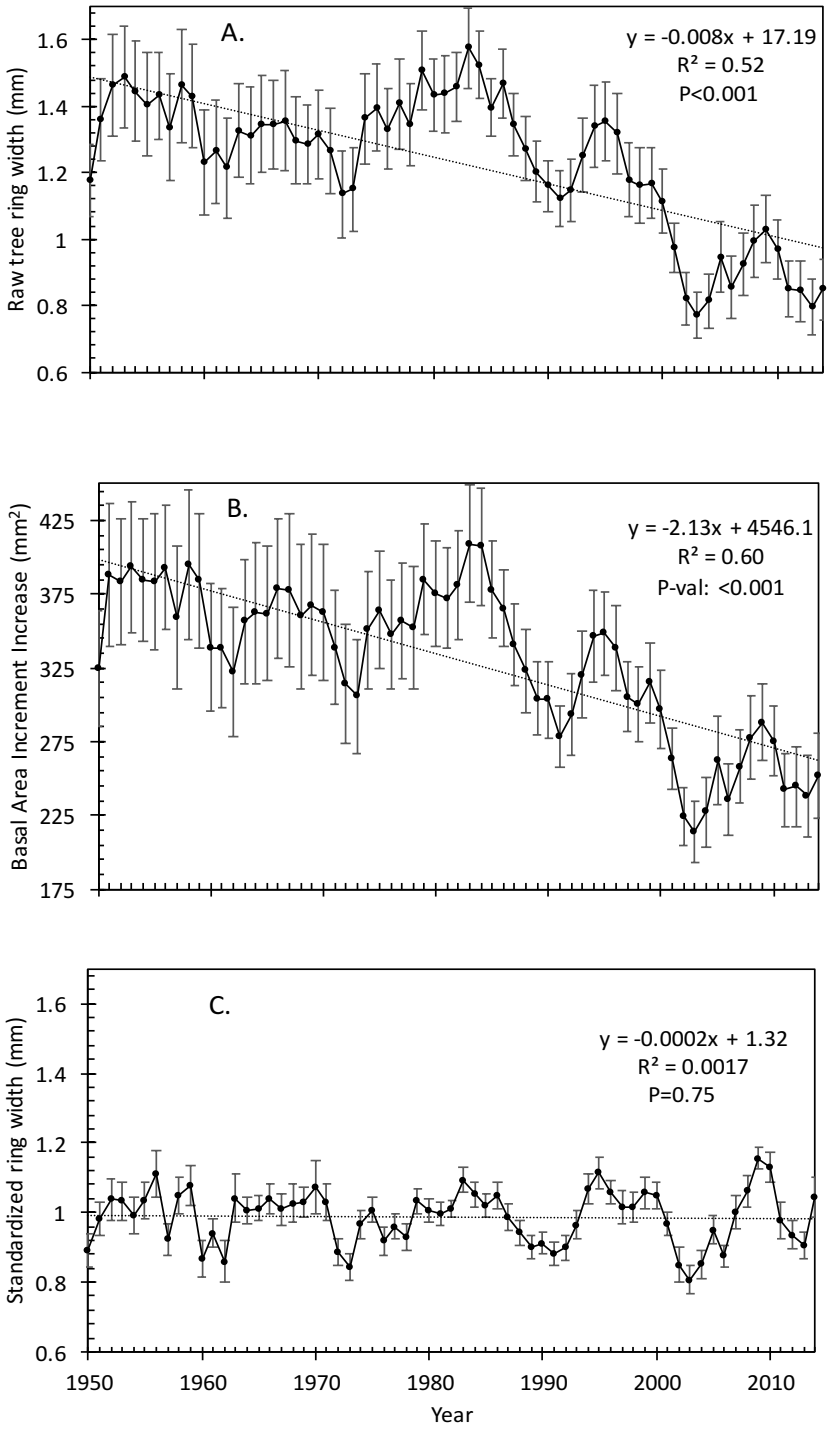

Figure 6. Average annual (A) Tree ring width (mm), (B) Basal area increment increase (mm^2), and (C) Standardized ring width (mm) of sampled *B. papyrifera* of the Niobrara River Valley between 1950 and 2014.

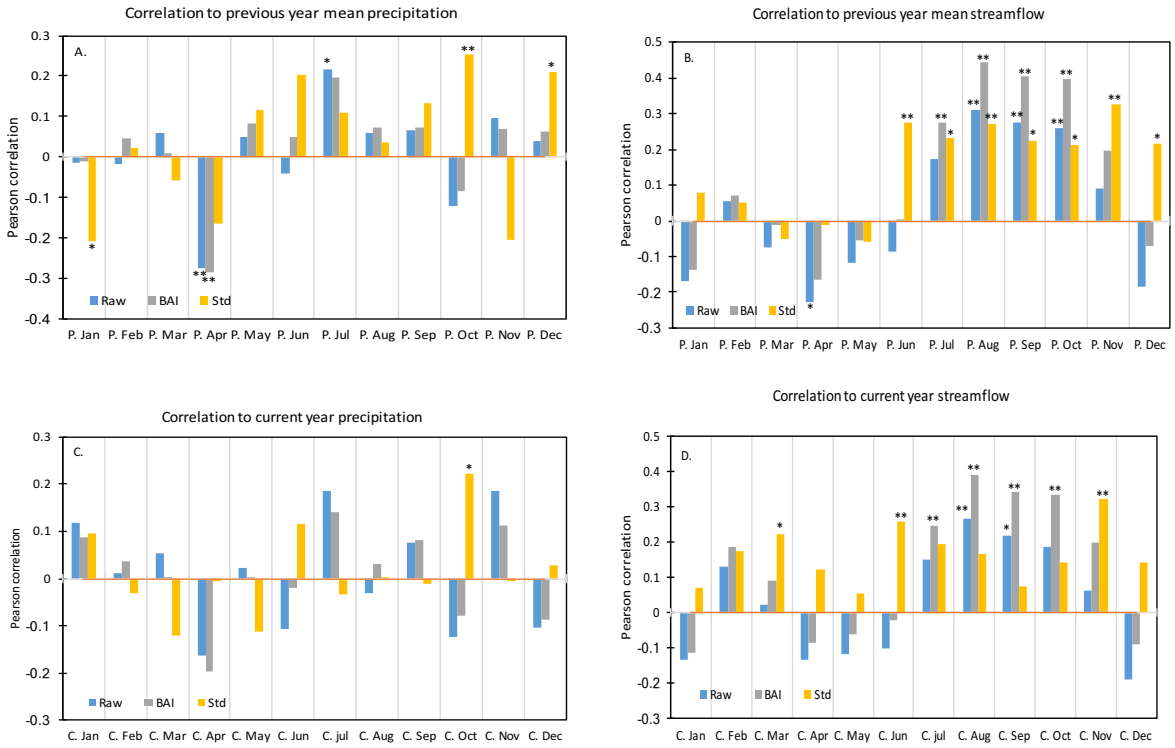

Figure 7. Pearson R^2 correlation between Tree ring width (Raw), Basal area increment increase (BAI) and standardized tree ring growth (Std) of *B. papyrifera* of the Niobrara River Valley, Nebraska between 1950 and 2014 and A) previous year precipitation (mm) (recorded by the Aisnworth, NE weather station), B) previous year streamflow (recorded by the USGS, measured near Sparks, NE), C) current year precipitation, and D) current year streamflow. * = significance at P = 0.1, ** = significance at the P = 0.05 level.

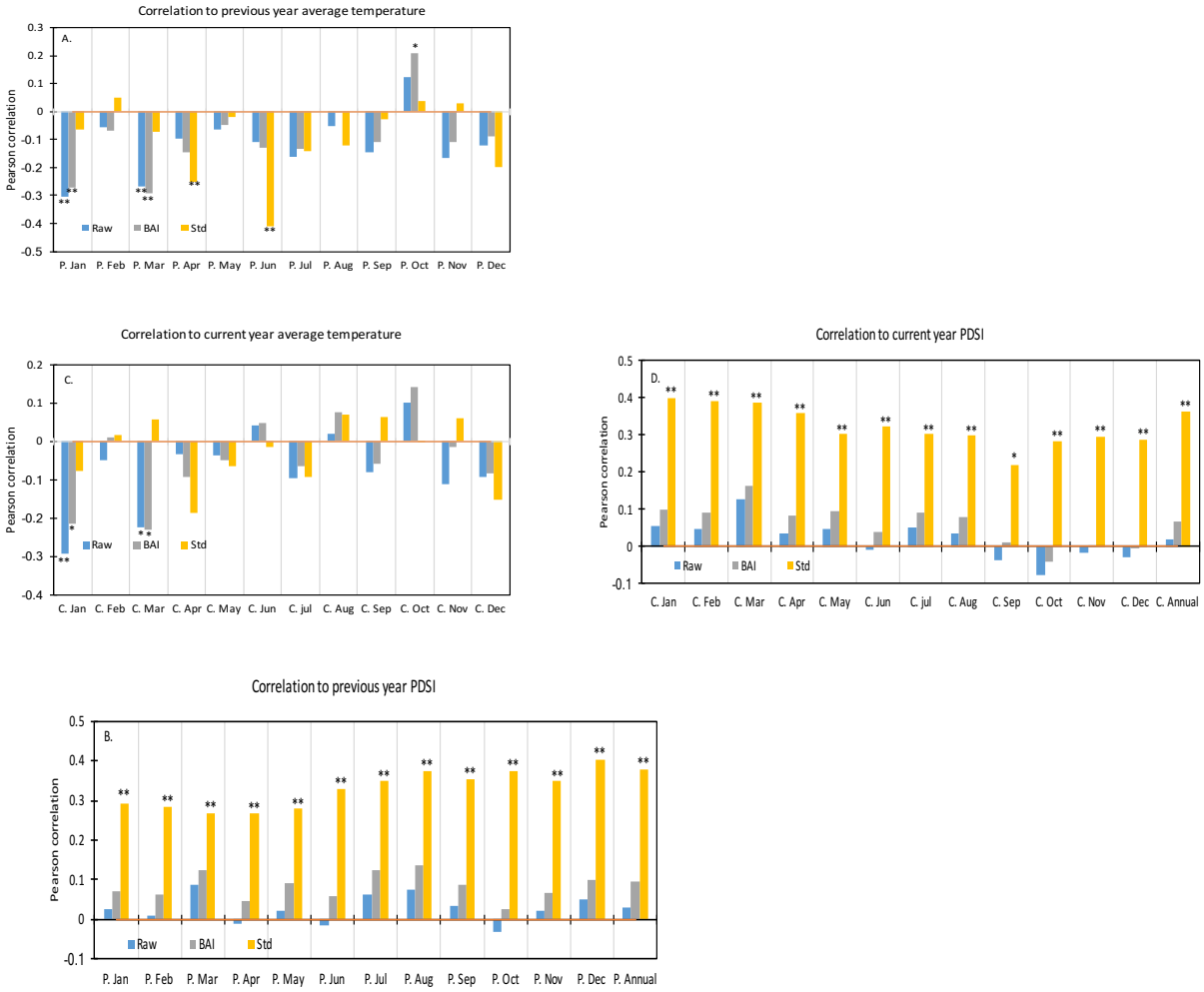

Figure 8. Pearson R^2 correlation between Tree ring width (Raw), Basal area increment increase (BAI) and standardized tree ring growth (Std) of *B. papyrifera* of the Niobrara River Valley, Nebraska between 1950 and 2014 and A) previous year average temperature (recorded by the Springview, NE weather station), B) previous year PDSI (of the North-central Nebraska region, obtained from NOAA), C) current year average temperature, and D) current year PDSI. * = significance at P = 0.1, ** = significance at the P = 0.05 level.

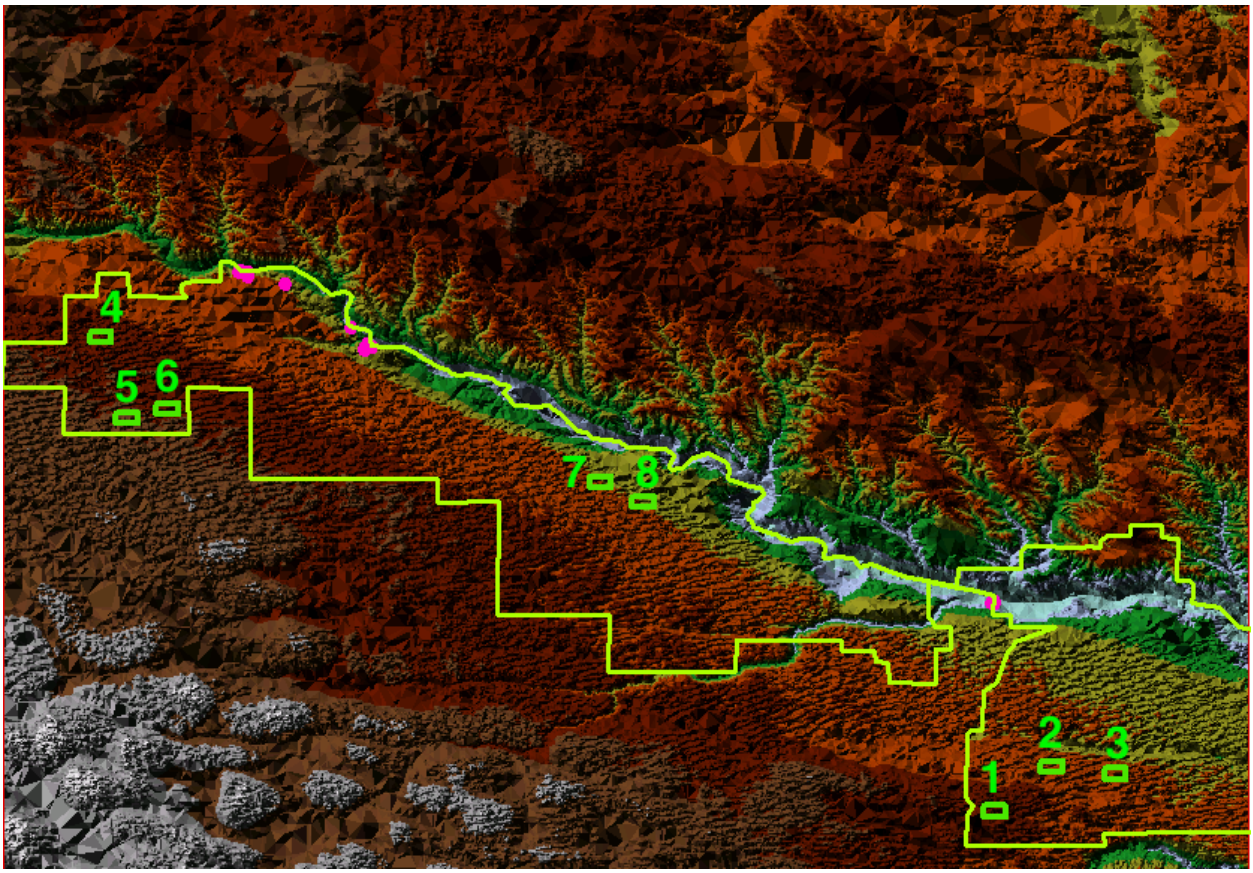

Figure 9. Perimeter of the Niobrara Valley Preserve as owned by The Nature Conservancy. 2016 vegetation composition plot locations, and tree sampling site locations with a Triangulated Irregular Network created from a USGS 30m DEM. This is used as a reference of topography for satellite image correlation rasters.

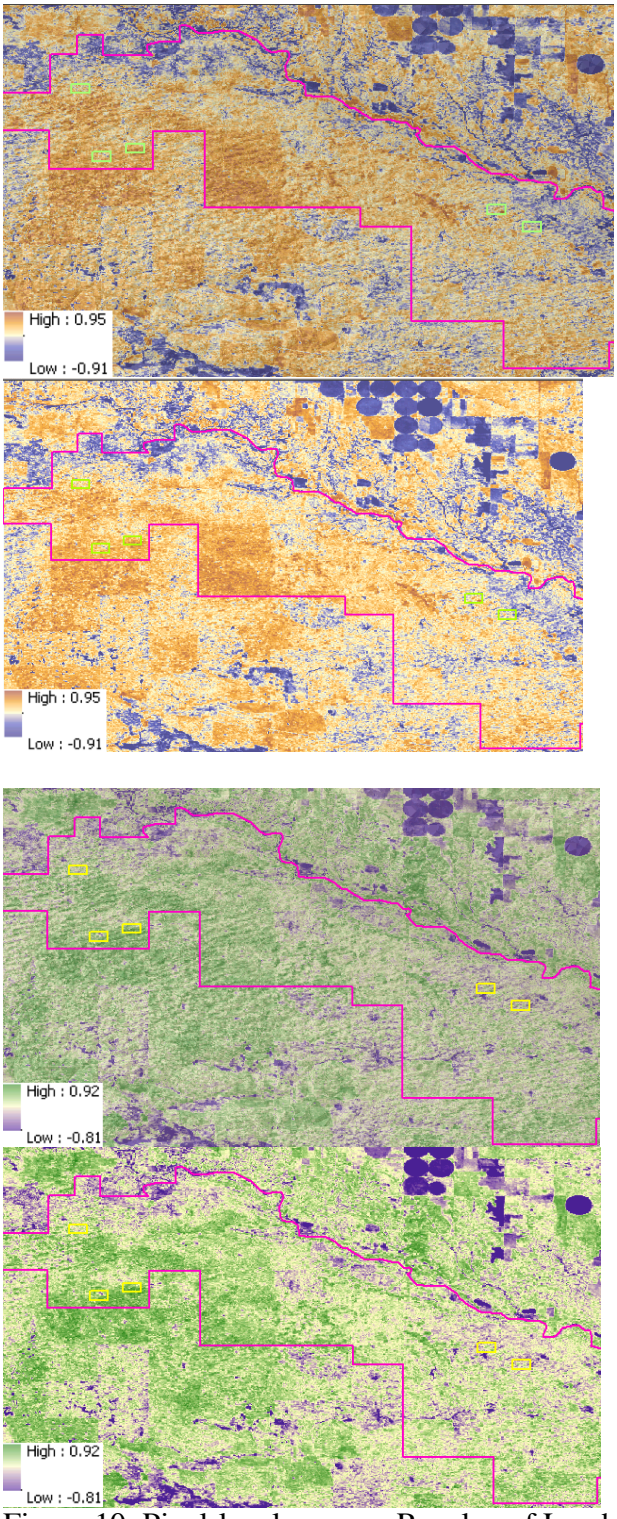

Figure 10. Pixel-level pearson R^2 value of Landsat 5 max-value NDVI to (top) Tree ring width and (bottom) standardized ring width of *B. papyrifera* of the Niobrara River Valley between 1985 and 2011, colored based on correlation value and magnitude. The left images are superimposed on a triangulated irregular network created from a USGS 30-meter DEM to observe a possible relationship between topography and vegetation composition with ring growth of *B. papyrifera* and potential area(s) for proxy monitoring

in real-time the growth of *B. papyrifera* at nearby sites along the river. The right images are the correlation rasters without the TIN to visually illustrate absence of influence from slope and aspect of the topographically varied pasture land

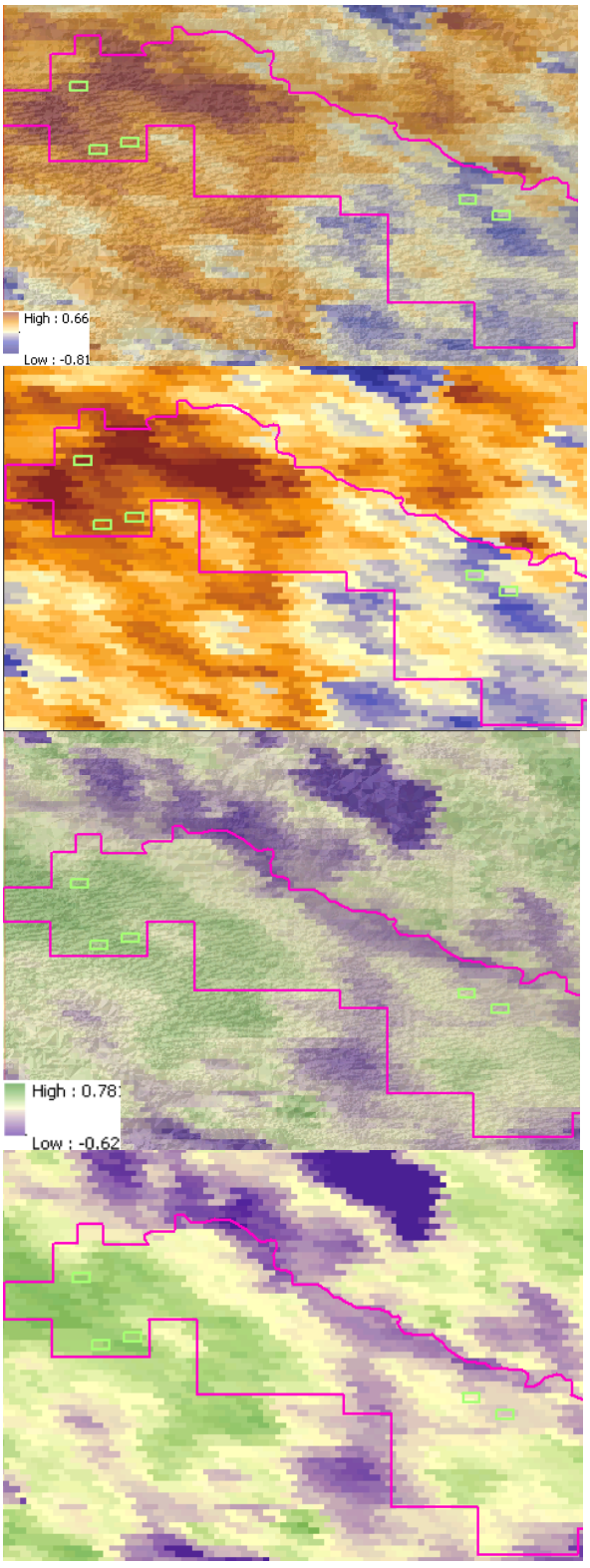
High : 0.66
Low : -0.81
High : 0.78
Low : -0.62

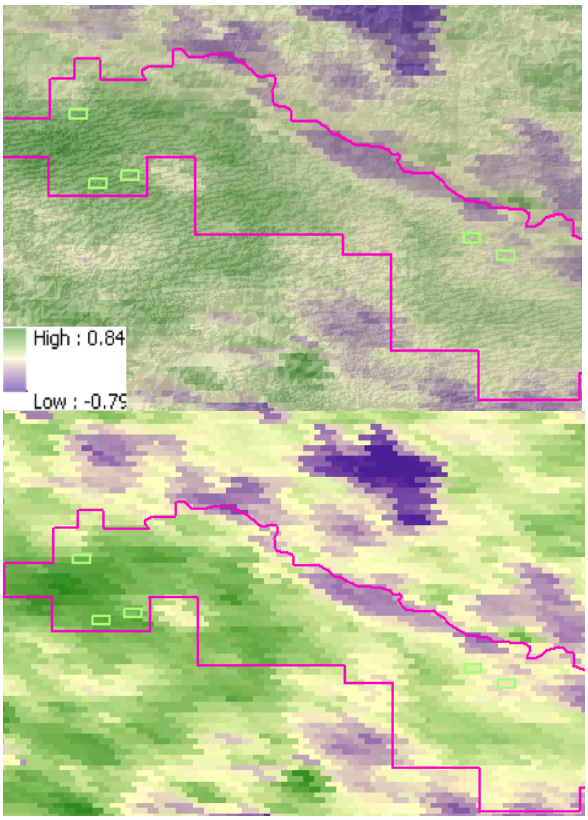

Figure 11. Pixel-level pearson R^2 value of MODIS sum-NDVI during July and tree ring width of *B. papyrifera* of the Niobrara River Valley (top), MODIS sum-NDVI during June – August to standardized ring width (middle), and MODIS sum-NDVI during July to standardized ring width (bottom), between 2000 and 2014, and colored based on correlation value and magnitude. The images are superimposed on a triangulated irregular network created from a USGS 30-meter DEM to observe a possible relationship between topography and vegetation composition with ring growth of *B. papyrifera* and potential area(s) for proxy monitoring in real-time the growth of *B. papyrifera* at nearby sites along the river (left).

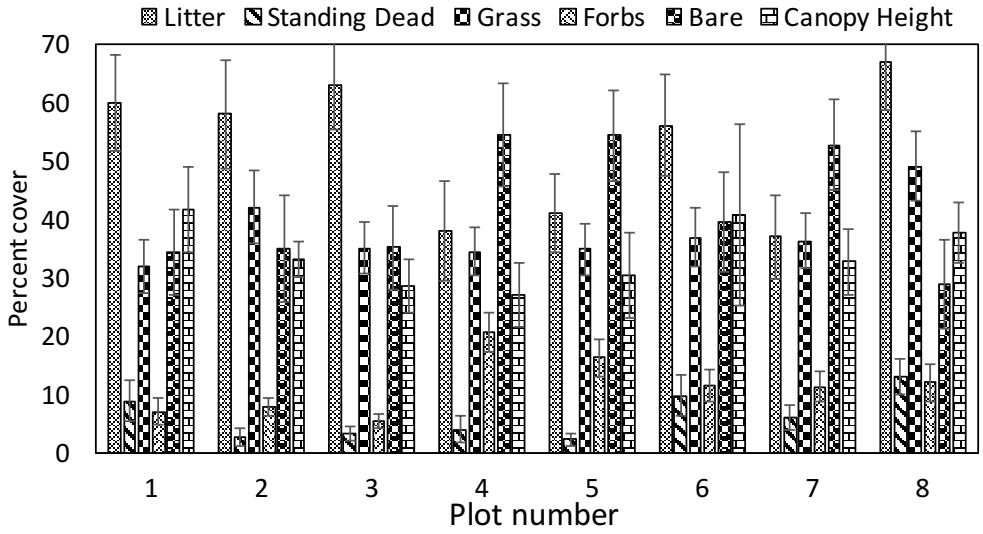

Figure 12. Vegetation was sampled from 8 plots located across a series of management treatments being compared on the Niobrara Valley Preserve owned by The Nature Conservancy on June 27, 2016. Each plot consists of an 8 x 6 grid (8 east – west, 6 north – south) of GPS points encompassed in a 640m x 480m area. This barplot shows canopy height (cm) and percent cover of litter, standing dead vegetation, grass, forbs, and bare soil.

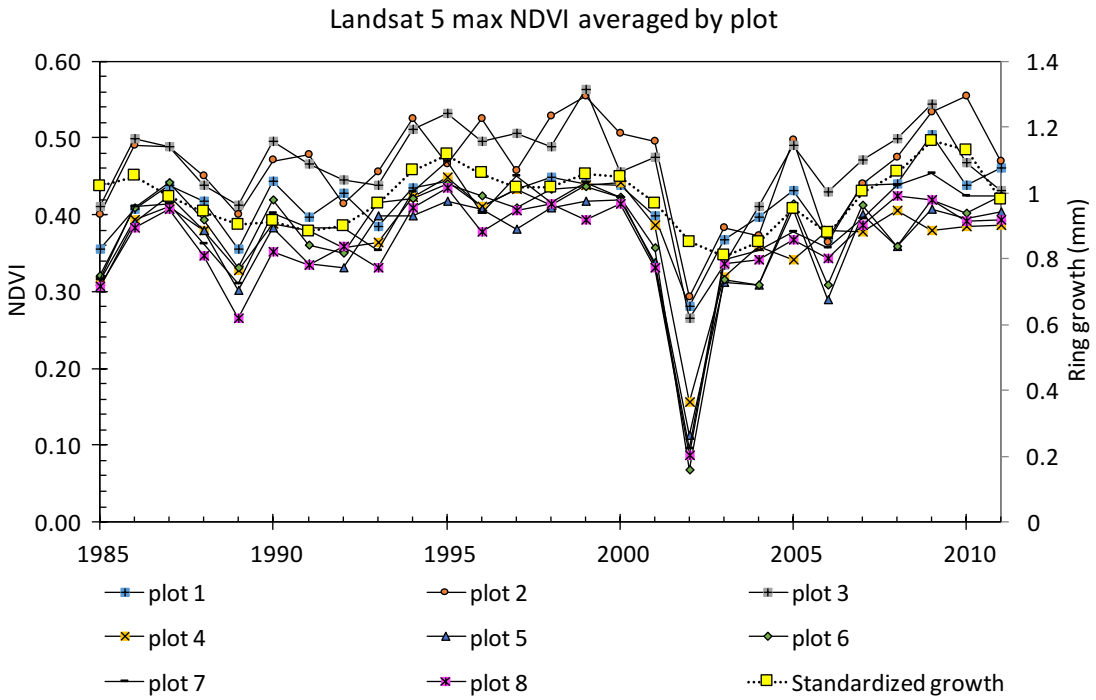

Figure 13. Average standardized growth of *B. papyifera* and max-value Landsat-5 NDVI between 1985 and 2011 within the 8 640m x 480m vegetation composition plots sampled in June, 2016 by the Nature Conservancy at the Niobrara Valley Preserve in Nebraska.

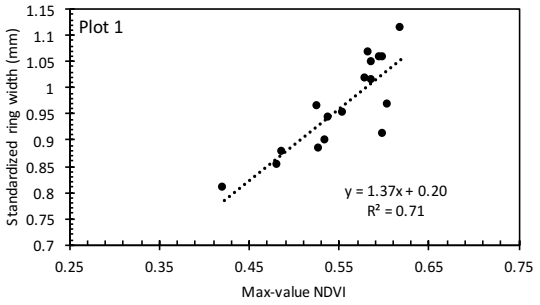
Plot 1
Standardized ring width (mm)
Max-value NDVI
y = 1.37x + 0.20
R² = 0.71

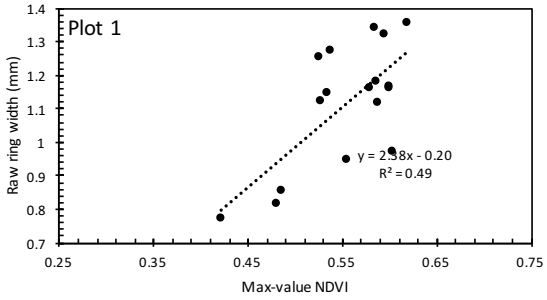
Plot 1
Raw ring width (mm)
Max-value NDVI
y = 2.38x - 0.20
R² = 0.49

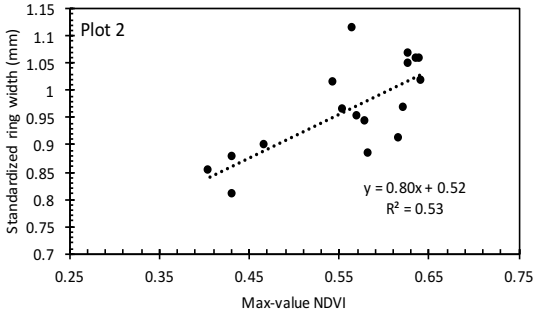
Plot 2
Standardized ring width (mm)
Max-value NDVI
y = 0.80x + 0.52
R² = 0.53

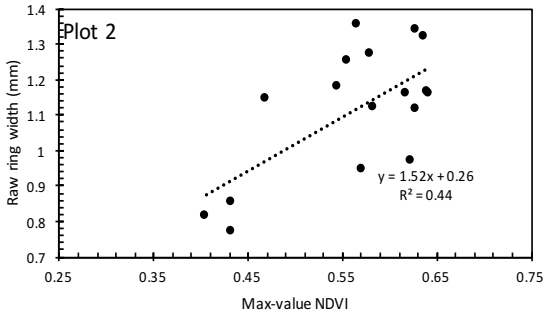
Plot 2
Raw ring width (mm)
Max-value NDVI
y = 1.52x + 0.26
R² = 0.44

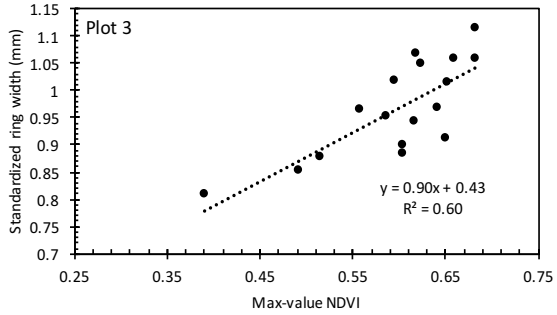
Plot 3
Standardized ring width (mm)
Max-value NDVI
y = 0.90x + 0.43
R² = 0.60

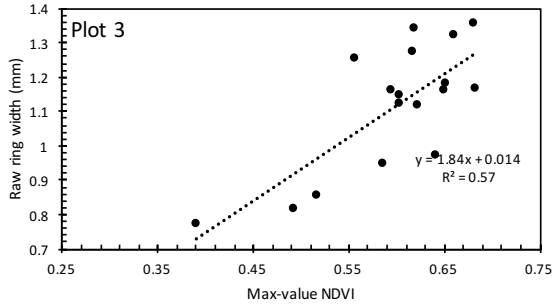
Plot 3
Raw ring width (mm)
Max-value NDVI
y = 1.84x + 0.014
R² = 0.57

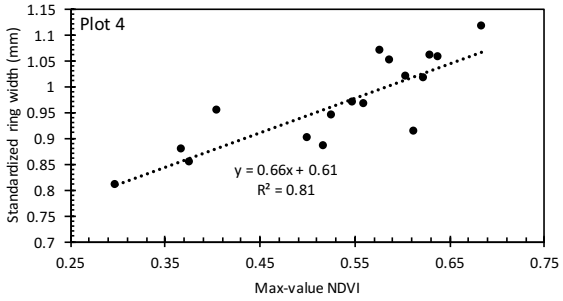
Plot 4
Standardized ring width (mm)
Max-value NDVI
y = 0.66x + 0.61
R² = 0.81

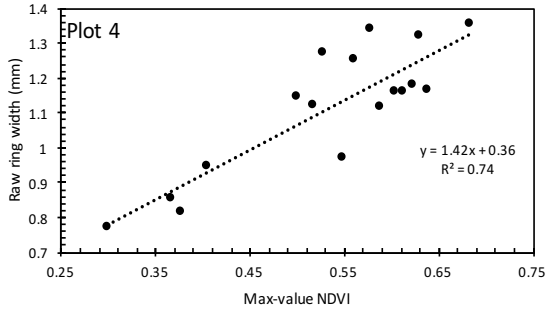
Plot 4
Raw ring width (mm)
Max-value NDVI
y = 1.42x + 0.36
R² = 0.74

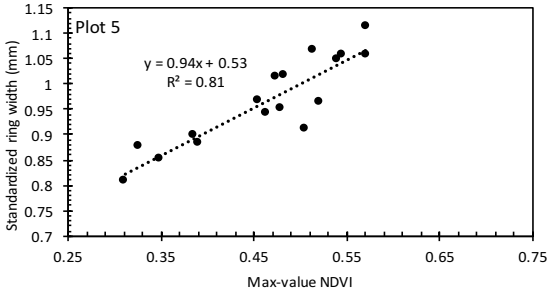
Plot 5
y = 0.94x + 0.53
R² = 0.81
Standardized ring width (mm)
Max-value NDVI

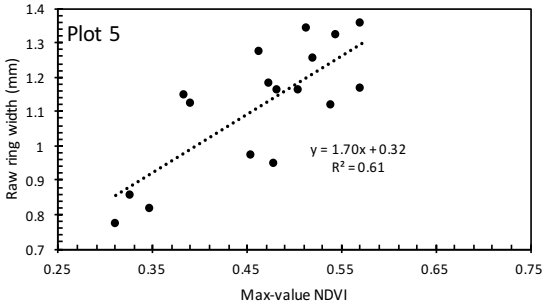
Plot 5
y = 1.70x + 0.32
R² = 0.61
Raw ring width (mm)
Max-value NDVI

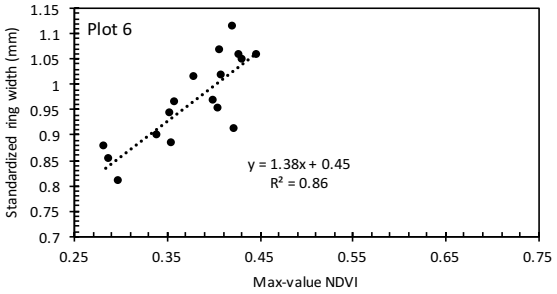
Plot 6
y = 1.38x + 0.45
R² = 0.86
Standardized ring width (mm)
Max-value NDVI

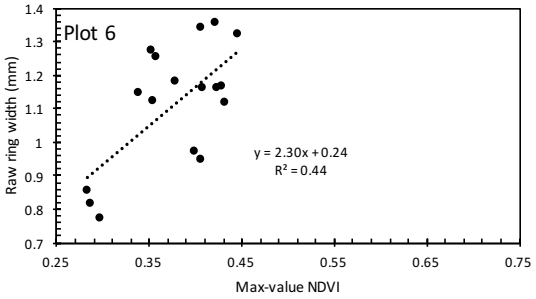
Plot 6
y = 2.30x + 0.24
R² = 0.44
Raw ring width (mm)
Max-value NDVI

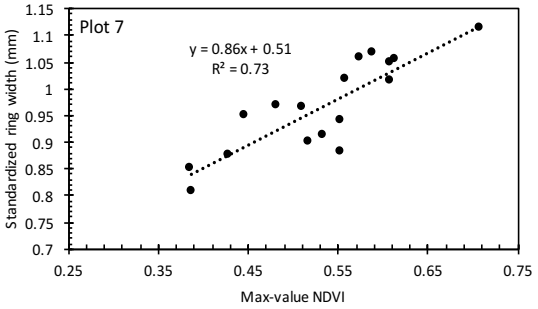
Plot 7
y = 0.86x + 0.51
R² = 0.73
Standardized ring width (mm)
Max-value NDVI

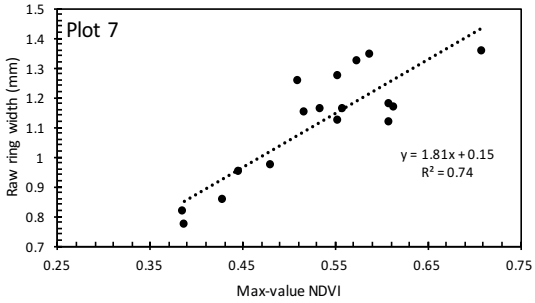
Plot 7
y = 1.81x + 0.15
R² = 0.74
Raw ring width (mm)
Max-value NDVI

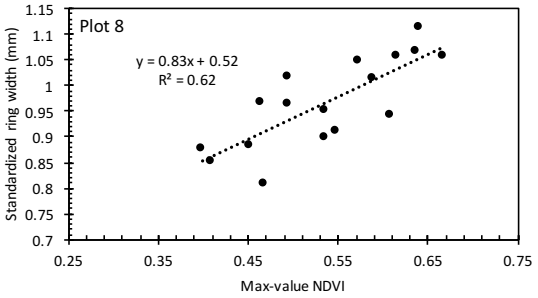
Plot 8
y = 0.83x + 0.52
R² = 0.62
Standardized ring width (mm)
Max-value NDVI

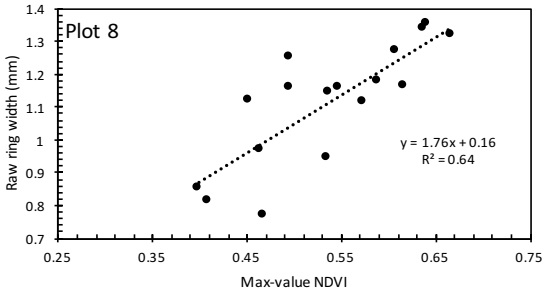
Plot 8
y = 1.76x + 0.16
R² = 0.64
Raw ring width (mm)
Max-value NDVI

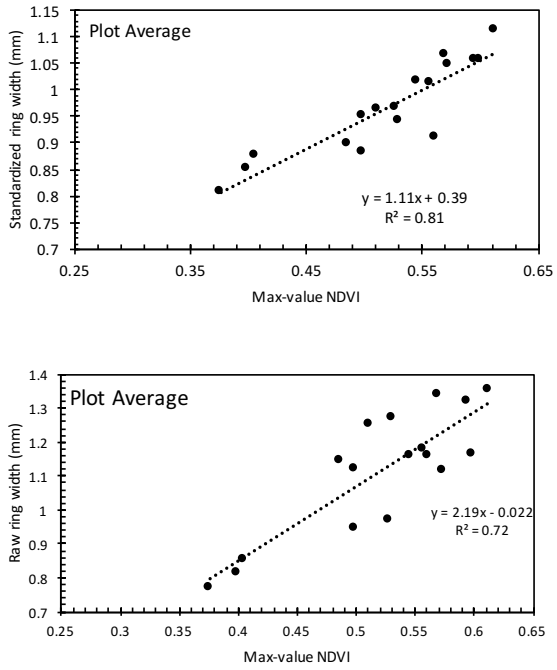

Figure 14. Average pixel value of maximum NDVI observed within each 2016 TNC vegetation sampling plot versus standardized and raw tree ring width of B. papyrifera of the Niobrara River Valley between 1985-2011

APPENDICES

Appendix A. Statistical summary of variables included in models which range between 1950 and 2014. Annual cumulative precipitation was obtained from the Ainsworth, NE weather station. Streamflow data of the Niobrara River was obtained from the USGS and measured near Sparks, NE. Temperature data was obtained from the Springview, NE weather station by way of the High Plains Regional Climate Center, UNL. Annual and monthly Palmer's Drought Severity Index (PDSI) information for North-central Nebraska was obtained from NOAA.

	Annual sum precipitation (mm)	Average annual streamflow (m3s-1)	Annual mean temperature (C)	Yearly PDSI	Monthly PDSI
hi	938.0	53.1	10.8	6.7	8.1
lo	241.3	0.3	6.5	-4.9	-5.9
mean	572.6	16.5	8.9	0.9	0.9
SE	17.6	0.3	0.1	0.3	0.1

Appendix B. Monthly and annual PDSI values for the North-central region of Nebraska from 1949 - 2014 as obtained from NOAA.

year	Jan_PDSI	Feb_PDSI	Mar_PDSI	Apr_PDSI	May_PDSI	Jun_PDSI	Jul_PDSI	Aug_PDSI	Sep_PDSI	Oct_PDSI	Nov_PDSI	Dec_PDSI	Annual_PDSI
2014	-0.25	-0.2	-0.48	-0.66	-1.09	1.95	1.84	3.25	3.2	2.87	2.53	2.99	1.33
2013	-5.07	-4.4	-4.36	0.07	0.89	0.48	0.56	1.4	1.08	1.91	0.02	-0.04	-0.62
2012	4.42	4.8	-1.22	-0.55	-1.36	-2.86	-4.24	-5.17	-5.82	-5.68	-5.67	-5.25	-2.38
2011	5.53	5.37	5.04	4.94	5.51	6.04	6.59	7.3	6.54	6.72	5.86	5.13	5.88
2010	6.55	6.35	6.16	6.26	5.84	7.59	8.04	8	7.47	6.93	6.05	5.51	6.73
2009	4.6	4.78	4.68	5.14	4.29	5.29	5.86	7.09	6.63	8.05	6.99	6.92	5.86
2008	1.87	1.53	0.92	1.23	2.28	2.61	2.98	3.24	3.63	5.35	4.96	4.68	2.94
2007	1.03	1.4	1.37	2.04	2.88	2.63	2.03	2.56	2.01	2.83	2	2.3	2.09
2006	-1.04	-1.25	-0.86	-0.93	-2.44	-2.75	-3.86	-3.53	0.91	0.74	0.21	1.21	-1.13
2005	-0.52	-0.79	-0.87	0.82	1.21	2.46	1.94	2.12	-0.39	-0.64	-0.5	-0.67	0.35
2004	-3.46	-3.23	-3.41	-3.7	-3.75	-3.72	-3.29	-3.45	0.94	0.92	0.88	-0.47	-2.15
2003	-3.23	-3.14	-3.26	-2.95	-2.71	-2.04	-2.51	-3.65	-3.84	-3.99	-3.65	-3.48	-3.2
2002	-0.69	-1.05	-1.22	-1.65	-2.23	-3.81	-5.2	-4.8	-4.61	-3.29	-3.44	-3.45	-2.95
2001	1.3	1.32	0.76	2.62	2.27	1.38	1.87	1.86	1.91	1.4	1.71	-0.4	1.5
2000	-1.49	-1.4	-1.9	-2.12	-1.99	-2.12	-2.15	-3.48	-3.61	0.73	1.15	0.86	-1.46
1999	4.38	4.15	3.72	4.65	4.33	4.73	4.72	4.2	4.33	-0.63	-1.31	-1.48	2.98
1998	2.69	2.3	2.56	2.29	2.16	3.37	4.11	4.5	3.71	5.03	5.51	4.87	3.59
1997	3.42	3.19	2.21	2.64	2.39	2.02	2.72	3.03	3.24	4.18	3.57	3.1	2.98
1996	4.94	4.21	3.58	2.96	4.07	3.18	2.92	3.04	4.55	4.34	4.31	3.86	3.83
1995	3.42	3.07	3.48	4.73	6.65	6.21	5.9	5.18	5.51	6.33	5.63	4.87	5.08
1994	6.48	6.33	5.3	5.12	3.6	3.75	4.79	4.66	4.19	4.44	4.09	3.95	4.73
1993	2.52	2.88	2.61	3.42	3.21	3.92	5.97	6.68	7.04	7.14	7.14	6.69	4.94
1992	0.7	0.72	1.38	-0.65	-1.65	0.63	1.77	3.42	3.21	3.01	2.89	2.53	1.5
1991	-2.37	-2.45	-2.7	-2.72	-1.55	-1.46	-1.87	-2.26	-2.12	0.45	0.86	0.44	-1.48
1990	-3.91	-4.01	-3.71	-3.86	-3.04	-3.35	-3.3	-2.7	-3.28	-2.87	-2.41	-2.35	-3.23
1989	-0.89	-0.95	-1.21	-2.36	-3.26	-3.55	-4.28	-4.4	-4.06	-4.2	-4.37	-4.08	-3.13
1988	3.3	2.95	2.35	2.36	3.13	2.19	2.5	2.56	3.12	-0.52	-0.61	-0.85	1.87
1987	3.12	3.73	5.65	4.62	4.12	3.11	2.82	2.59	2.8	2.2	2.34	2.78	3.32
1986	0.74	0.91	0.57	1.39	1.52	1.76	2.08	2.56	3.97	4.48	4.18	3.6	2.31
1985	0.09	-0.3	-0.74	-0.92	-1.48	-2.18	-2.02	0.27	1.06	0.88	1.32	1.15	-0.24
1984	4.03	4.2	4.01	5.32	4.58	4.31	4.75	4.2	3.37	3.81	3.96	0.02	3.88
1983	3.53	3.13	4.18	4.16	5.04	6.35	6.86	6.15	4.98	4.38	4.85	4.62	4.85
1982	1.03	-0.42	-0.55	-0.84	1.34	1.28	1.13	1.43	1.24	2.64	3.34	3.77	1.28
1981	-2.54	-2.7	-2.86	-4.12	-3.65	-4.15	0.85	0.98	0.18	0.52	0.63	1.02	-1.32
1980	3.51	3.61	4.13	-0.37	-0.53	-1.06	-1.82	-1.18	-2.09	-1.78	-2.27	-2.39	-0.19
1979	2.44	1.9	2.39	2.26	2.18	2.64	3.41	3.63	3.47	3.75	4.46	3.83	3.03
1978	3.3	3.69	3.1	3.81	3.75	2.82	3.77	3.99	2.96	2.18	2.05	2.28	3.14
1977	-3.02	-2.82	1.49	2.02	2.86	2.67	3.14	4.23	4.13	3.95	3.8	3.72	2.18
1976	-1.79	-1.94	-2.15	-1.79	-1.98	-2.97	-2.72	-3.01	-2.92	-2.81	-2.9	-2.96	-2.5
1975	-1.87	-2.05	-1.75	-1.83	-2.4	-1.59	-1.85	-2.55	-3.07	-3.38	-2.39	-2.34	-2.26
1974	3.94	3.67	-0.17	0.19	-0.05	-0.11	-0.88	-0.71	-1.25	-1.55	-1.91	-2.04	-0.07
1973	1.74	1.47	2.46	2.79	3.28	2.23	2.35	1.5	3.99	4.05	4.08	4.11	2.84
1972	-0.1	-0.4	-1.03	0.12	0.24	0.22	1.72	1.1	0.87	0.66	1.58	1.61	0.55
1971	-0.21	0.57	0.4	1.18	1.5	1.07	1.21	0.86	0.99	1.66	1.8	0.01	0.92
1970	-1.44	-1.65	-1.61	-0.61	-1.14	-1.26	-1.49	-2.37	-2.31	0.22	0.26	-0.13	-1.13
1969	1.05	1.21	-0.41	-1.35	-2.44	-2.47	-2	-2.48	-2.71	-1.15	-1.35	-1.31	-1.28
1968	-1.25	-1.48	-2.49	-1.81	-1.73	-1.83	-2.17	1.15	0.54	0.77	0.53	0.91	-0.74
1967	-0.71	-1.07	-1.93	-2.7	-2.54	-0.78	-0.73	-0.95	-0.93	-1.12	-1.27	-1.16	-1.32
1966	0.44	0.44	-0.29	-0.27	-1.5	0.35	0.11	1.19	1.51	-0.32	-0.68	-0.63	0.03
1965	-1.97	-2.04	-2.58	-3.17	0.08	0.8	1.02	0.85	2.74	2.6	-0.33	0.33	-0.14
1964	-1.48	-1.48	-1.54	-1.02	-1.71	-1.2	-1.19	-1.39	-1.24	-1.88	-2.11	-2.02	-1.52
1963	-0.1	-0.27	-0.25	-0.6	-1.44	-1.44	0.17	0.77	1.27	-0.66	-0.95	-1.17	-0.39
1962	-0.93	-0.51	-0.45	-1.25	1.36	3.33	5.17	5.12	4.77	-0.03	-0.54	-0.53	1.29
1961	-1.14	-1.26	-1.06	-1.32	0.62	-0.6	-0.48	-0.67	0.66	-0.28	-0.49	-0.64	-0.56
1960	0.62	1.18	1.14	1.69	2.54	2.4	2.04	2.2	-0.22	-0.7	-0.73	-0.79	0.95
1959	-0.97	-0.85	-0.79	-1.15	-1.08	-1.16	-1.37	-1.56	0.02	0.87	0.79	0.44	-0.57
1958	2.63	2.96	2.93	3.51	3.02	2.96	5.07	4.64	-0.16	-0.77	-0.87	-1.01	2.08
1957	-4.44	-4.54	-4.12	0.42	1.89	2.08	2.65	2.98	3.07	3.53	3.47	3.02	0.83
1956	-3.96	-3.88	-4.35	-4.21	-4.97	-5.59	-5.92	-5.31	-5.85	-5.5	-4.7	-4.59	-4.9
1955	-2.07	-1.61	-2.14	-3.29	-3.42	-3.18	-4.42	-5.48	-4.95	-5.15	-4.92	-4.32	-3.75
1954	-0.97	-1.49	-1.02	-1.35	-1.74	-0.99	-2.04	-1.74	-1.63	-1.37	-1.81	-2.07	-1.52
1953	0.03	0.93	0.56	1.71	1.56	1.39	1.82	-0.18	-1.12	-1.16	-1.08	-0.62	0.32
1952	7.51	7.46	7.24	6.53	6.59	-0.86	-1.52	-1.54	-2.36	-2.77	0.16	0.06	2.21
1951	2.49	2.53	2.28	2.56	3.47	4.8	5.59	7.07	7.96	7.92	7.33	7.67	5.14
1950	1.97	1.97	2.07	1.87	1.98	1.45	2.48	3.85	4.54	3.95	3.49	2.94	2.71
1949	1.48	1.02	2.55	2.47	2.89	2.67	2.63	2.72	2.47	3.13	2.41	2.17	2.38

Appendix C. Pearson R2 and associated P values for Tree ring width (Raw), Basal Area Increase (BAI), and Standardized ring width (Standardized) of *B. papyrifera* of the Niobrara River Valley between 1950 – 2014 correlated with current and previous years of monthly: A) precipitation , B) streamflow, C) average temperature, and D) Palmer's Drought Severity Index (PDSI). Annual cumulative precipitation data was obtained from the Ainsworth, NE weather station. Streamflow measurements of the Niobrara River was obtained from the USGS and recorded near Sparks, NE. Temperature data was obtained from the Springview, NE weather station by way of the High Plains Regional Climate Center, UNL. Annual and monthly PDSI data was obtained from NOAA.

A)	Raw		BAI		Standardized	
	correlation	P.value	correlation	P.value	correlation	P.value
C. Jan Precip	0.12	0.35	0.09	0.49	0.10	0.45
C. Feb Precip	0.01	0.92	0.04	0.78	-0.03	0.80
C. Mar Precip	0.05	0.67	0.00	0.99	-0.12	0.34
C. Apr Precip	-0.16	0.19	-0.20	0.11	-0.01	0.97
C. May Precip	0.02	0.85	0.00	1.00	-0.11	0.37
C. Jun Precip	-0.11	0.40	-0.02	0.89	0.12	0.36
C. jul Precip	0.18	0.14	0.14	0.27	-0.03	0.80
C. Aug Precip	-0.03	0.81	0.03	0.80	0.00	0.98
C. Sep Precip	0.07	0.55	0.08	0.53	-0.01	0.93
C. Oct Precip	-0.12	0.33	-0.08	0.53	0.22	0.08
C. Nov Precip	0.19	0.14	0.11	0.37	0.00	0.97
C. Dec Precip	-0.11	0.40	-0.09	0.49	0.03	0.82
P. Jan Precip	-0.01	0.92	-0.01	0.94	-0.21	0.10
P. Feb Precip	-0.02	0.88	0.05	0.72	0.02	0.86
P. Mar Precip	0.06	0.64	0.01	0.95	-0.06	0.64
P. Apr Precip	-0.28	0.03	-0.28	0.02	-0.16	0.19
P. May Precip	0.05	0.70	0.08	0.51	0.12	0.36
P. Jun Precip	-0.04	0.74	0.05	0.70	0.20	0.10
P. Jul Precip	0.22	0.08	0.20	0.12	0.11	0.39
P. Aug Precip	0.06	0.65	0.07	0.57	0.03	0.78
P. Sep Precip	0.06	0.61	0.07	0.57	0.13	0.29
P. Oct Precip	-0.12	0.34	-0.08	0.51	0.25	0.04
P. Nov Precip	0.10	0.45	0.07	0.59	-0.21	0.10
P. Dec Precip	0.04	0.75	0.06	0.62	0.21	0.09

B)	Raw		BAI		Standardized	
Raw	correlation	P.value	correlation	P.value	correlation	P.value
C. Jan Flow	-0.13	0.29	-0.11	0.37	0.07	0.57
C. Feb Flow	0.13	0.30	0.18	0.14	0.18	0.16
C. Mar Flow	0.02	0.87	0.09	0.48	0.22	0.07
C. Apr Flow	-0.13	0.29	-0.09	0.49	0.12	0.34
C. May Flow	-0.12	0.35	-0.06	0.62	0.05	0.67
C. Jun Flow	-0.10	0.42	-0.02	0.85	0.26	0.04
C. jul Flow	0.15	0.23	0.25	0.05	0.19	0.12
C. Aug Flow	0.27	0.03	0.39	0.00	0.17	0.18
C. Sep Flow	0.22	0.08	0.34	0.01	0.07	0.57
C. Oct Flow	0.19	0.13	0.33	0.01	0.14	0.26
C. Nov Flow	0.06	0.62	0.20	0.11	0.32	0.01
C. Dec Flow	-0.19	0.13	-0.09	0.47	0.14	0.25
P. Jan Flow	-0.17	0.18	-0.14	0.27	0.08	0.53
P. Feb Flow	0.06	0.65	0.07	0.58	0.05	0.68
P. Mar Flow	-0.08	0.55	-0.01	0.92	-0.05	0.69
P. Apr Flow	-0.23	0.07	-0.16	0.19	-0.01	0.94
P. May Flow	-0.12	0.35	-0.05	0.67	-0.06	0.64
P. Jun Flow	-0.09	0.49	0.00	0.99	0.27	0.03
P. Jul Flow	0.17	0.16	0.27	0.03	0.23	0.07
P. Aug Flow	0.31	0.01	0.44	0.00	0.27	0.03
P. Sep Flow	0.28	0.03	0.40	0.00	0.22	0.07
P. Oct Flow	0.26	0.04	0.40	0.00	0.21	0.09
P. Nov Flow	0.09	0.48	0.20	0.12	0.33	0.01
P. Dec Flow	-0.18	0.14	-0.07	0.58	0.22	0.08

C)	Raw		BAI		Standardized	
	correlation	P.value	correlation	P.value	correlation	P.value
C. Jan T mean	-0.29	0.02	-0.22	0.08	-0.08	0.55
C. Feb T mean	-0.05	0.70	0.01	0.94	0.02	0.90
C. Mar T mean	-0.22	0.07	-0.23	0.07	0.06	0.65
C. Apr T mean	-0.03	0.78	-0.09	0.46	-0.19	0.14
C. May T mean	-0.04	0.76	-0.05	0.69	-0.06	0.61
C. Jun T mean	0.04	0.73	0.05	0.70	-0.02	0.90
C. jul T mean	-0.10	0.44	-0.07	0.60	-0.09	0.46
C. Aug T mean	0.02	0.87	0.07	0.56	0.07	0.58
C. Sep T mean	-0.08	0.52	-0.06	0.64	0.06	0.61
C. Oct T mean	0.10	0.43	0.14	0.26	0.00	1.00
C. Nov T mean	-0.11	0.38	-0.02	0.90	0.06	0.64
C. Dec T mean	-0.09	0.46	-0.08	0.51	-0.15	0.22
P. Jan T mean	-0.30	0.01	-0.27	0.03	-0.06	0.61
P. Feb T mean	-0.06	0.66	-0.07	0.59	0.05	0.70
P. Mar T mean	-0.27	0.03	-0.29	0.02	-0.07	0.58
P. Apr T mean	-0.09	0.45	-0.15	0.24	-0.25	0.04
P. May T mean	-0.07	0.60	-0.05	0.70	-0.02	0.87
P. Jun T mean	-0.11	0.38	-0.13	0.31	-0.41	0.00
P. Jul T mean	-0.16	0.20	-0.13	0.29	-0.14	0.26
P. Aug T mean	-0.05	0.67	0.00	1.00	-0.12	0.33
P. Sep T mean	-0.15	0.25	-0.11	0.38	-0.03	0.83
P. Oct T mean	0.12	0.32	0.21	0.10	0.04	0.77
P. Nov T mean	-0.17	0.19	-0.11	0.38	0.03	0.82
P. Dec T mean	-0.12	0.33	-0.09	0.49	-0.20	0.11

D)	Raw		BAI		Standardized	
	correlation	P.value	correlation	P.value	correlation	P.value
C. Jan PDSI	0.06	0.65	0.10	0.43	0.40	0.00
C. Feb PDSI	0.05	0.72	0.09	0.47	0.39	0.00
C. Mar PDSI	0.13	0.31	0.16	0.19	0.39	0.00
C. Apr PDSI	0.04	0.78	0.08	0.52	0.36	0.00
C. May PDSI	0.05	0.70	0.10	0.45	0.30	0.01
C. Jun PDSI	-0.01	0.93	0.04	0.74	0.32	0.01
C. jul PDSI	0.05	0.69	0.09	0.48	0.30	0.01
C. Aug PDSI	0.04	0.78	0.08	0.53	0.30	0.02
C. Sep PDSI	-0.03	0.78	0.01	0.93	0.22	0.08
C. Oct PDSI	-0.08	0.55	-0.04	0.75	0.28	0.02
C. Nov PDSI	-0.02	0.90	0.00	0.97	0.30	0.02
C. Dec PDSI	-0.03	0.83	0.00	1.00	0.29	0.02
C. Annual PDSI	0.02	0.88	0.07	0.60	0.37	0.00
P. Jan PDSI	0.02	0.85	0.07	0.58	0.29	0.02
P. Feb PDSI	0.01	0.94	0.06	0.63	0.28	0.02
P. Mar PDSI	0.09	0.48	0.13	0.32	0.27	0.03
P. Apr PDSI	-0.01	0.92	0.05	0.72	0.27	0.03
P. May PDSI	0.02	0.87	0.09	0.48	0.28	0.02
P. Jun PDSI	-0.01	0.91	0.06	0.64	0.33	0.01
P. Jul PDSI	0.06	0.61	0.12	0.33	0.35	0.00
P. Aug PDSI	0.07	0.55	0.13	0.29	0.37	0.00
P. Sep PDSI	0.03	0.79	0.09	0.49	0.35	0.00
P. Oct PDSI	-0.03	0.81	0.03	0.84	0.37	0.00
P. Nov PDSI	0.02	0.86	0.07	0.60	0.35	0.00
P. Dec PDSI	0.05	0.70	0.10	0.44	0.40	0.00
P. Annual PDSI	0.03	0.80	0.09	0.45	0.38	0.00

Appendix D. Order of variable elimination and associated P values starting from the global model of tree ring width (Raw), standardized ring width (standardized), and Basal Area Increment increase (BAI), through backwards selection.

Raw		Standardized		BAI	
variable	p-val (Chi2)	variable	p-val (Chi2)	variable	p-val (Chi2)
C. May flo	0.965	C. Jun mean T	0.996	C. Apr precip	0.990
C. Jun Precip	0.934	C. Mar precip	0.937	P. Nov flow	0.984
C. Jun mean T	0.915	C. Jan mean T	0.920	C. Jun precip	0.902
C. Sep Precip	0.875	C. Jun flow	0.900	C. Aug precip	0.901
P. Nov flow	0.775	C. Mar mean T	0.820	P. Aug flow	0.701
C. Apr Precip	0.695	P. Dec precip	0.781	P. Sep flow	0.740
C. Aug Precip	0.665	P. Sep mean T	0.792	C. May flow	0.654
P. Sep mean T	0.621	P. Nov mean T	0.761	C. Sep precip	0.688
C. May mean T	0.612	C. Oct mean T	0.761	C. jun flow	0.673
C. Jun flow	0.642	C. May mean T	0.803	C. Mar mean T	0.646
C. jan precip	0.574	C. Jul precip	0.762	C. May mean T	0.667
P. Dec flow	0.623	P. Aug precip	0.722	P. Sep precip	0.677
P Aug precip	0.574	P. Aug flow	0.607	P. Oct precip	0.475
P. Jul flow	0.524	C. Jan precip	0.523	C. Sep flow	0.475
P. Oct precip	0.561	C. Sep flow	0.512	C. Oct flow	0.465
C. Mar flow	0.607	C. Oct flow	0.536	C. Apr mean T	0.432
P. Sep precip	0.477	C. Aug precip	0.567	P. Aug precip	0.454
C. Oct precip	0.498	C. May flow	0.457	C. Mar flow	0.410
C. Apr mean T	0.440	P. Nov precip	0.445	C. Jan precip	0.370
C. Sep Flow	0.490	P. Sep flow	0.388	C. Apr flow	0.267
C. Mar mean T	0.427	C. Apr precip	0.362	P. Dec flow	0.325
C. Oct flow	0.400	P. Jul precip	0.271	C. Jun mean T	0.418
C. Apr flow	0.304	P. Oct mean T	0.265	P. Dec precip	0.218
P. Sep flow	0.283	C. Aug mean T	0.302	P. Oct flow	0.153
C. Oct mean T	0.104	C. Jul mean T	0.378	C. Jan flow	0.132
P. Aug flow	0.121	C. Apr mean T	0.353	C. Oct mean T	0.268
C. Jan flow	0.106	P. Aug mean T	0.282	C. Feb flow	0.180
P. Dec precip	0.153	C. Sep mean T	0.282	P. Sep mean T	0.080
C. Feb flow	0.094	P. Sep precip	0.318		
		C. Aug flow	0.263		
		C. Jul flow	0.322		
		P. Nov flow	0.403		
		C. Jun precip	0.318		
		C. Feb flow	0.241		
		C. Feb mean T	0.218		
		P. Jul mean T	0.131		
		C. Annual PDSI	0.291		
		C. May precip	0.075		
		C. Sep precip	0.143		
		P. oct flow	0.098		
		P. Jul flow	0.128		
		C. Mar flow	0.128		
		C. Apr flow	0.079		
		C. Feb precip	0.167		

Appendix E. Comparison of GLMMs obtained through backwards stepwise linear regression and Pearson R^2 significance by monthly parameter; precipitation (A), streamflow (B), and temperature (C)

A			PRECIP			
	raw		BAI		STD	
	model	R2	model	R2	model	R2
P.Jan						-*
P.Feb						
P.Mar						
P.Apr		- **		-**		
P.May						
P.Jun						
P.Jul		+*	+			
P.Aug						
P.Sep						
P.Oct						+**
P.Nov					-	
P.Dec						+*
C.Jan						
C.Feb						
C.Mar	+					
C.Apr						
C.May						
C.Jun			+			+**
C.Jul						
C.Aug						
C.Sep						
C.Oct						+*
C.Nov						+**
C.Dec						

B			STREAMFLOW			
	raw		BAI		STD	
	model	R2	model	R2	model	R2
P.Jan						
P.Feb						
P.Mar						
P.Apr		-*				
P.May						
P.Jun						+**
P.Jul	-		-	+**		+*
P.Aug	+	+**	+	+**		+**
P.Sep		+**		+**		+*
P.Oct		+**		+**		+*
P.Nov						+**
P.Dec						+*
C.Jan						
C.Feb						
C.Mar						+*
C.Apr						
C.May	-					
C.Jun						
C.Jul				+**		
C.Aug	+	+**	+	+**		
C.Sep		+*		+**		
C.Oct				+**		
C.Nov						
C.Dec						

C			TEMPERATURE			
	raw		BAI		STD	
	model	R2	model	R2	model	R2
P.Jan		-**		-**		
P.Feb						
P.Mar		-**		-**		
P.Apr						-**
P.May						
P.Jun						-**
P.Jul						
P.Aug						
P.Sep						
P.Oct						
P.Nov	-					
P.Dec						
C.Jan	-	-**		-*		
C.Feb						
C.Mar		-*		-*		
C.Apr						
C.May						
C.Jun	+					
C.Jul						
C.Aug	+				+	
C.Sep	-					
C.Oct						
C.Nov						
C.Dec						

Appendix F. Minimum, maximum, average, and standard error of Pearson R^2 values of raw *B. papyrifera* ring growth (Raw) and standardized ring width (Std) to MODIS sum-NDVI of various examined time periods between 2000 and 2014 contained within the Niobrara Preserve boundary

	Raw	Std	Raw	Std
	May	**May**	**August-October**	**August-October**
min	-0.68	-0.58	-0.42	-0.23
max	0.00	0.14	0.08	0.34
mean	-0.30	-0.23	-0.21	0.09
SE	0.00	0.00	0.00	0.00
	June	**June**	**June-August**	**June-August**
min	-0.44	-0.15	-0.37	0.01
max	0.01	0.32	0.13	0.56
mean	-0.20	0.12	-0.10	0.35
SE	0.00	0.00	0.00	0.00
	July	**July**	**March-May**	**March-May**
min	-0.15	-0.07	-0.31	-0.28
max	0.53	0.70	0.15	0.14
mean	0.15	0.39	-0.17	-0.14
SE	0.00	0.00	0.00	0.00
	August	**August**	**March-October**	**March-October**
min	-0.37	-0.09	-0.49	-0.14
max	0.08	0.45	0.10	0.42
mean	-0.13	0.20	-0.26	0.17
SE	0.00	0.00	0.00	0.00

Appendix G. Summary of all (48) points measured in a 1.0m x 1.0m quadrat inside each of 8 plots measuring 640m x 480m: canopy height (cm), percent cover of litter, percent cover of standing dead vegetation, percent cover of grass, percent cover of forbs, and percent cover of bare soil, sampled in June, 2016 on The Niobrara Valley Preserve, owned by The Nature Conservancy.

Plot	Grs	Forb	Shrub	Litt	Sdead	Bare	Can Ht
plot 1							
max	85.0	50.0	50.0	100.0	80.0	99.0	105.0
min	0.0	0.0	0.0	1.0	0.0	0.0	8.5
avg	31.9	7.1	6.2	59.6	8.8	34.5	41.6
ste	2.3	1.2	1.3	4.2	1.8	3.7	3.7
plot 2							
max	90.0	25.0	100.0	100.0	20.0	99.0	62.5
min	5.0	0.0	0.0	2.0	0.0	1.0	15.0
avg	42.0	7.9	27.4	58.3	2.7	35.0	33.2
ste	3.2	0.8	3.5	4.8	0.7	4.6	1.5
plot 3							
max	73.0	20.0	95.0	100.0	25.0	95.0	83.0
min	15.0	0.0	0.0	3.0	0.0	0.0	8.5
avg	35.1	5.4	23.0	62.6	3.2	35.1	28.6
ste	2.3	0.7	2.8	3.9	0.6	3.7	2.3
plot 4							
max	65	50	95	98	40	95	126
min	1	0	0	5	0	1	9.5
avg	34.42	20.73	14.58	38.42	4	54.48	26.94
ste	2.108	1.681	3.068	4.276	1.159	4.568	2.778

Plot	Grs	Forb	Shrub	Litt	Sdead	Bare	Can Ht
plot 5							
max	85	45	99	85	20	95	190
min	5	0	0	5	0	3	11.5
avg	34.81	16.31	20.46	40.63	2.313	54.33	30.35
ste	2.262	1.615	3.092	3.376	0.543	3.928	3.709
plot 6							
max	75	40	100	100	50	90	400
min	1	0	0	10	0	0	12.5
avg	36.81	11.5	17.71	55.81	9.729	39.5	40.82
ste	2.574	1.414	3.733	4.42	1.764	4.417	7.941
plot 7							
max	75	45	90	100	30	95	110
min	10	0	0	5	0	0	11
avg	36.31	11.29	19.31	36.71	6	52.73	32.74
ste	2.363	1.367	3.56	3.668	1.102	3.947	2.906
plot 8							
max	85.0	45.0	70.0	100.0	40.0	95.0	103.5
min	15.0	0.0	0.0	5.0	0.0	0.0	13.5
avg	49.0	12.1	13.9	67.2	13.0	28.8	37.7
ste	3.0	1.6	2.5	4.2	1.5	3.8	2.6

Plot	Grs	Forb	Shrub	Litt	Sdead	Bare	Can Ht
all plots							
max	49.0	20.7	27.4	67.2	13.0	54.5	41.6
min	31.9	5.4	6.2	36.7	2.3	28.8	26.9
avg	37.6	11.5	17.8	52.4	6.2	41.8	34.0
ste	0.9	0.5	1.1	1.5	0.5	1.5	1.4

Appendix H. Statistical description of R^2 values of average tree ring width (RAW) and standardized ring width (DET) of *B. papyrifera* of the Niobrara River Valley to annual max-value Landsat-5 NDVI between 1985 and 2011 within the 8 vegetation plots sampled in June, 2016 by the Nature Conservancy

RAW plot	Min	Max	Mean	Range
6	0.31	0.87	0.63	0.56
2	0.34	0.86	0.61	0.52
3	0.24	0.90	0.57	0.66
5	-0.03	0.79	0.56	0.82
4	-0.18	0.89	0.51	1.07
7	0.07	0.87	0.47	0.80
1	-0.15	0.83	0.40	0.98
8	-0.12	0.68	0.35	0.81
DET plot	Min	Max	Mean	Range
2	0.48	0.90	0.76	0.42
6	0.34	0.86	0.66	0.53
5	-0.08	0.84	0.61	0.92
3	0.06	0.78	0.59	0.72
4	-0.05	0.81	0.49	0.85
7	0.05	0.75	0.40	0.69
1	-0.24	0.81	0.37	1.05
8	0.00	0.66	0.36	0.67

Appendix I. Average R^2 value of standardized growth of *B. papyrifera* of the Niobrara River valley to max-value MODIS sum-NDVI between 1985 and 2011 within the 8 vegetation plots sampled in June, 2016 by the Nature Conservancy at the Niobrara Valley Preserve

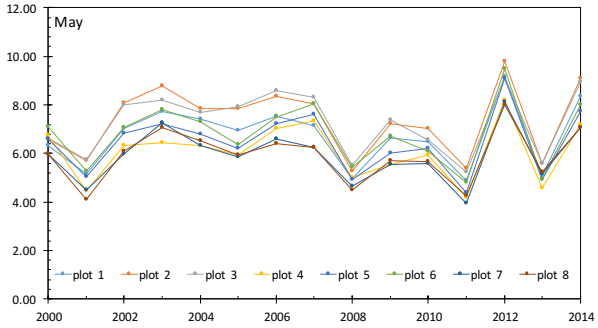

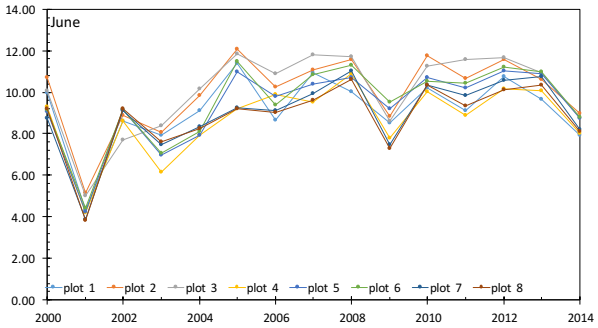

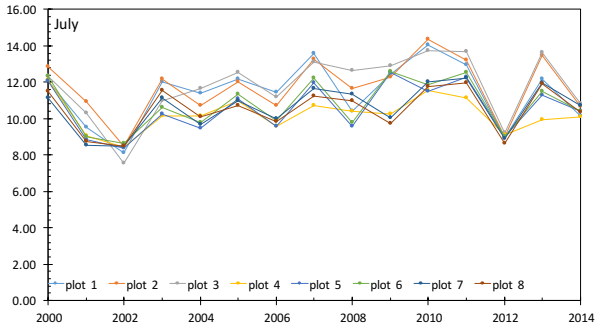

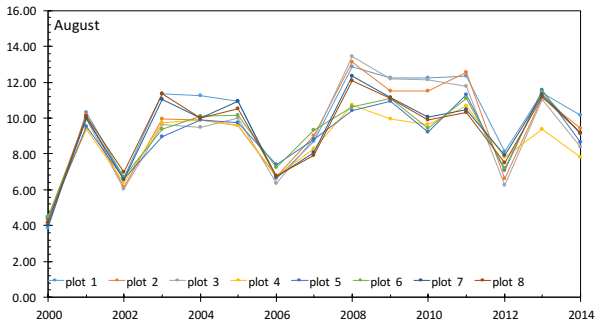

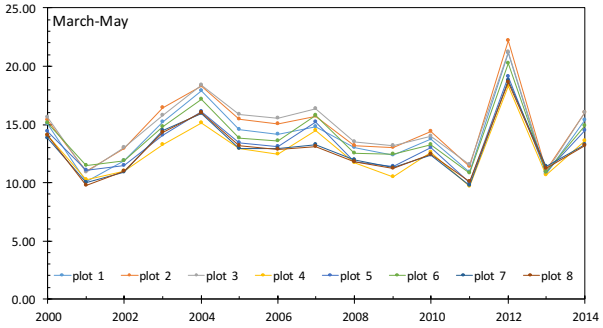
March-May
25.00
20.00
15.00
10.00
5.00
0.00
2000
2002
2004
2006
2008
2010
2012
2014
plot 1
plot 2
plot 3
plot 4
plot 5
plot 6
plot 7
plot 8

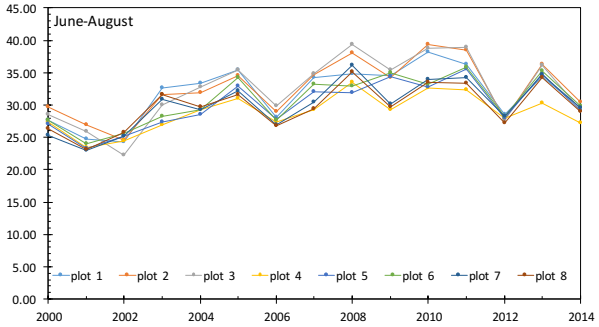
June-August
45.00
40.00
35.00
30.00
25.00
20.00
15.00
10.00
5.00
0.00
2000
2002
2004
2006
2008
2010
2012
2014
plot 1
plot 2
plot 3
plot 4
plot 5
plot 6
plot 7
plot 8

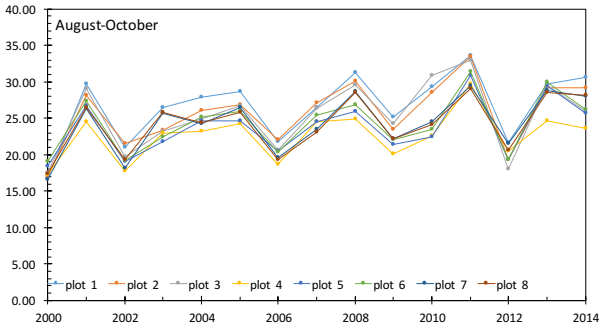
August-October
40.00
35.00
30.00
25.00
20.00
15.00
10.00
5.00
0.00
2000
2002
2004
2006
2008
2010
2012
2014
plot 1
plot 2
plot 3
plot 4
plot 5
plot 6
plot 7
plot 8

Appendix J. Statistical description of R^2 values of average tree ring width (top) and standardized ring width (bottom) of *B. papyrifera* of the Niobrara River Valley to MODIS sum-NDVI between 2000 and 2014 within the 8 vegetation composition plots sampled in June, 2016 by the Nature Conservancy at the Niobrara Valley Preserve.

Plot		May_Raw	Jun_Raw	Jul_Raw	Aug_Raw	Mar-May_Raw	Jun-Aug_Raw	Aug-Oct_Raw	Mar-Oct_Raw
1	min	-0.35	-0.09	0.17	-0.16	-0.22	-0.07	-0.24	-0.28
	max	-0.32	-0.09	0.23	-0.15	-0.20	-0.03	-0.21	-0.22
	mean	-0.34	-0.09	0.20	-0.16	-0.21	-0.05	-0.22	-0.25
	range	0.03	0.00	0.06	0.02	0.02	0.04	0.03	0.06
2	min	-0.41	-0.12	0.23	-0.09	-0.24	0.03	-0.23	-0.25
	max	-0.38	-0.07	0.36	0.01	-0.23	0.11	-0.13	-0.13
	mean	-0.39	-0.09	0.30	-0.05	-0.23	0.07	-0.19	-0.20
	range	0.03	0.05	0.13	0.10	0.01	0.08	0.10	0.11
3	min	-0.33	-0.19	0.26	0.05	-0.20	0.08	-0.03	-0.06
	max	-0.32	-0.18	0.29	0.06	-0.19	0.09	-0.02	-0.05
	mean	-0.33	-0.18	0.27	0.05	-0.20	0.08	-0.03	-0.06
	range	0.01	0.01	0.03	0.01	0.01	0.01	0.01	0.01
4	min	-0.37	-0.32	-0.03	-0.20	-0.26	-0.26	-0.30	-0.42
	max	-0.37	-0.31	-0.01	-0.19	-0.24	-0.25	-0.29	-0.41
	mean	-0.37	-0.32	-0.01	-0.19	-0.25	-0.25	-0.29	-0.42
	range	0.00	0.01	0.02	0.01	0.03	0.01	0.02	0.01
5	min	-0.42	-0.30	-0.07	-0.21	-0.24	-0.29	-0.29	-0.44
	max	-0.40	-0.29	0.03	-0.21	-0.23	-0.25	-0.28	-0.41
	mean	-0.40	-0.30	-0.01	-0.21	-0.24	-0.26	-0.29	-0.42
	range	0.02	0.00	0.10	0.00	0.00	0.04	0.01	0.03
6	min	-0.27	-0.18	0.35	-0.20	-0.17	-0.05	-0.22	-0.22
	max	-0.27	-0.17	0.39	-0.20	-0.16	-0.03	-0.22	-0.20
	mean	-0.27	-0.18	0.36	-0.20	-0.17	-0.05	-0.22	-0.21
	range	0.00	0.01	0.03	0.00	0.00	0.02	0.00	0.03
7	min	-0.24	-0.15	0.33	-0.19	-0.15	-0.03	-0.17	-0.13
	max	-0.19	-0.10	0.36	-0.17	-0.11	0.00	-0.16	-0.13
	mean	-0.21	-0.13	0.35	-0.18	-0.13	-0.02	-0.17	-0.13
	range	0.04	0.05	0.03	0.02	0.04	0.03	0.00	0.00
8	min	-0.17	-0.12	0.36	-0.18	-0.17	-0.04	-0.25	-0.21
	max	-0.15	-0.11	0.48	-0.14	-0.15	0.05	-0.21	-0.14
	mean	-0.17	-0.11	0.42	-0.16	-0.16	0.00	-0.23	-0.18
	range	0.02	0.01	0.12	0.05	0.02	0.09	0.04	0.07

Plot		May_Std	Jun_Std	Jul_Std	Aug_Std	Mar-May_Std	Jun-Aug_Std	Aug-Oct_Std	Mar-Oct_Std
1	min	-0.29	0.17	0.40	0.26	-0.16	0.42	0.16	0.23
	max	-0.25	0.19	0.47	0.29	-0.14	0.45	0.19	0.29
	mean	-0.27	0.18	0.43	0.28	-0.15	0.43	0.18	0.26
	range	0.04	0.01	0.07	0.02	0.02	0.04	0.03	0.06
2	min	-0.34	0.23	0.42	0.31	-0.19	0.49	0.15	0.27
	max	-0.31	0.26	0.61	0.41	-0.18	0.56	0.25	0.39
	mean	-0.33	0.25	0.53	0.36	-0.19	0.54	0.19	0.32
	range	0.03	0.02	0.18	0.10	0.02	0.07	0.10	0.11
3	min	-0.33	0.17	0.59	0.44	-0.18	0.53	0.30	0.39
	max	-0.29	0.19	0.59	0.44	-0.17	0.54	0.31	0.41
	mean	-0.30	0.18	0.59	0.44	-0.17	0.54	0.31	0.40
	range	0.04	0.01	0.00	0.00	0.01	0.01	0.01	0.02
4	min	-0.32	0.11	0.37	0.18	-0.21	0.31	0.11	0.14
	max	-0.30	0.12	0.39	0.20	-0.21	0.33	0.11	0.15
	mean	-0.31	0.11	0.38	0.18	-0.21	0.32	0.11	0.14
	range	0.02	0.01	0.02	0.02	0.00	0.02	0.00	0.01
5	min	-0.30	0.08	0.27	0.13	-0.21	0.26	0.08	0.09
	max	-0.30	0.10	0.27	0.14	-0.21	0.27	0.09	0.10
	mean	-0.30	0.09	0.27	0.13	-0.21	0.26	0.08	0.10
	range	0.00	0.02	0.01	0.01	0.01	0.01	0.01	0.01
6	min	-0.26	0.25	0.59	0.18	-0.16	0.47	0.05	0.26
	max	-0.25	0.26	0.61	0.20	-0.15	0.50	0.07	0.30
	mean	-0.25	0.26	0.60	0.19	-0.16	0.48	0.05	0.28
	range	0.00	0.01	0.02	0.02	0.00	0.03	0.02	0.04
7	min	-0.25	0.27	0.53	0.18	-0.15	0.47	0.08	0.30
	max	-0.21	0.32	0.56	0.20	-0.12	0.48	0.10	0.32
	mean	-0.23	0.29	0.55	0.19	-0.13	0.47	0.09	0.31
	range	0.04	0.05	0.04	0.02	0.03	0.01	0.02	0.02
8	min	-0.19	0.23	0.44	0.13	-0.16	0.43	0.03	0.18
	max	-0.14	0.24	0.58	0.19	-0.13	0.50	0.07	0.24
	mean	-0.16	0.24	0.52	0.16	-0.14	0.46	0.05	0.20
	range	0.05	0.02	0.14	0.05	0.03	0.07	0.04	0.07

Appendix K. Maximum, minimum, standard error, and average horizontal (X dist to river (m)), vertical (Y to river (m)), and Pythagorean (P to river (m)) distance to the river's edge of B. papyrifera sampled on the Niobrara river in 2016 based on measured via GPS coordinate over 2014 NAIP satellite imagery in ArcMap.

	X to river (m)	Y to river (m)	P to river (m)
max	173.00	22.86	173.62
min	1.00	0.00	0.00
SE	6.83	0.90	6.59
avg	41.52	9.94	43.28

Appendix L. Plot level regression of maximum value-NDVI from Landsat 5 TM versus Annual PDSI of the north-central region of Nebraska between 1985 – 2011.

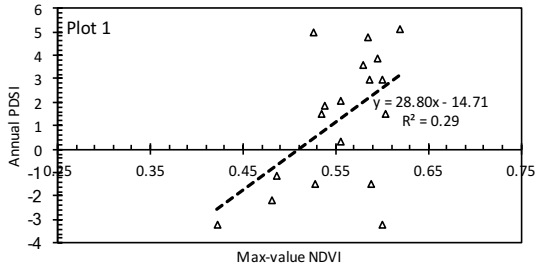

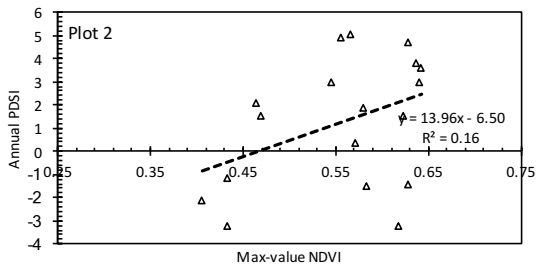

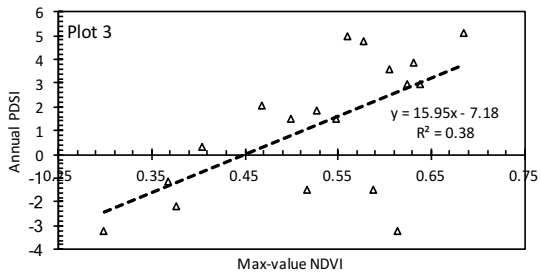

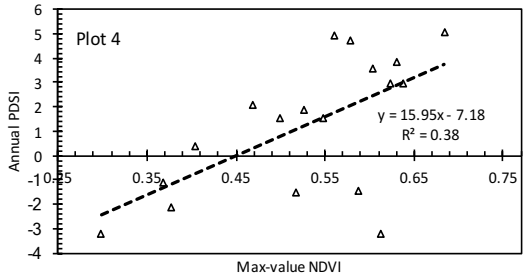

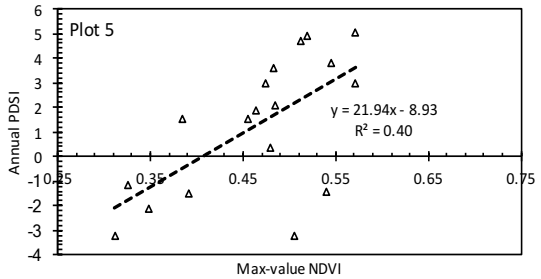

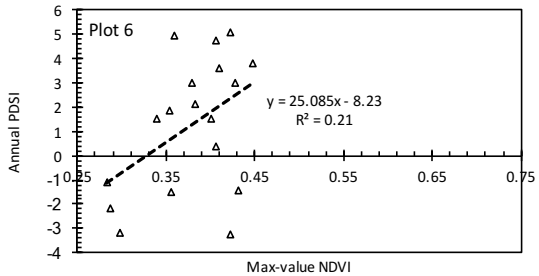

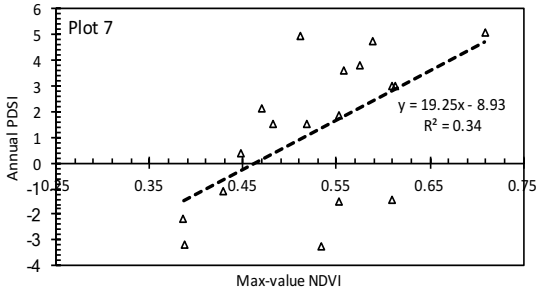
Plot 7
y = 19.25x - 8.93
R² = 0.34
Annual PDSI
Max-value NDVI
6
5
4
3
2
1
0
-1
-2
-3
-4
-0.25
0.35
0.45
0.55
0.65
0.75

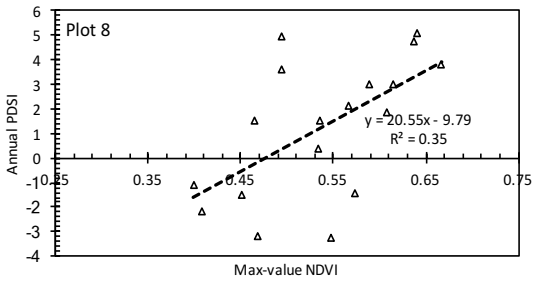
Plot 8
y = 20.55x - 9.79
R² = 0.35
Annual PDSI
Max-value NDVI
6
5
4
3
2
1
0
-1
-2
-3
-4
-0.25
0.35
0.45
0.55
0.65
0.75

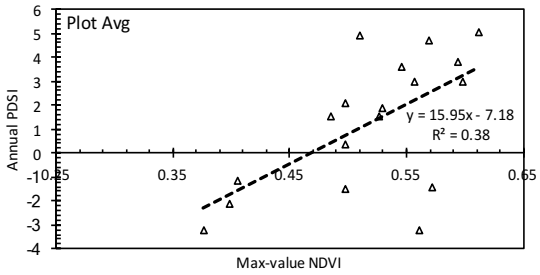
Plot Avg
y = 15.95x - 7.18
R² = 0.38
Annual PDSI
Max-value NDVI
6
5
4
3
2
1
0
-1
-2
-3
-4
-0.25
0.35
0.45
0.55
0.65

Appendix M. Plot level regression of sum-NDVI from MODIS Terra during July versus standardized and raw tree ring growth of *B. papyrifera* of the Niobrara river valley between 2000 – 2014.

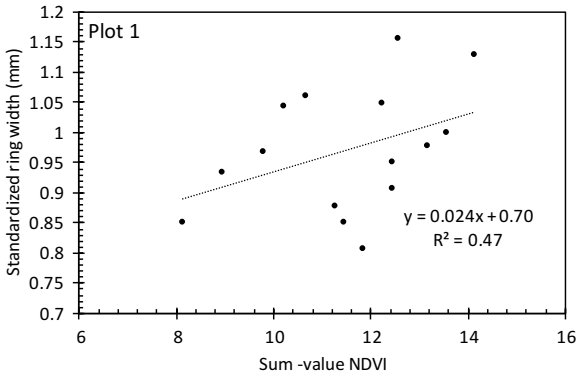

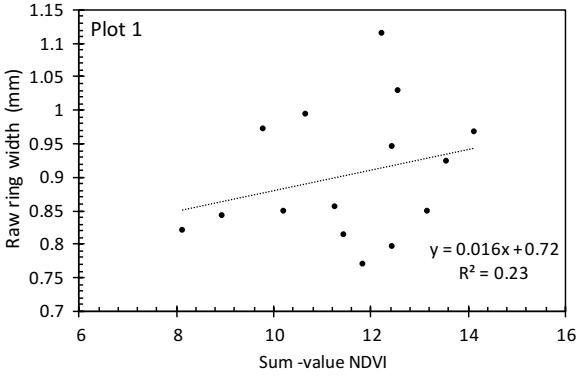

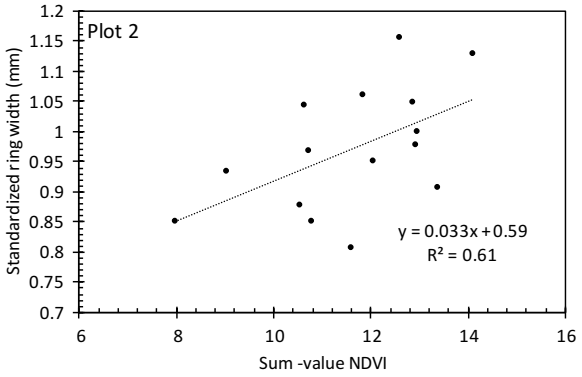
Plot 2
y = 0.033x + 0.59
R² = 0.61
Standardized ring width (mm)
Sum -value NDVI

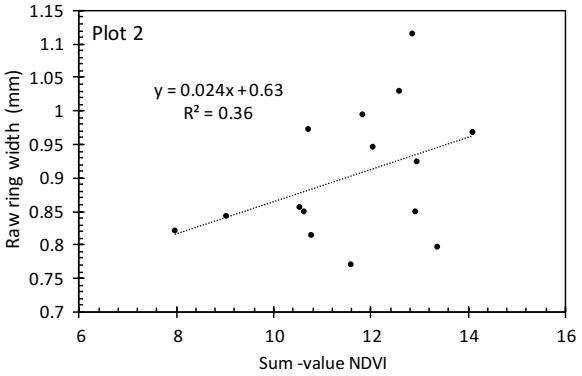
Plot 2
y = 0.024x + 0.63
R² = 0.36
Raw ring width (mm)
Sum -value NDVI

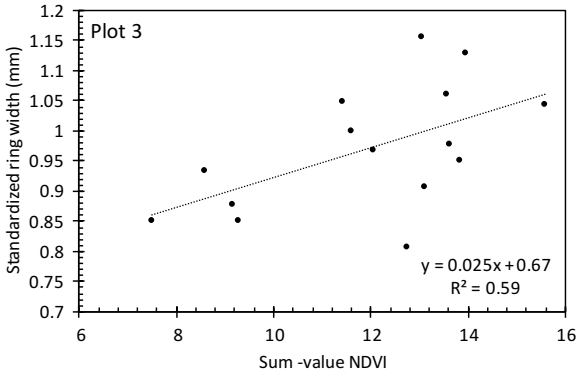
Plot 3
y = 0.025x + 0.67
R² = 0.59
Standardized ring width (mm)
Sum -value NDVI

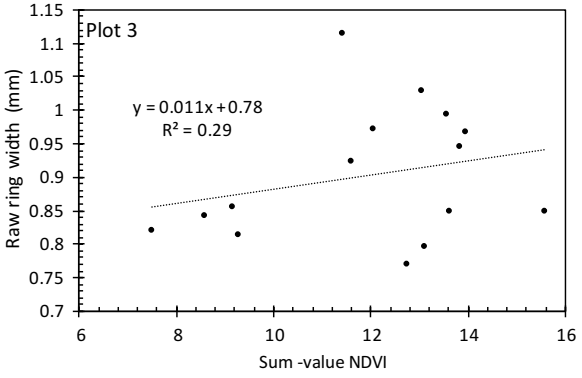
Plot 3
y = 0.011x + 0.78
R² = 0.29
Raw ring width (mm)
Sum -value NDVI

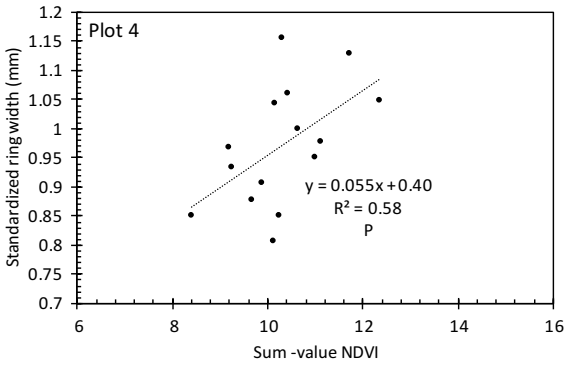
Plot 4
Standardized ring width (mm)
y = 0.055x + 0.40
R² = 0.58
P
Sum -value NDVI

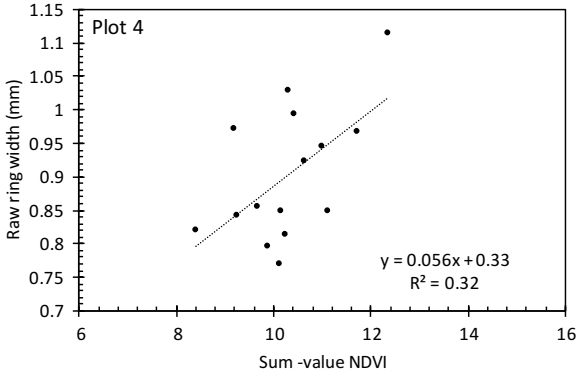
Plot 4
Raw ring width (mm)
y = 0.056x + 0.33
R² = 0.32
Sum -value NDVI

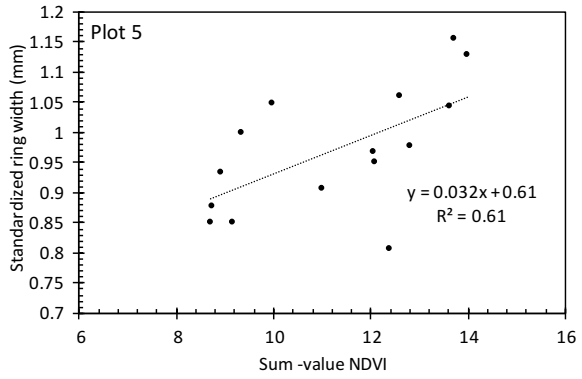
Plot 5
Standardized ring width (mm)
y = 0.032x + 0.61
R² = 0.61
Sum -value NDVI

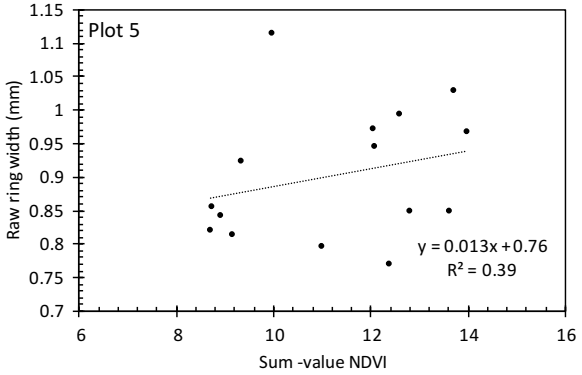
Plot 5
Raw ring width (mm)
y = 0.013x + 0.76
R² = 0.39
Sum -value NDVI

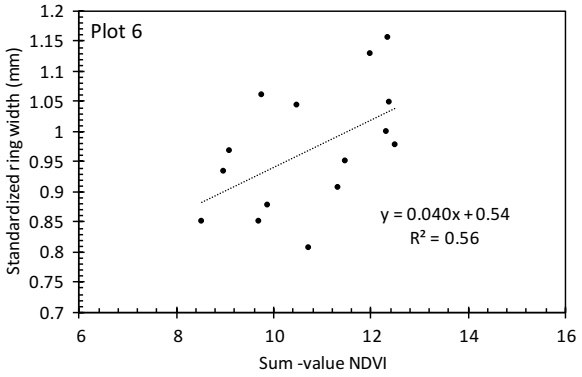
Plot 6
Standardized ring width (mm)
Sum -value NDVI
y = 0.040x + 0.54
R² = 0.56

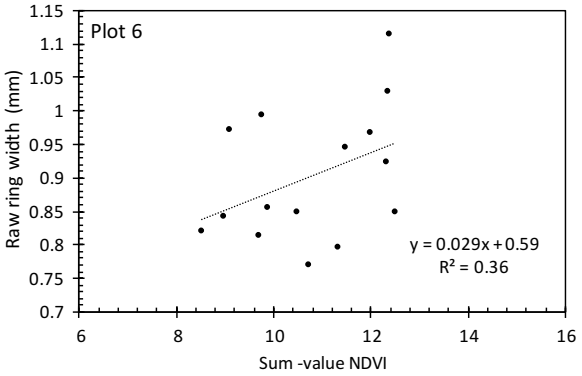
Plot 6
Raw ring width (mm)
Sum -value NDVI
y = 0.029x + 0.59
R² = 0.36

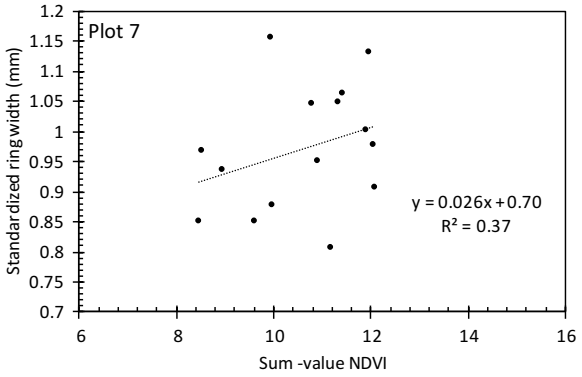
Plot 7
Standardized ring width (mm)
Sum -value NDVI
y = 0.026x + 0.70
R² = 0.37

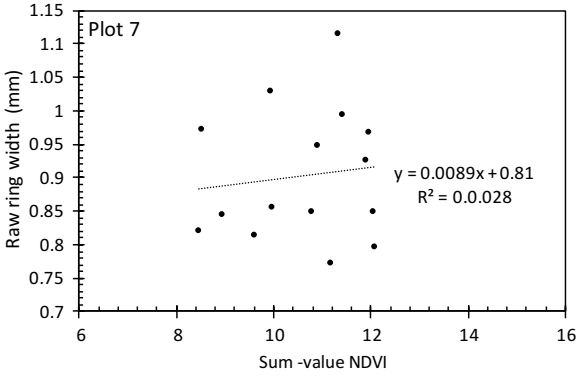
Plot 7
Raw ring width (mm)
Sum -value NDVI
y = 0.0089x + 0.81
R² = 0.0.028

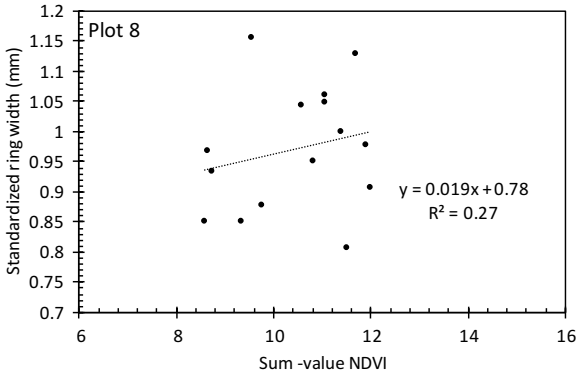
Plot 8
Standardized ring width (mm)
y = 0.019x + 0.78
R² = 0.27
Sum -value NDVI

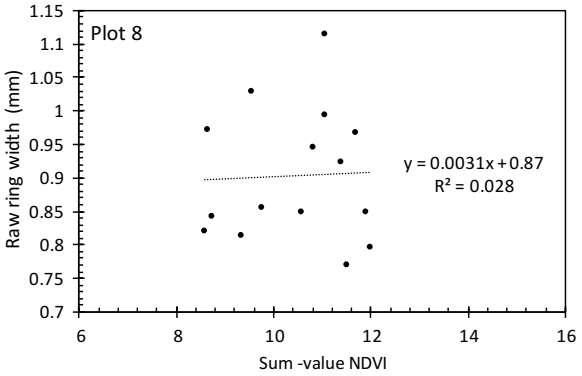
Plot 8
Raw ring width (mm)
y = 0.0031x + 0.87
R² = 0.028
Sum -value NDVI

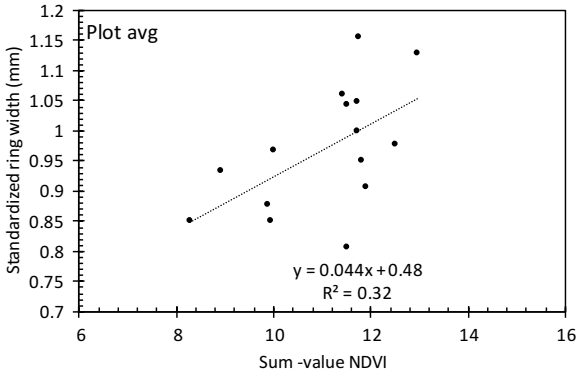
Plot avg
Standardized ring width (mm)
y = 0.044x + 0.48
R² = 0.32
Sum -value NDVI

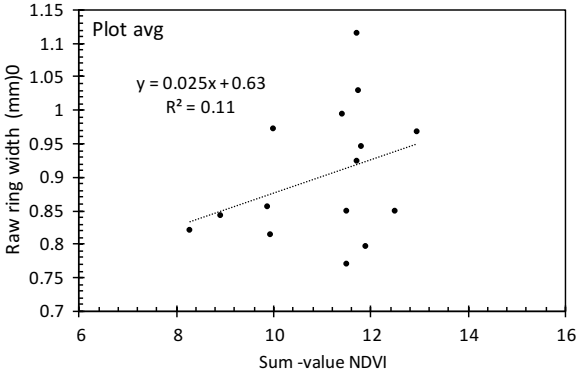
Plot avg
Raw ring width (mm)0
y = 0.025x + 0.63
R² = 0.11
Sum -value NDVI

Appendix N. Plot level regression of sum-value NDVI from MODIS Terra during July versus annual PDSI of the north-central region of Nebraska between 2000-2014.

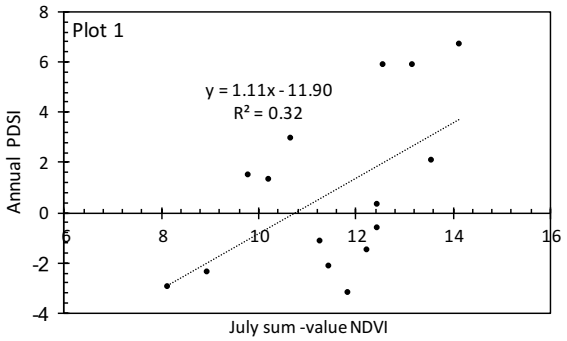

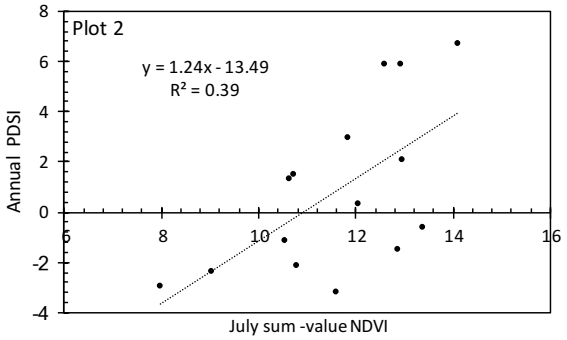

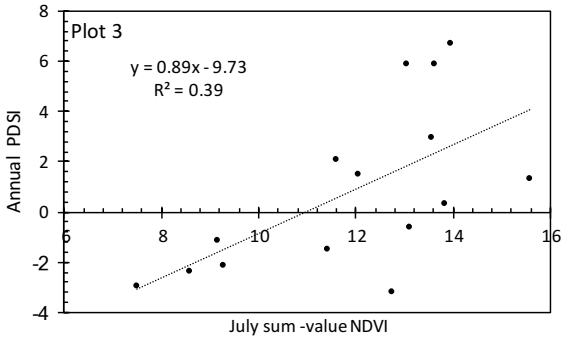
Plot 3
y = 0.89x - 9.73
R² = 0.39
Annual PDSI
July sum -value NDVI

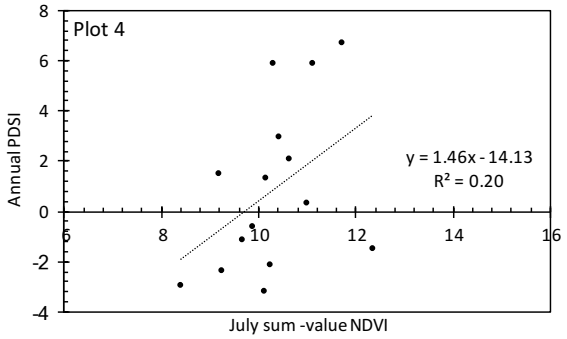
Plot 4
y = 1.46x - 14.13
R² = 0.20
Annual PDSI
July sum -value NDVI

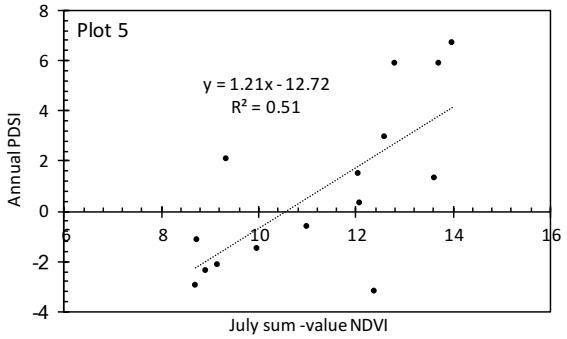
Plot 5
y = 1.21x - 12.72
R² = 0.51
Annual PDSI
July sum -value NDVI

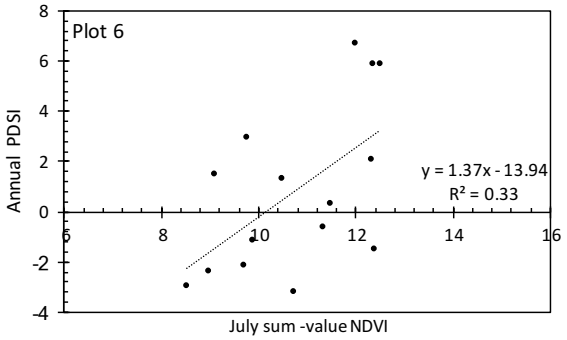
Plot 6
y = 1.37x - 13.94
R² = 0.33
Annual PDSI
July sum -value NDVI

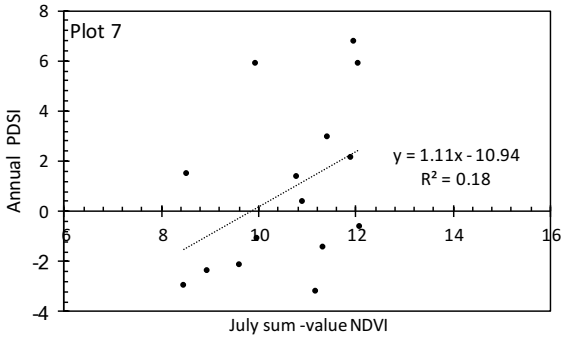
Plot 7
y = 1.11x - 10.94
R² = 0.18
Annual PDSI
July sum -value NDVI

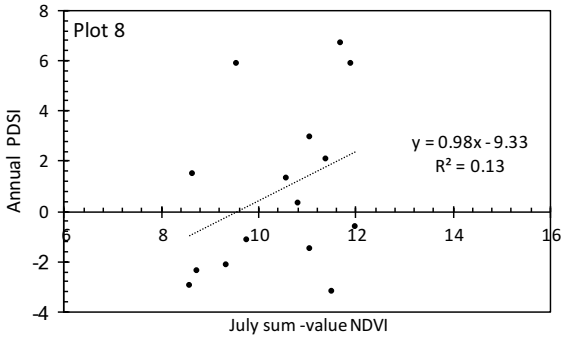
Plot 8
y = 0.98x - 9.33
R² = 0.13
Annual PDSI
July sum -value NDVI

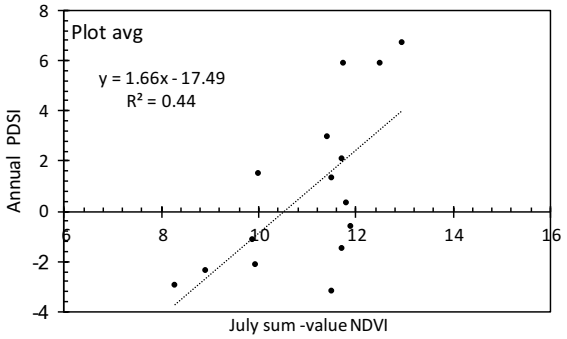
Plot avg
y = 1.66x - 17.49
R² = 0.44
Annual PDSI
July sum -value NDVI

Appendix O. Plot level regression of sum-NDVI from MODIS Terra during June - August versus standardized ring growth of *B. papyrifera* of the Niobrara river valley between 2000 – 2014.

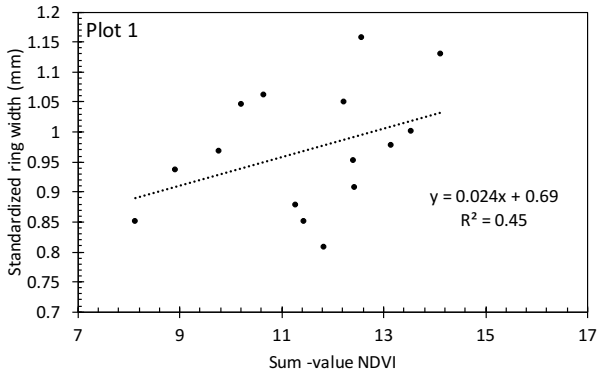

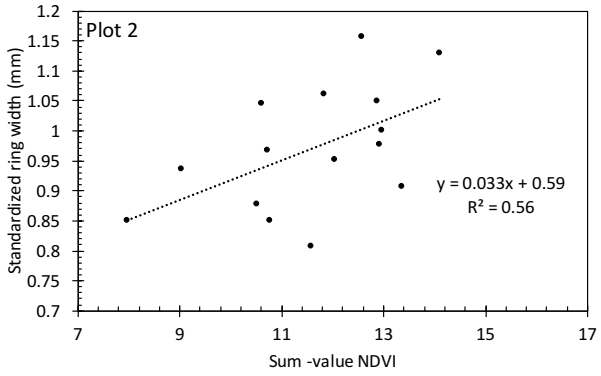

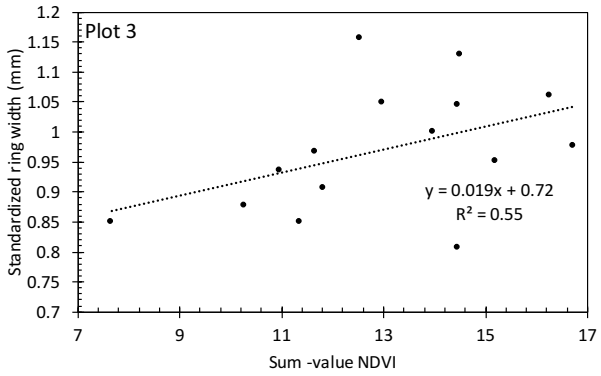
Plot 3
y = 0.019x + 0.72
R² = 0.55
Standardized ring width (mm)
Sum -value NDVI

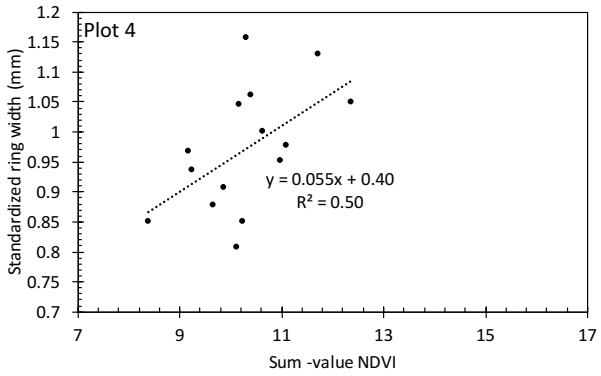
Plot 4
y = 0.055x + 0.40
R² = 0.50
Standardized ring width (mm)
Sum -value NDVI

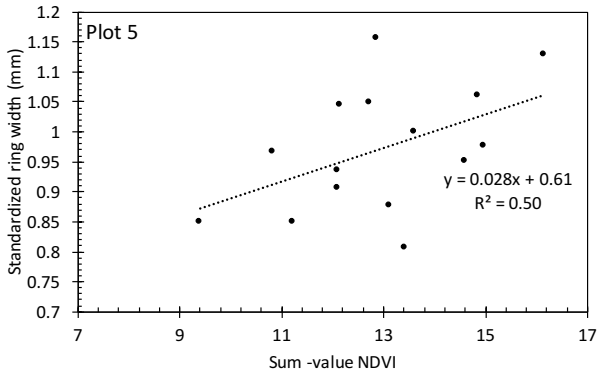
Plot 5
y = 0.028x + 0.61
R² = 0.50
Standardized ring width (mm)
Sum -value NDVI

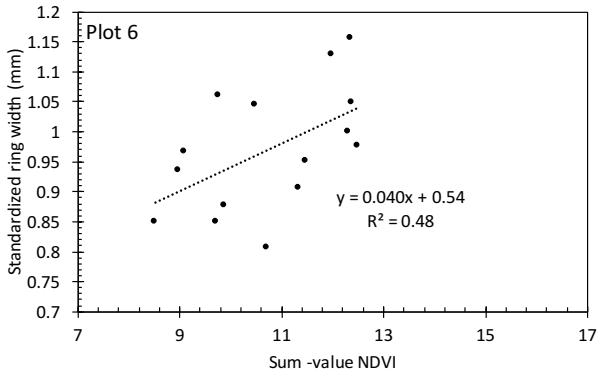
Plot 6
y = 0.040x + 0.54
R² = 0.48
Standardized ring width (mm)
Sum -value NDVI

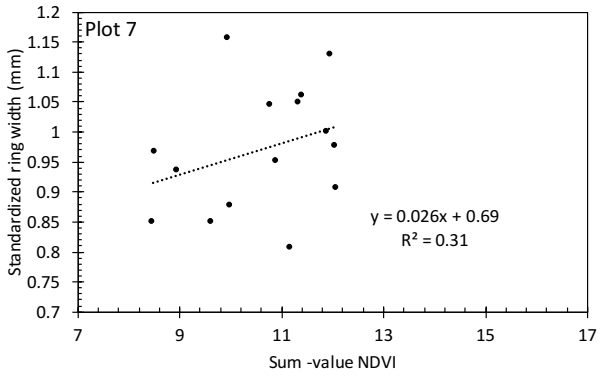
Plot 7
Standardized ring width (mm)
Sum -value NDVI
y = 0.026x + 0.69
R² = 0.31

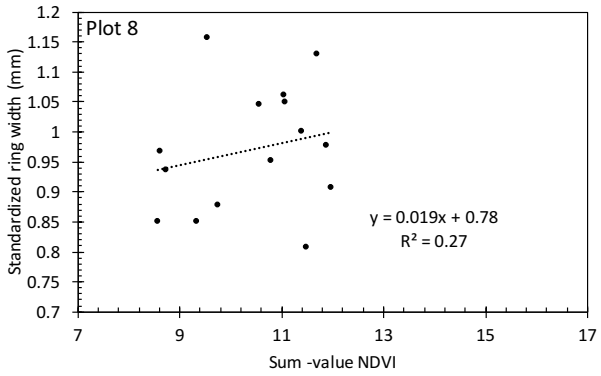
Plot 8
Standardized ring width (mm)
Sum -value NDVI
y = 0.019x + 0.78
R² = 0.27

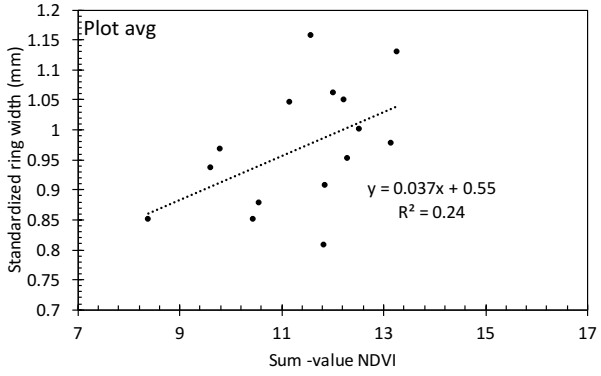
Plot avg
Standardized ring width (mm)
Sum -value NDVI
y = 0.037x + 0.55
R² = 0.24

Appendix P. Plot level regression of sum-value NDVI from MODIS Terra during July versus annual PDSI of the north-central region of Nebraska between 2000-2014.

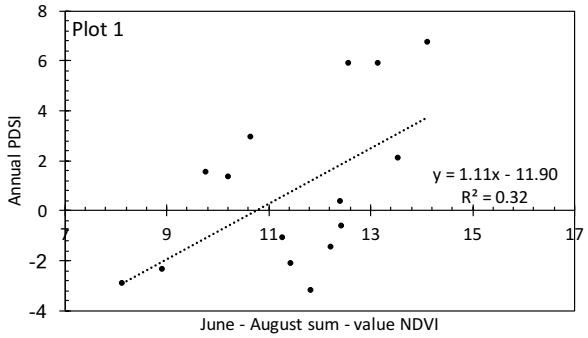

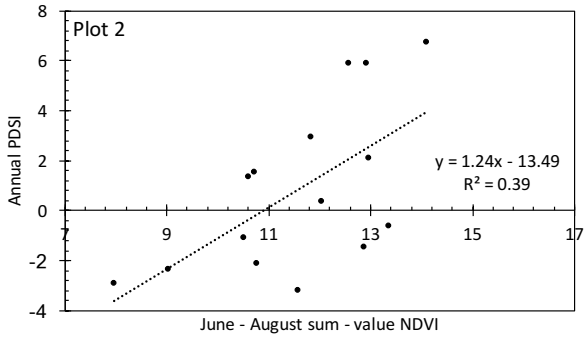

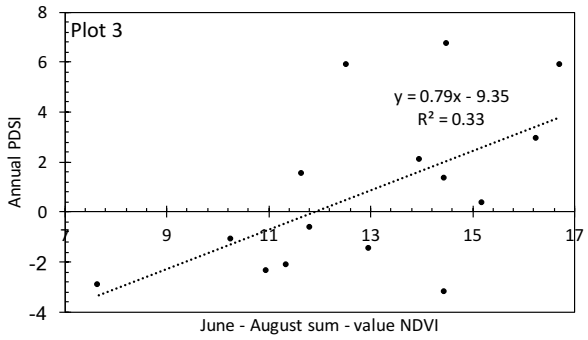
Plot 3
y = 0.79x - 9.35
R² = 0.33
Annual PDSI
June - August sum - value NDVI

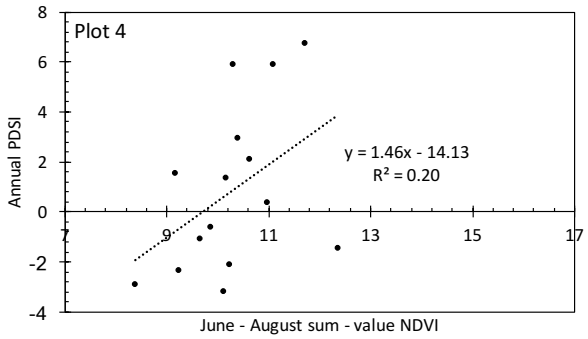
Plot 4
y = 1.46x - 14.13
R² = 0.20
Annual PDSI
June - August sum - value NDVI

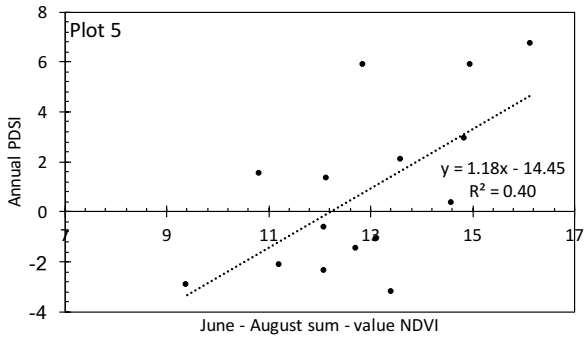
Plot 5
y = 1.18x - 14.45
R² = 0.40
Annual PDSI
June - August sum - value NDVI

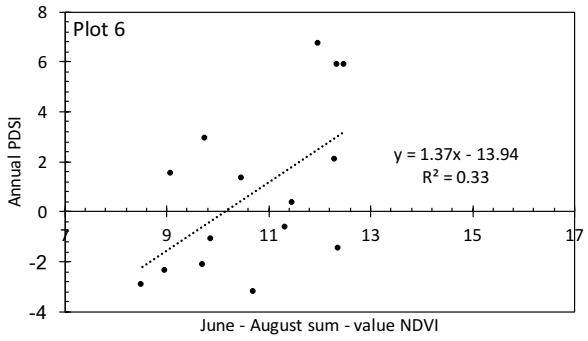
Plot 6
y = 1.37x - 13.94
R² = 0.33
Annual PDSI
June - August sum - value NDVI

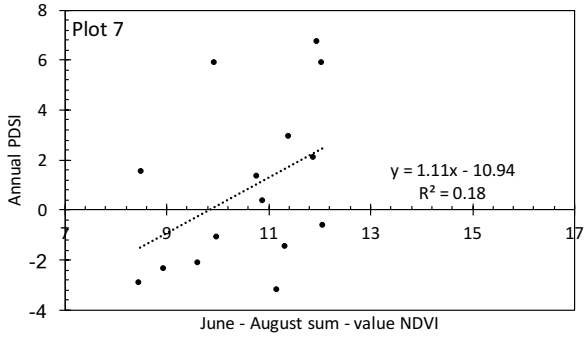
Plot 7
y = 1.11x - 10.94
R² = 0.18
Annual PDSI
June - August sum - value NDVI

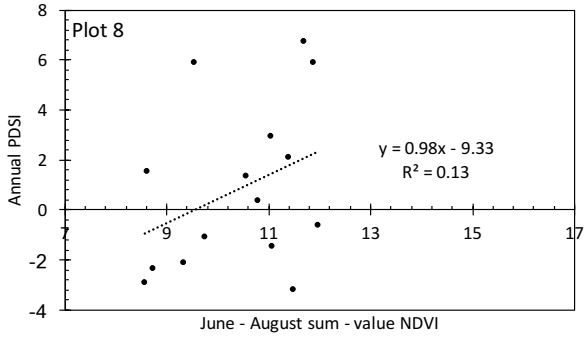
Plot 8
y = 0.98x - 9.33
R² = 0.13
Annual PDSI
June - August sum - value NDVI

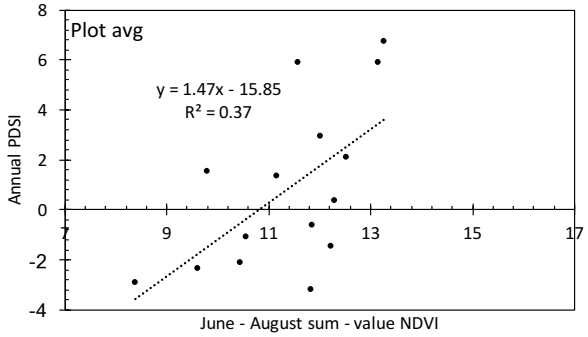
Plot avg
y = 1.47x - 15.85
R² = 0.37
Annual PDSI
June - August sum - value NDVI

Appendix Q. Pearson's R^2 correlation of B. papyrifera tree ring growth (raw) and standardized ring growth (std) to groundwater well observations surrounding the Niobrara River Valley study sites between 1950 – 2014

station ID	424441100320001	424802100310701	425350100122301	425416100130401	425434100342101
raw	0.2917914	0.5786209	-0.02905303	-0.4282874	-0.5581398
raw.p	0.02251	0.0002715	0.9181	0.1648	0.02465
std	-0.0925433	0.07040475	0.3539098	-0.01708916	0.06416785
std.p	0.4781	0.6878	0.1956	0.958	0.8134

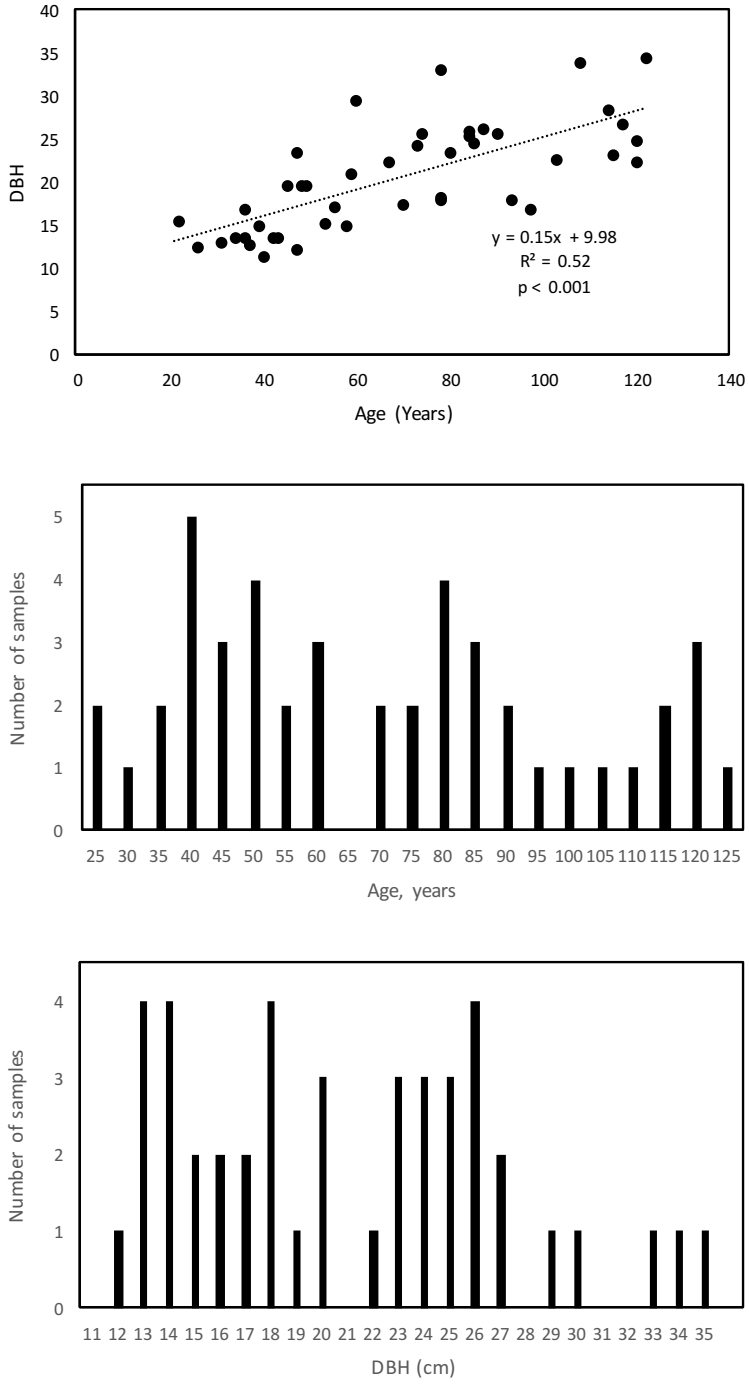

Appendix R. Age and diameter at breast height (DBH) of the observed Niobrara River Valley B. papyrifera samples from 1894 – 2016

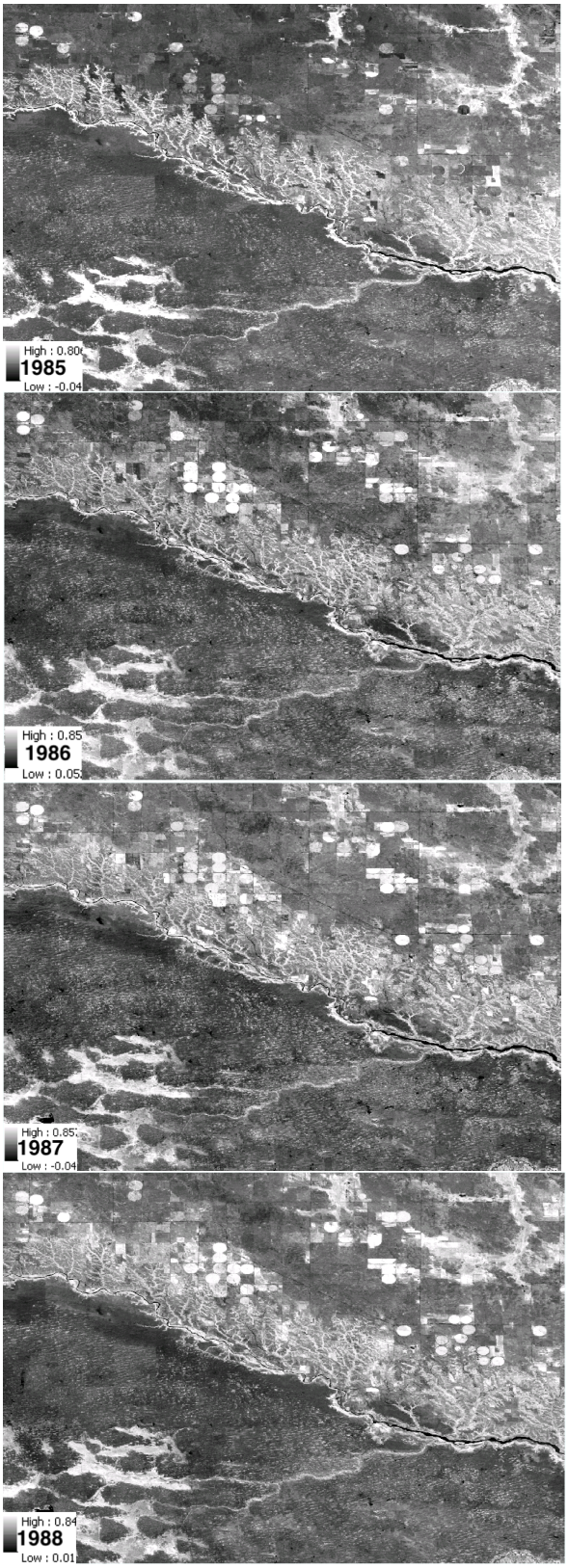
High : 0.80
1985
Low : -0.04
High : 0.85
1986
Low : 0.05
High : 0.85
1987
Low : -0.04
High : 0.84
1988
Low : 0.01

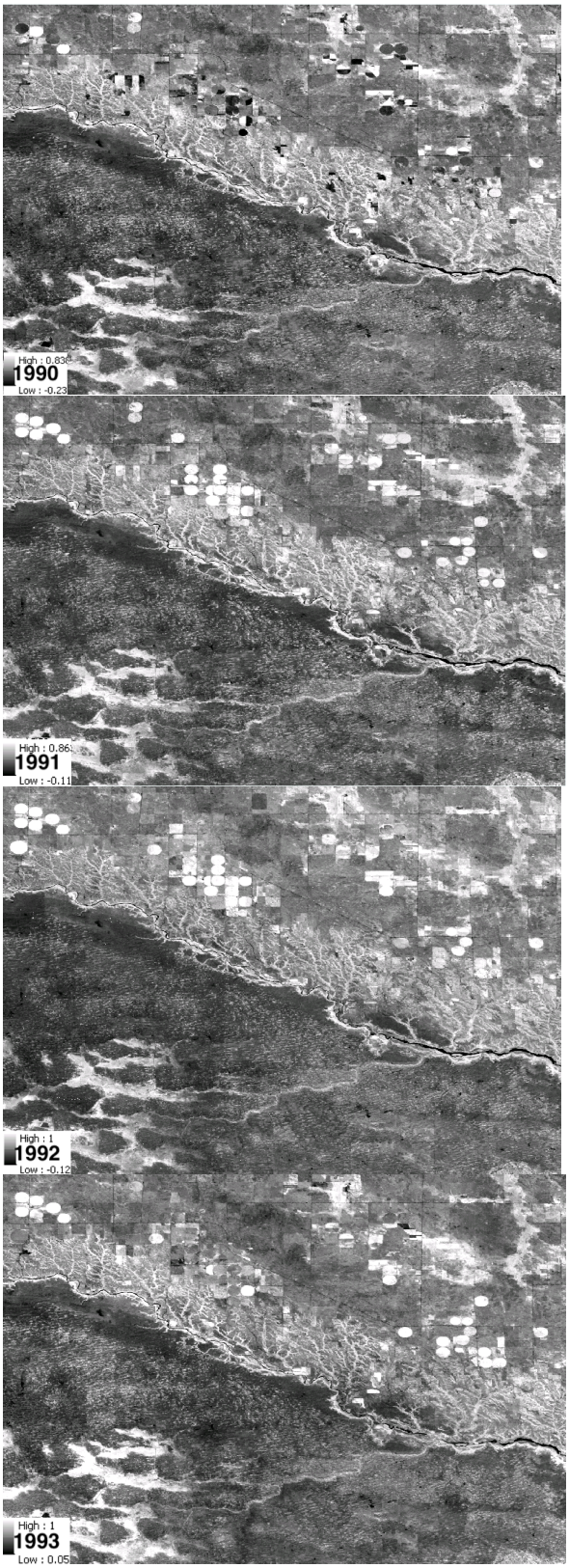
High : 0.83
1990
Low : -0.23
High : 0.86
1991
Low : -0.11
High : 1
1992
Low : -0.12
High : 1
1993
Low : 0.05

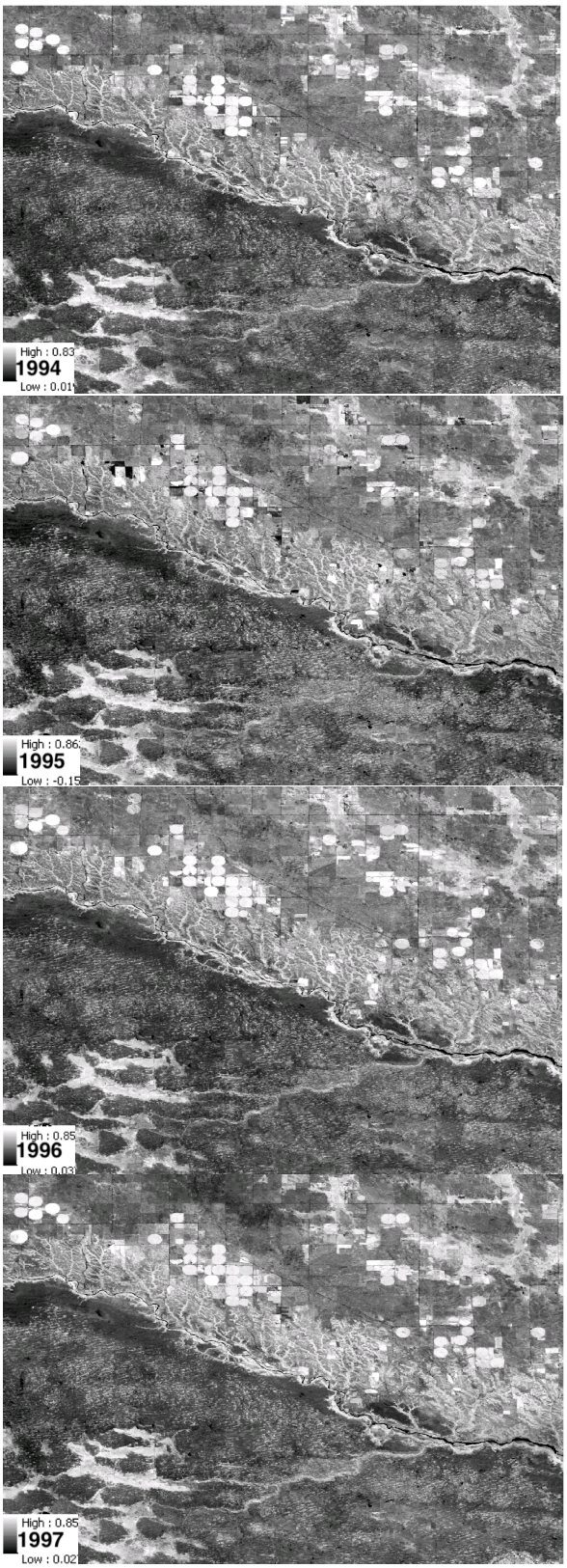
High : 0.83
1994
Low : 0.01
High : 0.86
1995
Low : -0.15
High : 0.85
1996
High : 0.85
1997
Low : 0.02

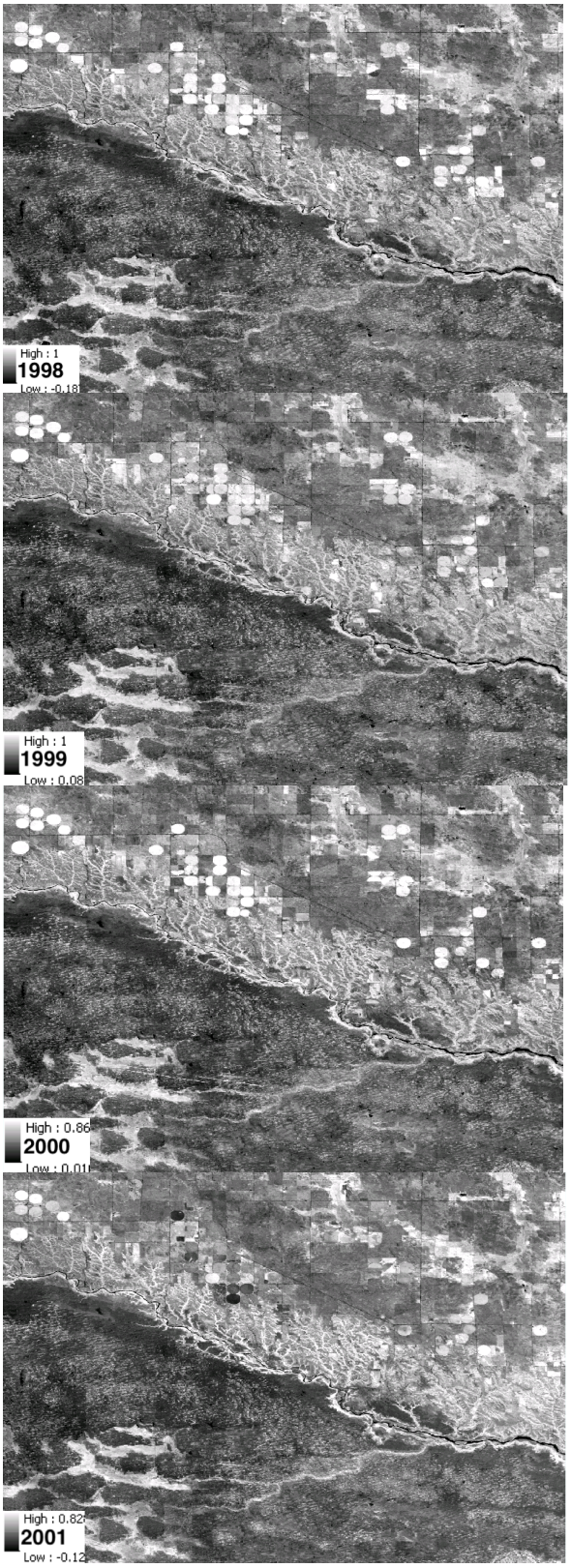
High : 1
1998
High : 1
1999
Low : 0.08
High : 0.86
2000
2001
Low : -0.12

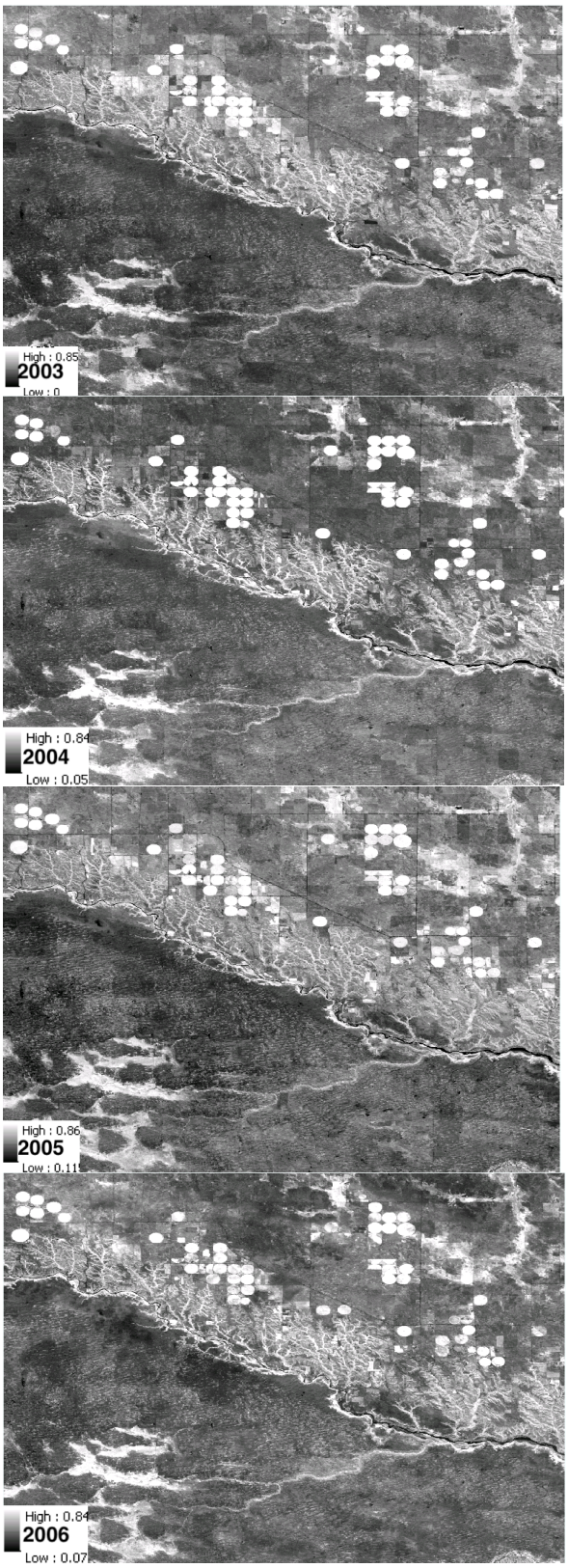
High : 0.85
2003
Low : 0
High : 0.84
2004
Low : 0.05
High : 0.86
2005
High : 0.84
2006
Low : 0.07

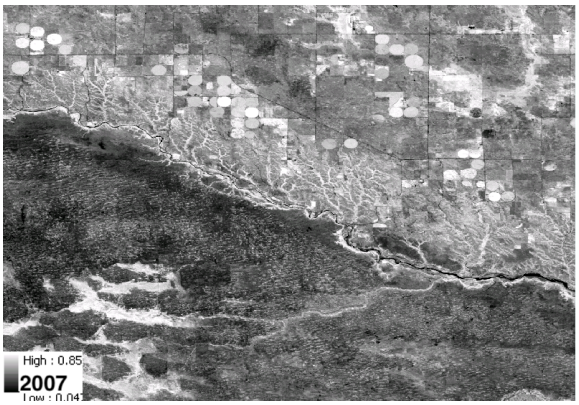

Appendix S. Maximum-value NDVI images used in the Pearson's R2 correlation to raw tree ring growth and standardized ring growth of B. Papyrifera of the Niobrara River Valley between 1985-2007